

Steam-Water Mixing and System Hydrodynamics Program - Task 4

Quarterly Progress Report
July - September 1979

Manuscript Completed: July 1980
Date Published: August 1980

Prepared by
R. P. Collier, J. A. Dworak, L. J. Flanigan
J. S. K. Liu, A. Segev

Battelle-Columbus Laboratories
505 King Avenue
Columbus, OH 43201

Prepared for
Division of Reactor Safety Research
Office of Nuclear Regulatory Research
U.S. Nuclear Regulatory Commission
Washington, D.C. 20555
NRC FIN No. A4048

8009100043

THIS DOCUMENT CONTAINS
POOR QUALITY PAGES

STEAM-WATER MIXING AND SYSTEM HYDRODYNAMICS PROGRAM

by

Robert P. Collier, Joseph A. Dworak,
Lawrence J. Flanigan, Jim S. Liu,
and Aryeh Segev

ABSTRACT

During this quarter we analyzed results from high bypass air-water tests and from low subcooling steam-water tests in the 2/15-scale model, continued development of a mechanistic model for ECC penetration, and analyzed results from steam-water tests in the simple tube facility.

The experimental efforts during this quarter were directed to completion of the installation of the annulus void measurement system and the instrumented spool piece for the break leg, and subsequent check out and acquisition of initial data.

SUMMARY

This report describes progress during the fourth quarter of FY '79 on the BCL Steam-Water Mixing and System Hydrodynamics Program. Progress during the quarter is reported under four technical tasks: analysis, testing and data reduction, RIL support and technical assistance, and acquisition and application of advanced instrumentation.

Analysis

Results from high bypass air-water tests in the 2/15-scale model were analyzed. These tests have indicated that the penetration rate is independent of the injected water flow rate for high bypass operating conditions. This is consistent with data obtained previously.

The data also show that the penetration to the lower plenum is dependent on the injected water temperature. The addition of evaporated water vapor to the reverse core air flow has been identified as the cause of the air-water temperature dependent penetration.

These data have been compared with air-water data obtained in previous 1/15- and 2/15-scale studies. Penetration data from the two different scale models do not overlay on J^* coordinates. The presence of VDM probes in the annulus has also been shown to affect the penetration behavior for air-water flows.

Results of low subcooling steam-water tests in the 2/15-scale model were also evaluated. The effects of pressure, injected water flow rate, and test mode were consistent with previous results. The presence of VDM probes in the annulus did not appear to influence the penetration behavior for steam-water tests over the range tested. The NLINMLE program was used to correlate the steam-water data in a form originally proposed by Beckner, et al. Good agreement between the correlation and the experimental data is shown.

During this quarter, results of a countercurrent flow condensation study were incorporated into the mechanistic model for ECC penetration which is currently under development. Results of calculations made with the revised mechanistic model were compared with data from neutral wall experiments. Relatively good agreement was shown.

Results of countercurrent flow flooding tests in 2-6 inch I.D. tubes were reviewed. Both steam-water and air-water tests were performed. A hysteresis effect is clearly indicated for steam-water flooding data.

Testing and Data Reduction

The experimental efforts during the quarter were directed toward completion of the installation of the annulus void distribution (VDM) system and completion of the instrumented spool piece for the broken leg. Initial shakedown tests utilizing the advanced instrumentation were completed.

RIL Support and Technical Assistance

BCL staff assisted in review of final material for the RIL summarizing small scale ECC bypass research results.

Acquisition and Application of Advanced Instrumentation

The three beam gamma densitometer for the break leg spool piece was received and installed. The annulus VDM system was completed and installed during the quarter.

TABLE OF CONTENTS

	<u>Page</u>
ABSTRACT.	i
SUMMARY	ii
INTRODUCTION.	xii
PART I:	
TASK 1.0 ANALYSIS.	1
Objectives	1
Work During Quarter.	1
Plans for Future Work.	
TASK 2.0	
Objectives	45
Work During Quarter.	45
Plans for Future Work.	46
TASK 3.0	
Objectives	47
Work During Quarter.	47
Plans for Future Work.	47
TASK 4.0	
Objectives	48
Work During Quarter.	48
Plans for Future Work.	48
PART II:	
COUNTERCURRENT FLOODING FLOW IN TUBES	50
REFERENCES.	R-1
APPENDIX A.	A-1
APPENDIX B.	B-1

LIST OF TABLES

PART I

Progress for the Quarter
July 1, 1979 - September 30, 1979

	<u>Page</u>
Table 1. Air-Water Plenum Fill Test Matrix--Nominal Conditions.	2
Table 2. Wallis Correlation Parameters Calculated from 2/15-Scale, Air-Water Plenum Fill Tests--J* Parameters.	13
Table 3. Effects of Evaporation for Three Injected Water Temperatures.	15
Table 4. Steam-Water Plenum Fill Test Matrix--Nominal Conditions.	27
Table 5. Correlation Parameters Calculated from 2/15-Scale Steam-Water Plenum Fill Tests	31

LIST OF FIGURES

PART I

Progress for the Quarter
July 1, 1979 - September 30, 1979

	<u>Page</u>
Figure 1. Air-Water Plenum Fill Penetration Data Obtained With $J_{Lin}^* = 0.064$ and $P_V = 170$ kPa (25 psia)	3
Figure 2. Air-Water Plenum Fill Penetration Data Obtained With $J_{Lin}^* = 0.098$ and $P_V = 170$ kPa (25 psia)	4
Figure 3. Air-Water Plenum Fill Penetration Data Obtained With $J_{Lin}^* = 0.122$ and $P_V = 170$ kPa (25 psia)	5
Figure 4. Air-Water Plenum Fill Penetration Data Obtained With $T_{Lin} = 25^\circ\text{C}$ (77°F) and $P_V = 170$ kPa (25 psia)	6
Figure 5. Air-Water Plenum Fill Penetration Data Obtained With $T_{Lin} = 57^\circ\text{C}$ (135°F) and $P_V = 190$ kPa (28 psia)	7
Figure 6. Air-Water Plenum Fill Penetration Data Obtained With $T_{Lin} = 93^\circ\text{C}$ (200°F) and $P_V = 204$ kPa (30 psia)	8
Figure 7. Data of Figure 4 on $J^{*1/2}$ Coordinates	9
Figure 8. Data of Figure 5 on $J^{*1/2}$ Coordinates	10
Figure 9. Data of Figure 6 on $J^{*1/2}$ Coordinates	12
Figure 10. Comparison of 1/15- and 2/15-Scale Air-Water Penetration Data - $J_{Lin}^* = 0.064-0.150$, $T_{Lin} = 25^\circ\text{C}$ (77°F)	17
Figure 11. Comparison of Quasi-Steady State and Plenum Fill Air-Water Penetration Data Obtained With $J_{Lin}^* = 0.064$ and 0.098 and $T_{Lin} = 27^\circ\text{C}$ (82°F) - VDM Probes in Annulus	20
Figure 12. Comparison of 2/15-Scale Air-Water Penetration Data Obtained With and Without VDM Probes in the Downcomer Annulus - $J_{Lin}^* = 0.064$, $P_V = 153$ kPa (23 psia), $T_{Lin} = 27^\circ\text{C}$ (80°F)	21
Figure 13. Comparison of 2/15-Scale Air-Water Penetration Data Obtained With and Without VDM Probes in the Downcomer Annulus - $J_{Lin}^* = 0.098$, $P_V = 153$ kPa (23 psia), $T_{Lin} = 27^\circ\text{C}$ (80°F)	22

LIST OF FIGURES
(continued)

	<u>Page</u>
Figure 14. Comparison of Data With and Without VDM Probes In Annulus on $J^{*1/2}$ Coordinates.	24
Figure 15. Penetration Data Corrected for VDM Probe Influence.	25
Figure 16. Steam-Water Plenum Fill Penetration Data Obtained With $T_{Lin} = 99^{\circ}\text{C}$ (210°F) and $J_{Lin}^{*} = 0.064$	28
Figure 17. Steam-Water Plenum Fill Penetration Data Obtained With $T_{Lin} = 99^{\circ}\text{C}$ (210°F) and $P_V = 306$ kPa (45 psia).	29
Figure 18. Comparison of Quasi-Steady State and Plenum Fill Steam-Water Penetration Data With $J_{Lin}^{*} = 0.064$, $P_V = 306$ kPa (45 psia), $T_{Lin} = 99^{\circ}\text{C}$ (210°F).	30
Figure 19. Comparison of Correlation and Steam-Water Penetration Data For $J_{Lin}^{*} = 0.064$ and $T_{Lin} =$ 99°C (210°F)	32
Figure 20. Comparison of Correlation and Steam-Water Penetration Data for $J_{Lin}^{*} = 0.098$, $T_{Lin} =$ 99°C (210°F), and $P_V = 306$ kPa (45 psia)	33
Figure 21. Comparison of Steam-Water Penetration Data Taken With and Without VDM Probes in the Annulus For $J_{Lin}^{*} = 0.098$, $T_{Lin} = 99^{\circ}\text{C}$ (210°F), $P_V = 306$ kPa (45 psia).	35
Figure 22. Comparison of Steam-Water Penetration Data With Earlier Results, $J_{Lin}^{*} = 0.064$	36
Figure 23. Comparison of Steam-Water Penetration Data With Earlier Results, $J_{Lin}^{*} = 0.064$	37
Figure 24. Comparison of Steam-Water Penetration Data With Earlier Results, $J_{Lin}^{*} = 0.097$	38
Figure 25. Comparison of Predicted and Measured J_{gc}^{*} For Battelle's 1/15-Scale Geometry	41
Figure 26. Comparison of Predicted and Measured J_{gc}^{*} For Battelle's 2/15-Scale Geometry	42
Figure 27. Comparison of Predicted and Measured J_{gc}^{*} For Battelle's 2/15-Scale Geometry - Extended Core Barrel	43

LIST OF FIGURES
(continued)

	<u>Page</u>
Figure 28. Comparison of Predicted and Measured J_{gc}^* For Battelle's 2/15-Scale Geometry - Short Core Barrel	44
Figure 29. Schematic Sketch of Test Facility.	54
Figure 30. Lower Tank Pressure for Three Countercurrent Flows With $T_W = 21^\circ\text{C}$	58
Figure 31. Flooding Velocities for Air-Water Flows in 2-Inch Diameter Tube With $T_W = 85^\circ\text{F}$	60
Figure 32. Flooding Velocities for Air-Water Flows in 2-Inch Diameter Tube With $T_W = 140^\circ\text{F}$	61
Figure 33. Flooding Velocities for Air-Water Flows in 2-Inch Diameter Tube With $T_W = 75^\circ\text{F}$	62
Figure 34. Flooding Velocities for Air-Water Flows in 4-Inch Diameter Tube With $T_W = 140^\circ\text{F}$	63
Figure 35. Flooding Velocities for Air-Water Flows in 6-Inch Diameter Tube With $T_W = 75^\circ\text{F}$	64
Figure 36. Flooding Velocities for Air-Water Flows in 6-Inch Diameter Tube With $T_W = 140^\circ\text{F}$	65
Figure 37. Variation of Flooding Velocities as a Function of Tube Diameter for Air-Water Flows with $T_W = 80^\circ\text{F}$ and $J_{Lin}^* = 0.05$	66
Figure 38. Variation of Flooding Velocities as a Function of Tube Diameter for Air-Water Flows with $T_W = 80^\circ\text{F}$ and $J_{Lin}^* = 0.125$	67
Figure 39. Variation of Flooding Velocities as a Function of Tube Diameter for Air-Water Flows with $T_W = 140^\circ\text{F}$ and $J_{Lin}^* = 0.05$	68
Figure 40. Variation of Flooding Velocities as a Function of Tube Diameter for Air-Water Flows with $T_W = 140^\circ\text{F}$ and $J_{Lin}^* = 0.125$	69
Figure 41. Variation of Flooding Velocities as a Function of Tube Diameter for Air-Water Flows with $T_W = 80^\circ\text{F}$. .	70
Figure 42. Variation of Flooding Velocities as a Function of Tube Diameter for Air-Water Flows with $T_W = 80^\circ\text{F}$. .	71

LIST OF FIGURES
(continued)

	<u>Page</u>
Figure 43. Variation of Flooding Velocities as a Function of Tube Diameter for Air-Water Flows with $T_W = 140^\circ\text{F}$. . .	72
Figure 44. Variation of Flooding Velocities as a Function of Tube Diameter for Air-Water Flows with $T_W = 140^\circ\text{F}$. . .	73
Figure 45. Flooding Velocities for Steam-Water Flows in 2-Inch Diameter Tube with $T_W = 85^\circ\text{F}$	74
Figure 46. Flooding Velocities for Steam-Water Flows in 2-Inch Diameter Tube with $T_W = 140^\circ\text{F}$	75
Figure 47. Flooding Velocities for Steam-Water Flows in 4-Inch Diameter Tube with $T_W = 80^\circ\text{F}$	76
Figure 48. Flooding Velocities for Steam-Water Flows in 4-Inch Diameter Tube with $T_W = 140^\circ\text{F}$	77
Figure 49. Flooding Velocities for Steam-Water Flows in 6-Inch Diameter Tube with $T_W = 75^\circ\text{F}$	78
Figure 50. Flooding Velocities for Steam-Water Flows in 6-Inch Diameter Tube with $T_W = 140^\circ\text{F}$	79
Figure 51. Variation of Flooding Velocities as a Function of Diameter for Steam-Water Flows with $T_W = 80^\circ\text{F}$ and $J_{Lin}^* = 0.05$	80
Figure 52. Variation of Flooding Velocities as a Function of Diameter for Steam-Water Flows with $T_W = 75^\circ\text{F}$ and $J_{Lin}^* = 0.13$	81
Figure 53. Variation of Flooding Velocities as a Function of Diameter for Steam-Water Flows with $T_W = 140^\circ\text{F}$ and $J_{Lin}^* = 0.05$	82
Figure 54. Variation of Flooding Velocities as a Function of Diameter for Steam-Water Flows with $T_W = 140^\circ\text{F}$ and $J_{Lin}^* = 0.13$	83
Figure 55. Variation of Flooding Velocities as a Function of Diameter for Steam-Water Flows with $T_W = 80^\circ\text{F}$	84
Figure 56. Variation of Flooding Velocities as a Function of Diameter for Steam-Water Flows with $T_W = 80^\circ\text{F}$	85

LIST OF FIGURES
(continued)

	<u>Page</u>
Figure 57. Variation of Flooding Velocities as a Function of Diameter for Steam-Water Flows with $T_W = 140^\circ\text{F}$. . .	86
Figure 58. Variation of Flooding Velocities as a Function of Diameter for Steam-Water Flows with $T_W = 140^\circ\text{F}$. . .	87
Figure 59. Comparison of the Experimental Data for 2-Inch Diameter Tube.	88
Figure 60. Comparison of the Experimental Data for 6- and 10-Inch Diameter Tube.	89

PREVIOUS REPORTS IN THIS SERIES

<u>Report No.</u>	<u>Period Covered</u>	<u>Date Issued</u>
BMI-X-657	January-March 1975	April, 1975
BMI- 1936	April-June 1975	August, 1975
BMI- 1940	July-September 1975	November, 1975
BMI-NUREG-1945	October-December 1975	March, 1976
BMI-NUREG-1949	January-March 1976	May, 1976
BMI-NUREG-1962	April-June 1976	November, 1976
BMI-NUREG-1964	July-September 1976	December, 1976
BMI-NUREG-1968	October-December 1976	February, 1977
BMI-NUREG-1972	January-March 1977	May, 1977
BMI-NUREG-1979	April-June 1977	September, 1977
BMI-NUREG-1987	July-September 1977	December, 1977
NUREG/CR-0034 (BMI-1993)	October-December 1977	March, 1978
NUREG/CR-0147 (BMI-2003)	January-March 1978	June, 1978
NUREG/CR-0526 (BMI-2011)	April-June 1978	November, 1978
NUREG/CR-0565 (BMI-2013)	July-September 1978	December, 1978
NUREG/CR-0845 (BMI-2028)	October-December 1978	May, 1979
NUREG/CR-0897 (BMI-2029)	January-March 1979	June, 1979
NUREG/CR- (BMI-2038)	April-June 1979	June, 1980

INTRODUCTION

The U.S. Nuclear Regulatory Commission is responsible for assessing and assuring the safety of nuclear reactors under abnormal conditions such as a postulated loss-of-coolant accident (LOCA), as well as under normal operating conditions. Prediction of the thermal-hydraulic behavior of the reactor system following such a LOCA is of particular interest, and NRC supports a very large research effort aimed at increasing that predictive capability. In the Steam-Water Mixing and System Hydrodynamics Program currently in progress at Battelle-Columbus Laboratories (BCL) both analytical and experimental work are directed toward a more thorough understanding and description of steam-water interaction and its influence on the effectiveness of emergency core cooling systems under LOCA conditions. The phenomena of ECC penetration and bypass are of primary interest.

Fiscal Year 1979 activities include identification and establishment of the physical basis for scaling ECC bypass phenomena, development of and understanding of condensation and vaporization processes in the downcomer, determination of the validity of using steady-state results to predict transient behavior, and preparation of a summary technical report for the planned Research Information Letter (RIL).

The scope of technical work on the program has been subdivided into four tasks: (1) Analysis, (2) Testing and Data Reduction, (3) RIL Support and Technical Assistance and (4) Acquisition and Application of Advanced Instrumentation.

The quarterly Progress Reports consist of two parts, the first is a description of activities and progress during the quarter in the technical tasks. This part is more informational in nature as results are presented as early as possible to expedite the dissemination of data and analyses. The second part is a discussion of a specific topic or topics important to meeting the overall program objectives. In this sense, the second part is a "mini-topical" which may include results of work completed during several quarters. This part is more interpretational in nature.

This report summarizes progress made on the program during the quarter ending September 30, 1979, for the individual technical tasks. Although progress is reported by task, it should be recognized that there is significant interaction between the tasks in both the scope and conduct of the research. A section discussing countercurrent flow air-water and steam-water tests in tubes is also included.

PART 1

Progress for the Quarter

July 1, 1979 - September 30, 1979

TASK 1.0 ANALYSIS

Objectives

The objectives of this task are to:

- (1) Develop an improved theoretical understanding of steam-water interaction phenomena,
- (2) Analyze and correlate the experimental data obtained from the studies conducted under Task 2.0,
- (3) Evaluate and interpret experimental data from offsite steam-water mixing experimental efforts, and
- (4) Use this knowledge to verify and improve current LOCA/ECC analysis methods.

Work During Quarter

During this quarter we analyzed results from high bypass air-water tests and from low subcooling steam-water tests in the 2/15-scale model, continued development of a mechanistic model for ECC penetration, and analyzed results from steam-water tests in the simple tube facility.

Analysis of High Bypass Air-Water Tests in the 2/15-Scale Model

Nominal operating conditions for 2/15-scale high bypass air-water tests are listed in Table 1. The operating conditions were selected to study penetration dependence on ECC water injection rate and temperature. The tests were conducted in the plenum fill mode with the oversized break leg and with VDM probes in the annulus. The penetration data are plotted in Figures 1 through 6 and are listed in Table A-1.

Temperature and Flow Rate Effects. Examination of Figures 1 through 3 reveals that for low-to-medium reverse core air flows the penetration to the lower plenum is dependent upon ECC water temperature. The

TABLE 1. AIR-WATER PLENUM FILL TEST MATRIX--NOMINAL CONDITIONS

Test No.	Model Pressure kPa	ECC Water Temp., C	ECC Water Injection Flow Rate, gpm	J* Lin	J* g
1	Minimum of 136 kPa-Maximum pressure dependent on operating conditions	70	250	0.064	air flows to span range from full penetration to full bypass
2		135	250	0.064	
3		210	250	0.064	
4		70	380	0.098	
5		135	380	0.098	
6		210	380	0.098	
7		70	480	0.120	
8		135	480	0.120	
9		210	480	0.120	

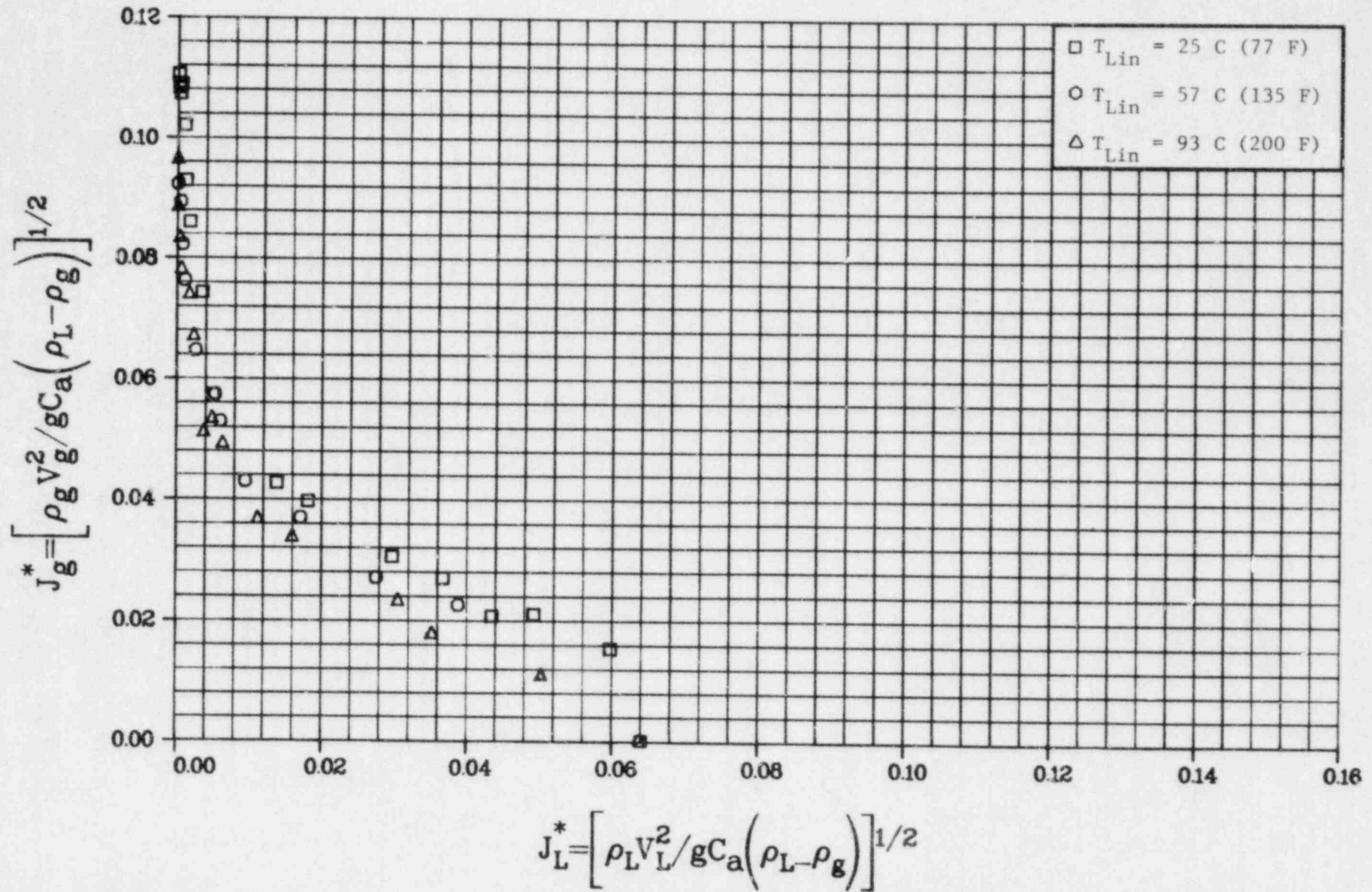
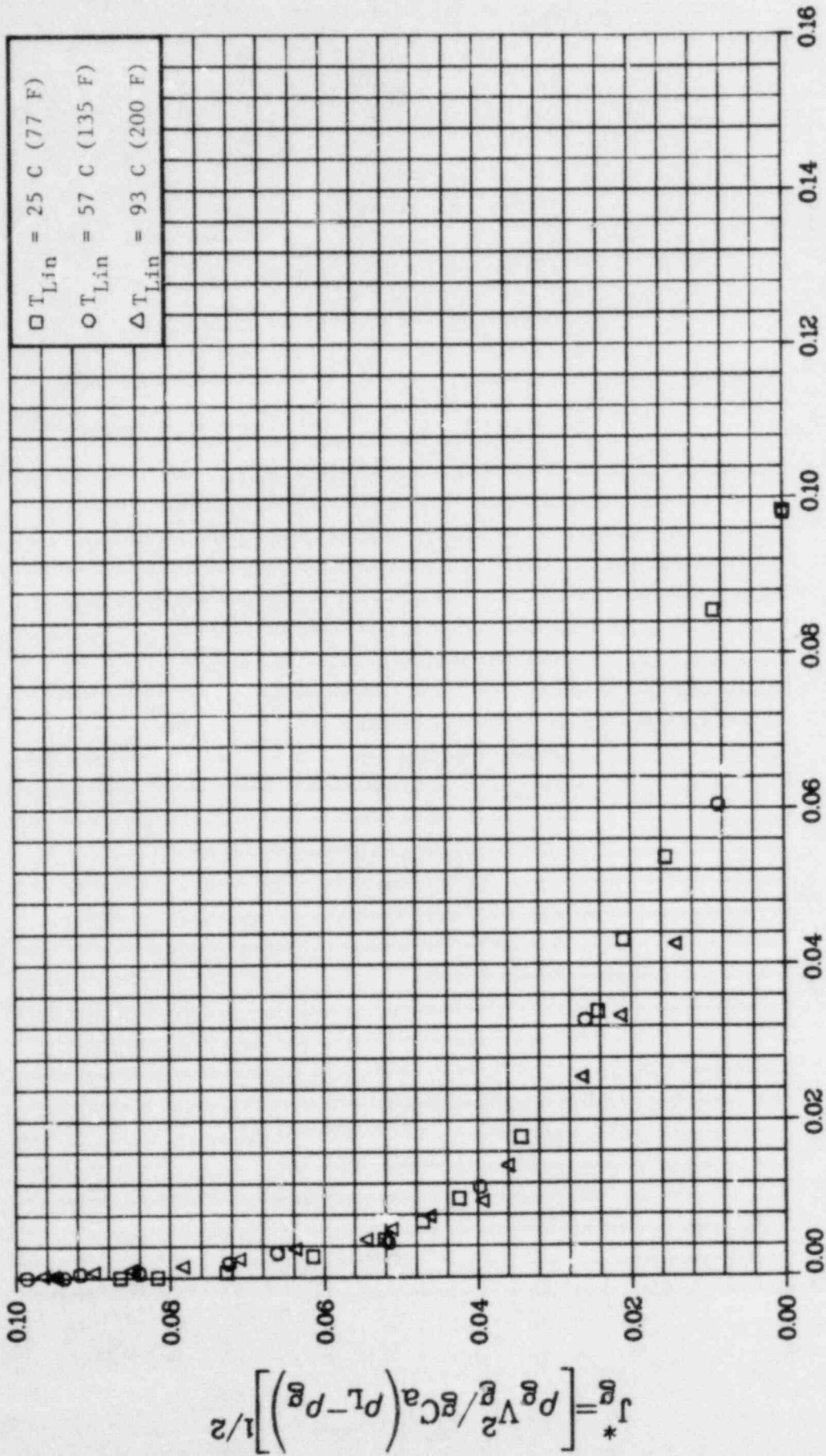


FIGURE 1. AIR-WATER PLENUM FILL PENETRATION DATA OBTAINED WITH $J_{Lin}^* = 0.064$ AND $P_V = 170 \text{ kPa (25 psia)}$



$$J_L^* = \left[\rho_L V_L^2 / g C_a (\rho_L - \rho_g) \right]^{1/2}$$

FIGURE 2. AIR-WATER PLENUM FILL PENETRATION DATA OBTAINED

WITH $J_{Lin}^* = 0.098$ AND $P_v = 170\text{ kPa (25 psia)}$

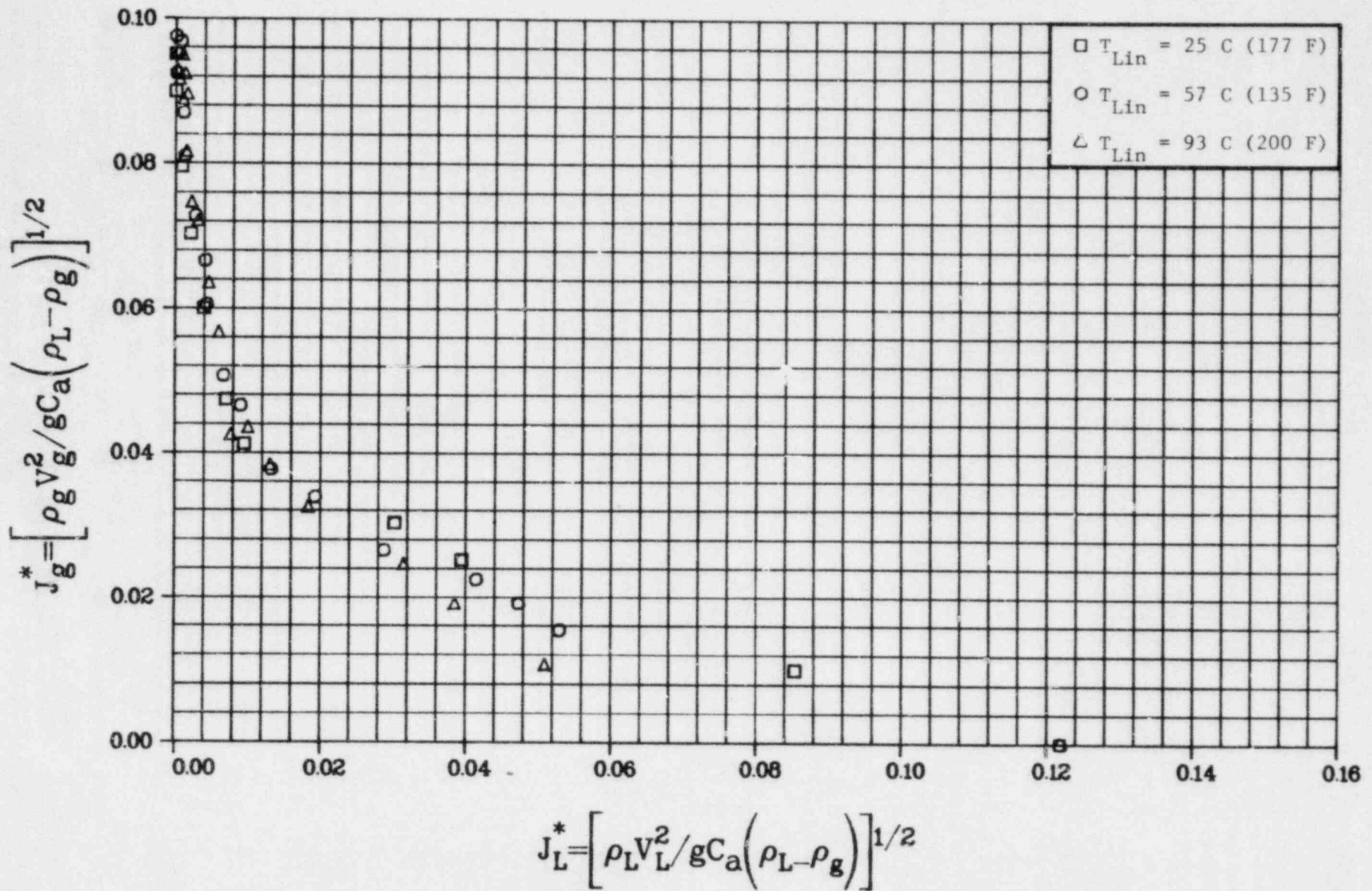
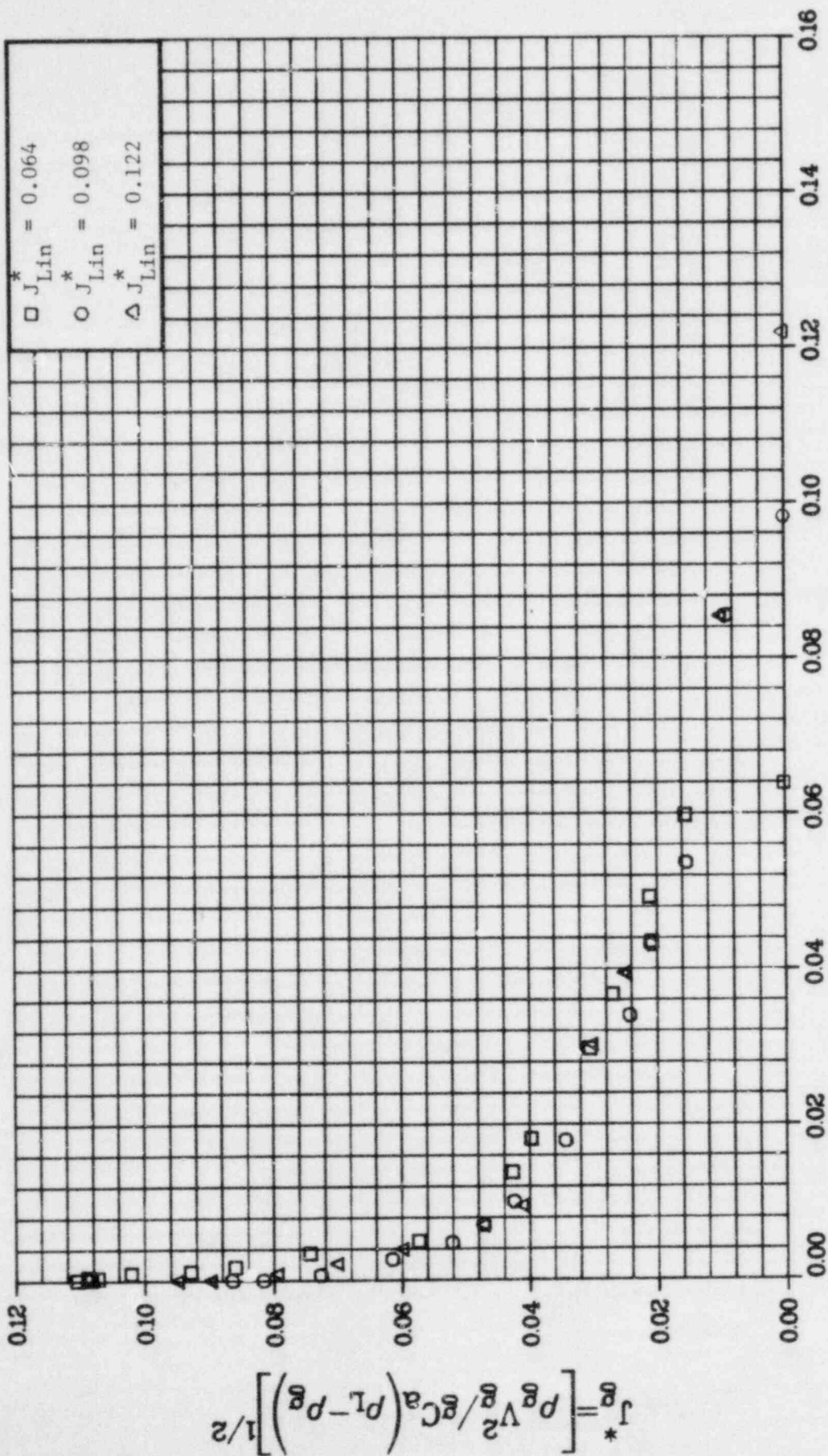


FIGURE 3. AIR-WATER PLENUM FILL PENETRATION DATA OBTAINED WITH $J_{Lin}^* = 0.122$ AND $P_v = 170 \text{ kPa (25 psia)}$



$$J_L^* = \left[\rho_L V_L^2 / g C_a (\rho_L - \rho_g) \right]^{1/2}$$

FIGURE 4. AIR-WATER PLENUM FILL PENETRATION DATA OBTAINED

WITH $T_{Lin} = 25 \text{ C (77 F)}$ AND $P_V = 170 \text{ kPa (25 psia)}$

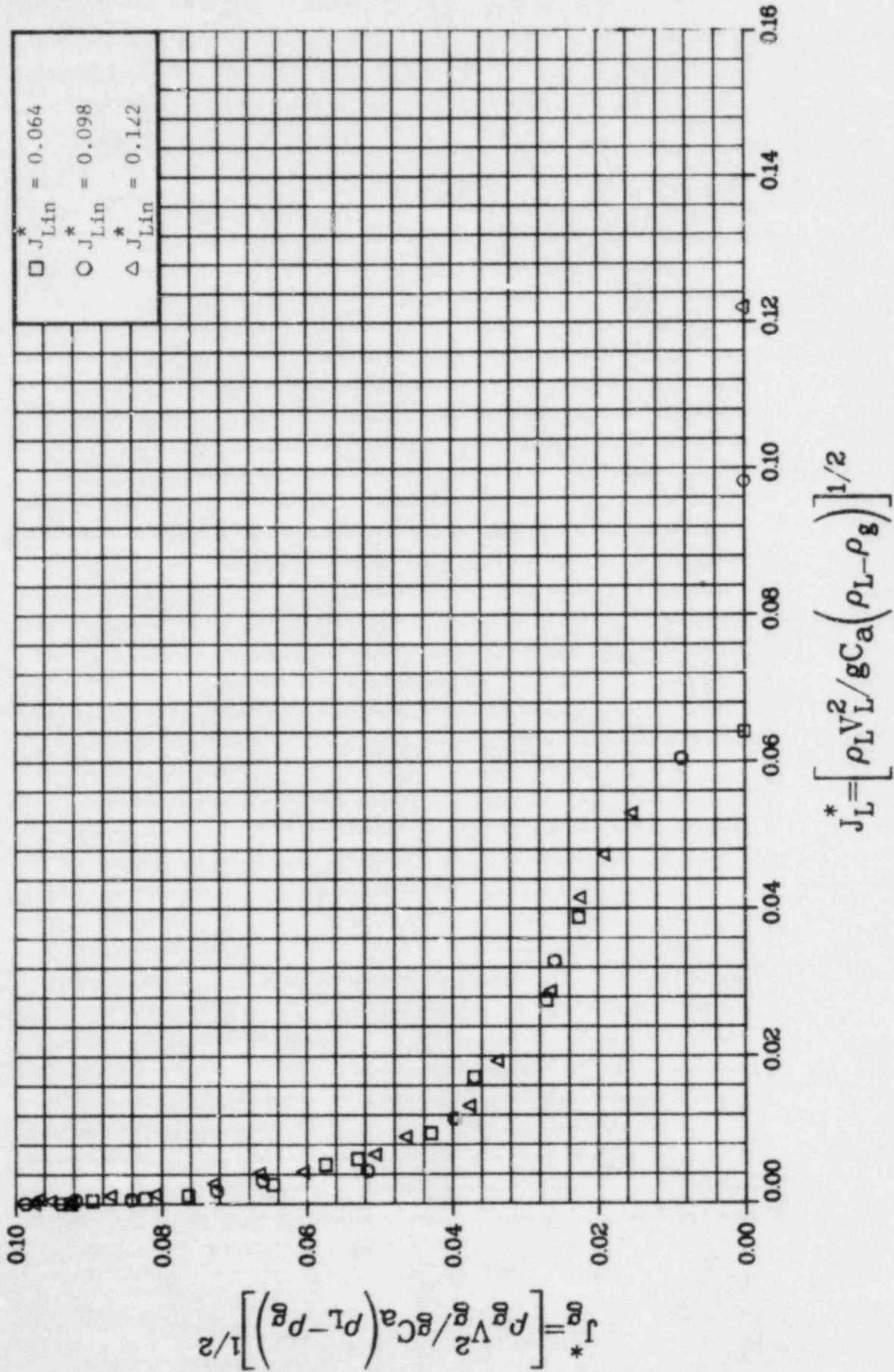


FIGURE 5. AIR-WATER PLENUM FILL PENETRATION DATA OBTAINED WITH $T_{Lin} = 57$ C (135 F) AND $P_V = 190$ kPa (28 psia)

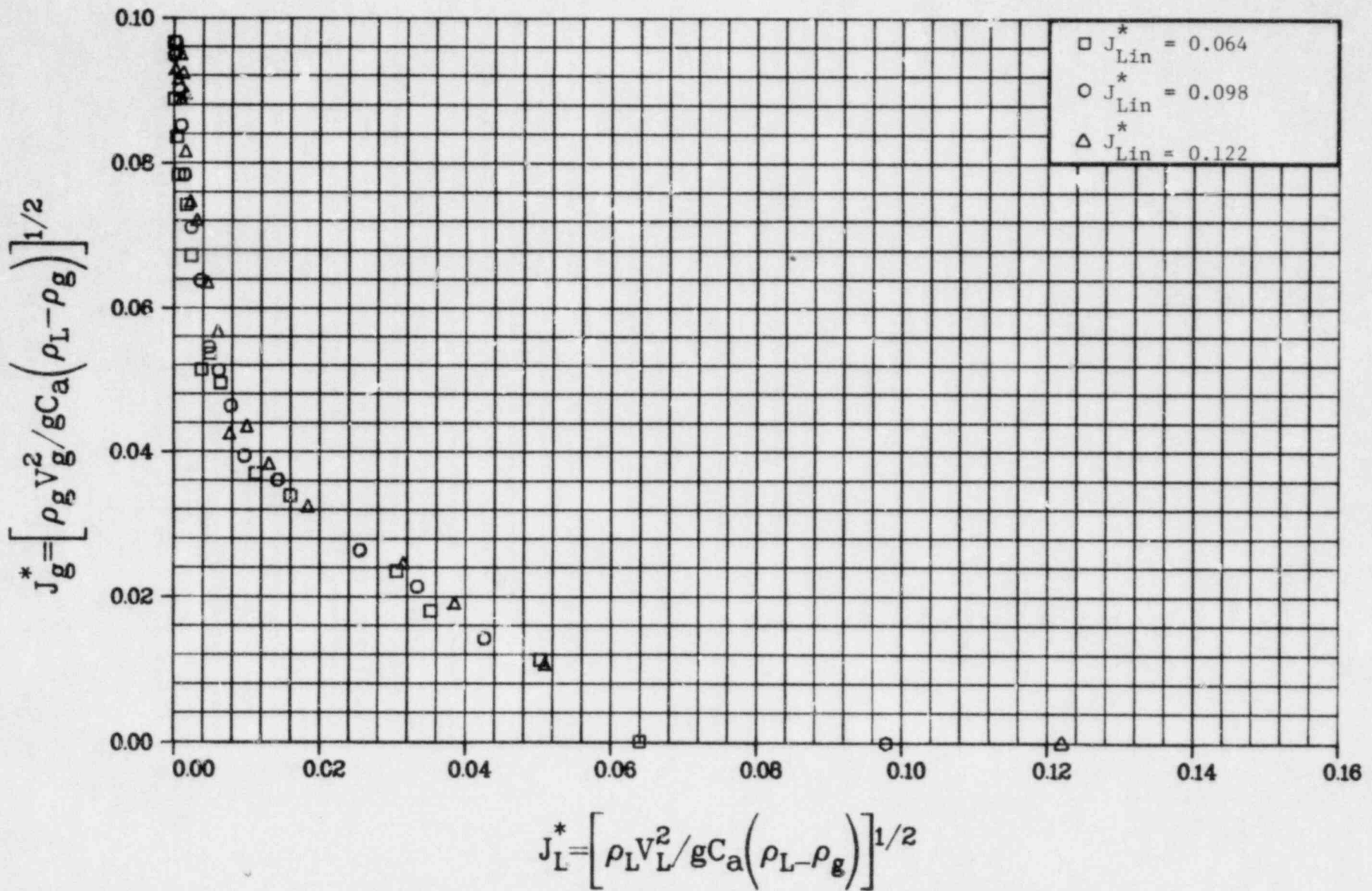
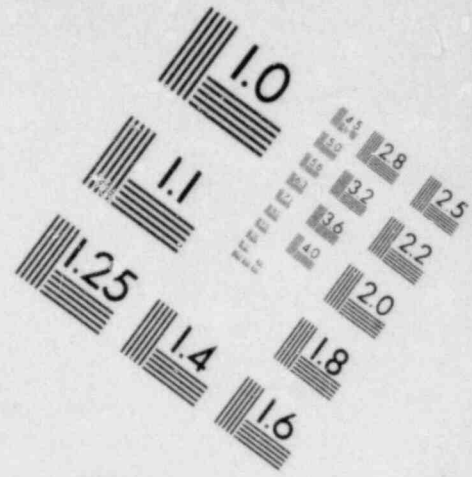
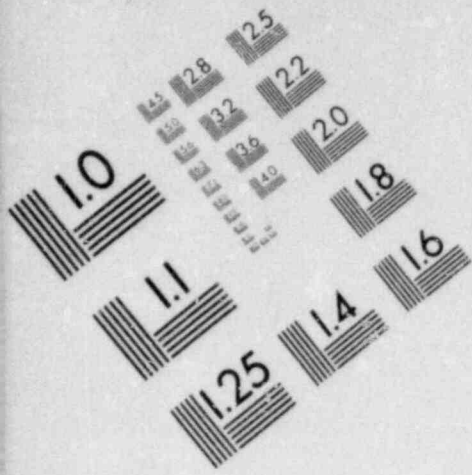
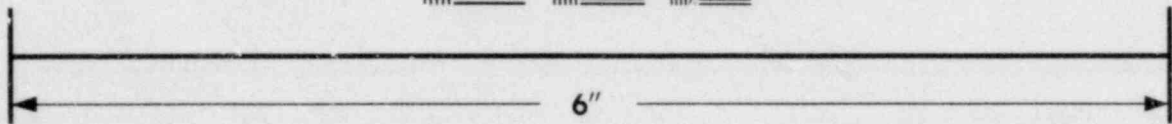
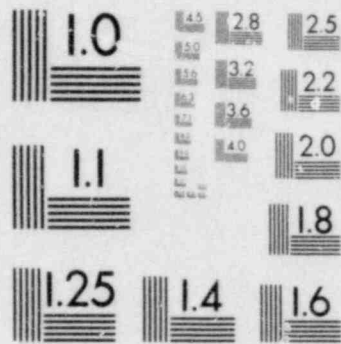


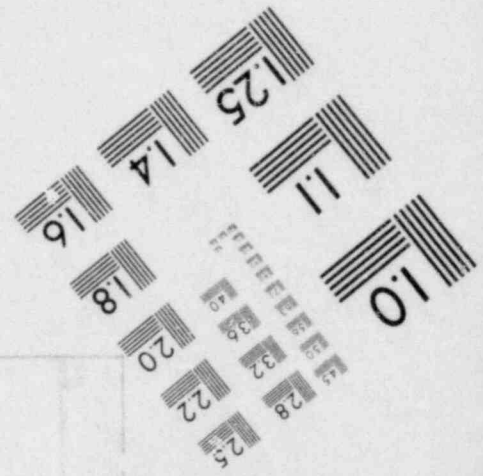
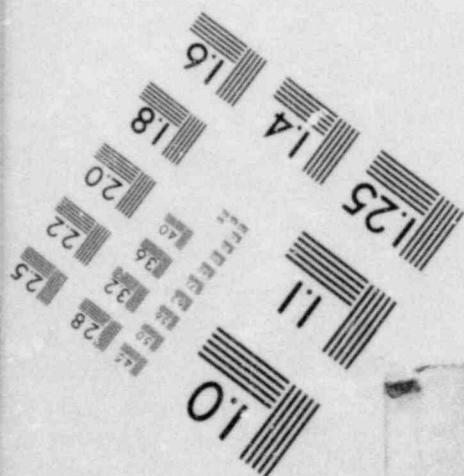
FIGURE 6. AIR-WATER PLENUM FILL PENETRATION DATA OBTAINED
 WITH $T_{Lin} = 93$ C (200 F) AND $P_V = 204$ kPa (30 psia)



**IMAGE EVALUATION
TEST TARGET (MT-3)**



MICROCOPY RESOLUTION TEST CHART



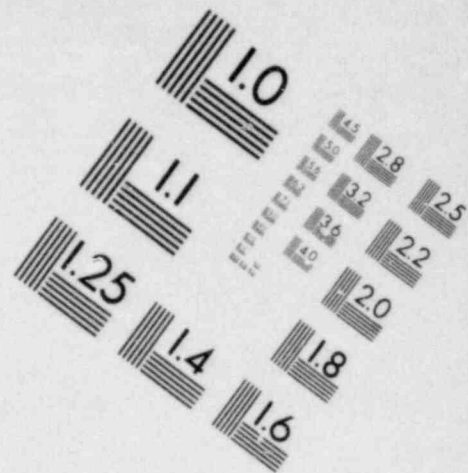
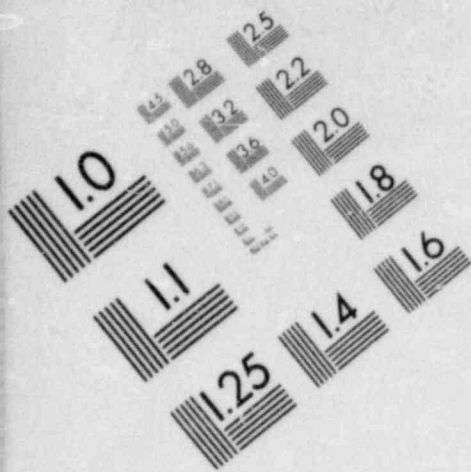
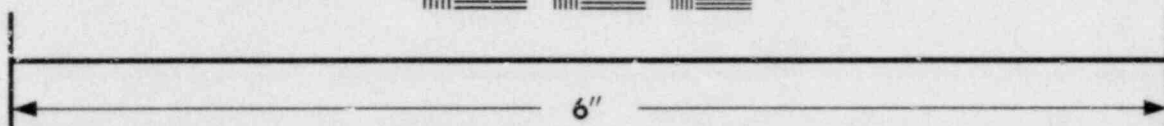
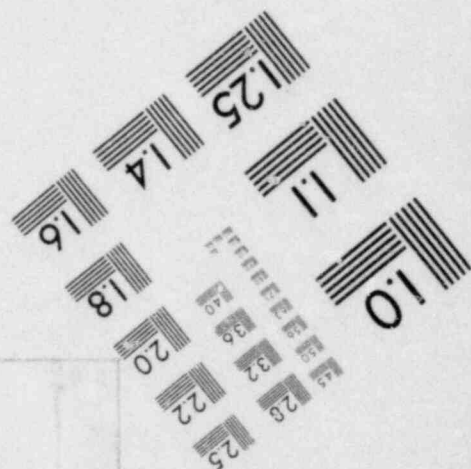
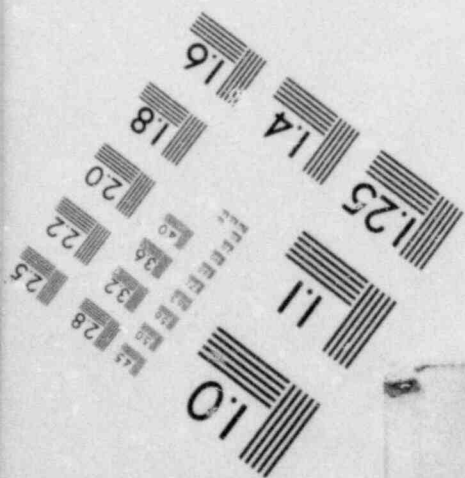


**IMAGE EVALUATION
TEST TARGET (MT-3)**



MICROCOPY RESOLUTION TEST CHART



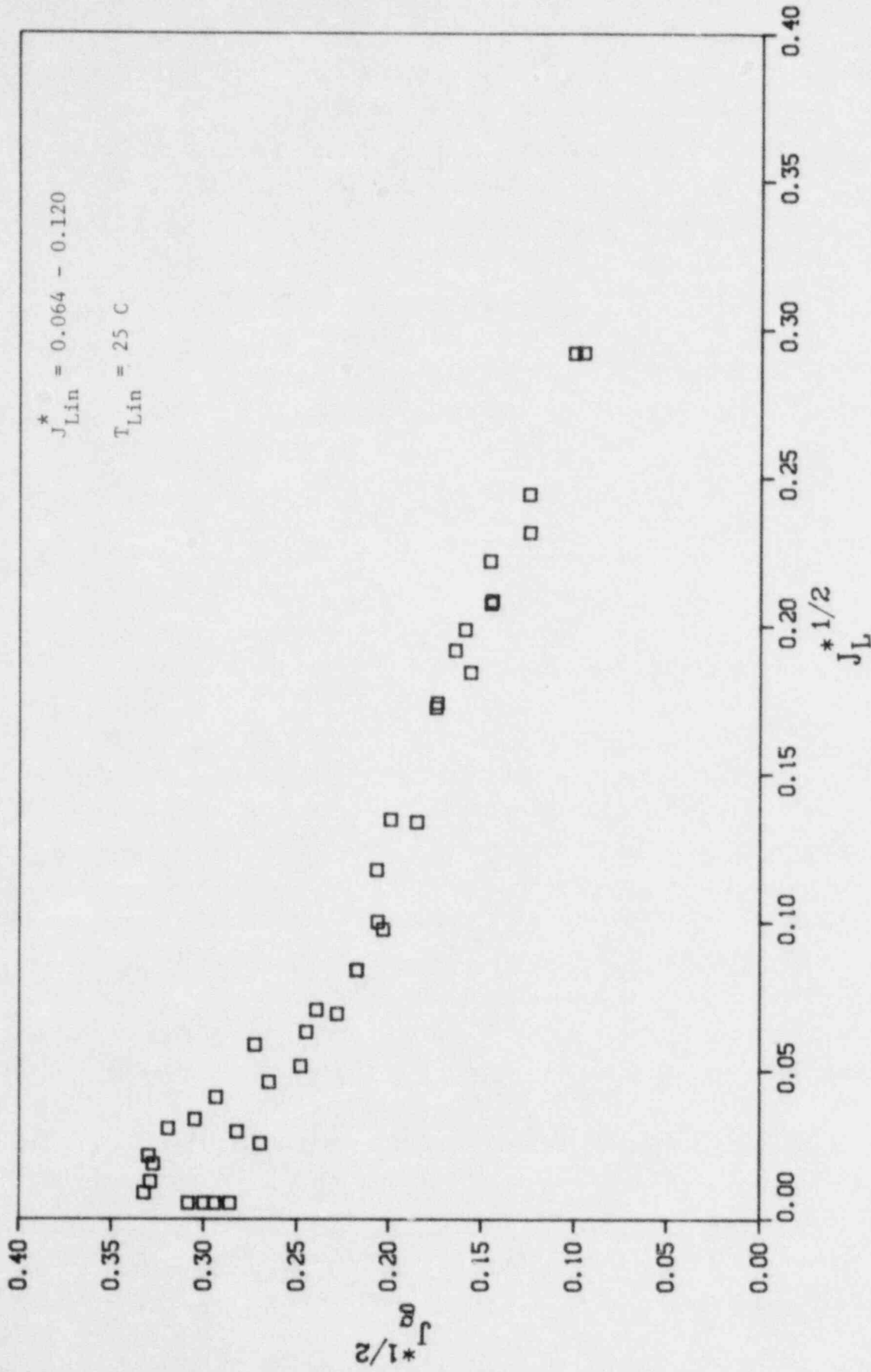
effect is observed for the three different injection rates tested. Specifically, increased ECC water temperature results in a decrease in penetration to the lower plenum. This behavior has been observed in 1/15-scale studies reported earlier (for example, see NUREG/CR-0565, BMI-2013, Appendix A). The decrease in penetration at higher water temperatures may be due to evaporated water vapor which increases the equivalent mass flow rate of the air. A more detailed discussion is presented below.

The data are replotted in each of Figures 4 through 6 for a constant water temperature and three injection flow rates. For these air-water flow rates the penetration rate is independent of the injected water flow rate. This 2/15-scale behavior is also consistent with the 1/15-scale data referenced above.

The data in Table A-1 were analyzed with the NLINMLE program using the Wallis correlation. The data and correlations are compared on $J^{*1/2}$ coordinates in Figures 7 through 9. The calculated fit parameters are given in Table 2. Examination of the parameters reveals that an increase in ECC water temperature results in an increase in the m and C values for the correlation.

Possible Effects of Evaporation on Air-Water Penetration Data. Both 1/15- and 2/15-scale data show that increased ECC water temperature decreases penetration to the lower plenum. This temperature effect is evident whether the data are plotted on J^* or K^* coordinates. The J^* parameter accounts for density changes with temperature while the K^* parameter contains both a density and surface tension term. Comparisons of the data using J^* and K^* parameters⁽¹⁾ show that the temperature effect is decreased when the K^* parameter is used, but the same trend of decreased penetration with increased water temperature can still be observed. These results indicate that surface tension and density variations with temperature are not the only water properties affecting penetration.

It has been suggested recently that the addition of evaporated water vapor to the reverse core air flow might explain the air-water temperature-dependent penetration. In the present 2/15-scale facility the temperature of the reverse core air entering the vessel is normally maintained within a


 FIGURE 7. DATA OF FIGURE 4 ON $J^{*1/2}$ COORDINATES

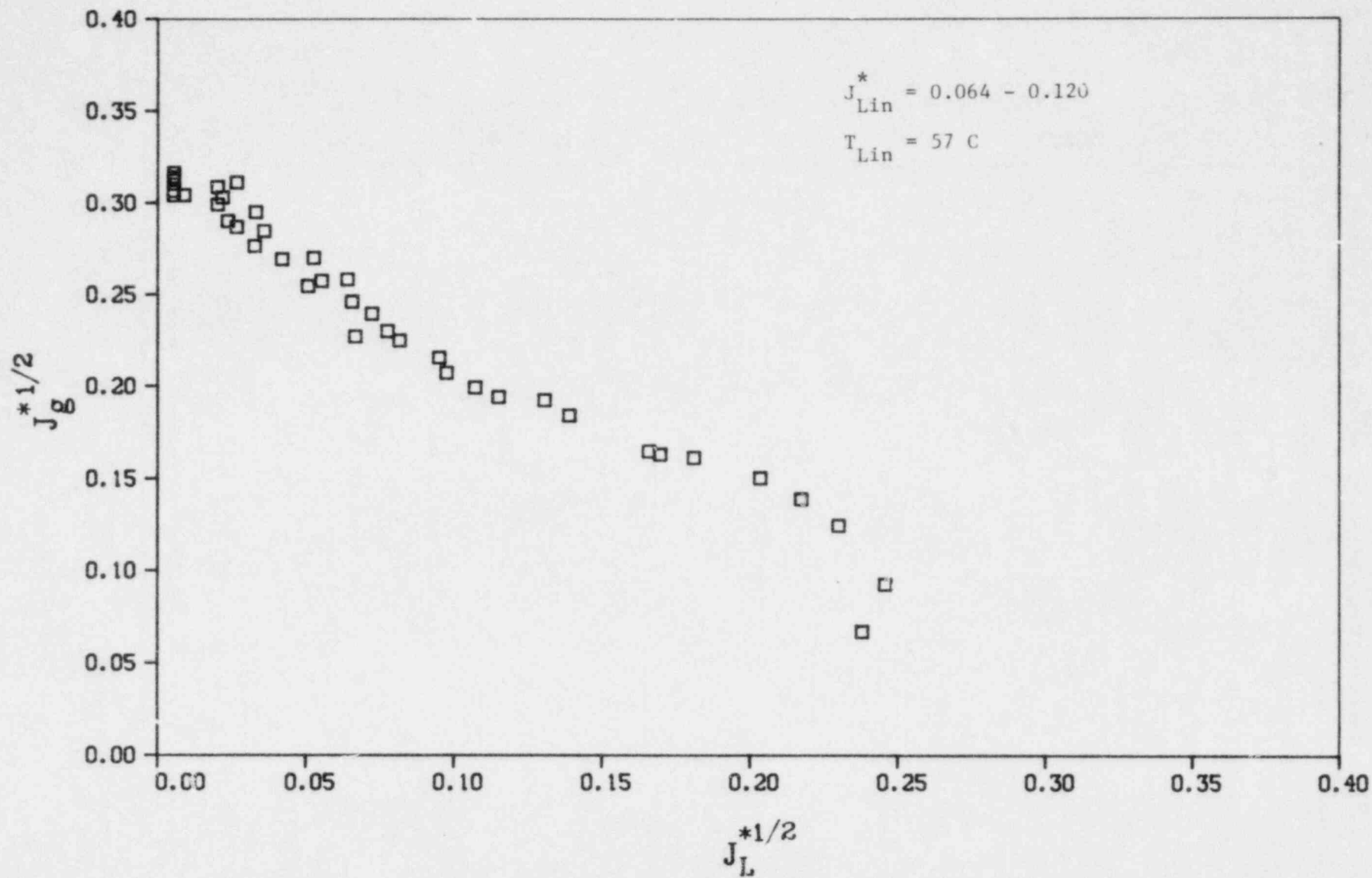


FIGURE 8. DATA ON FIGURE 5 ON $J^{*1/2}$ COORDINATES

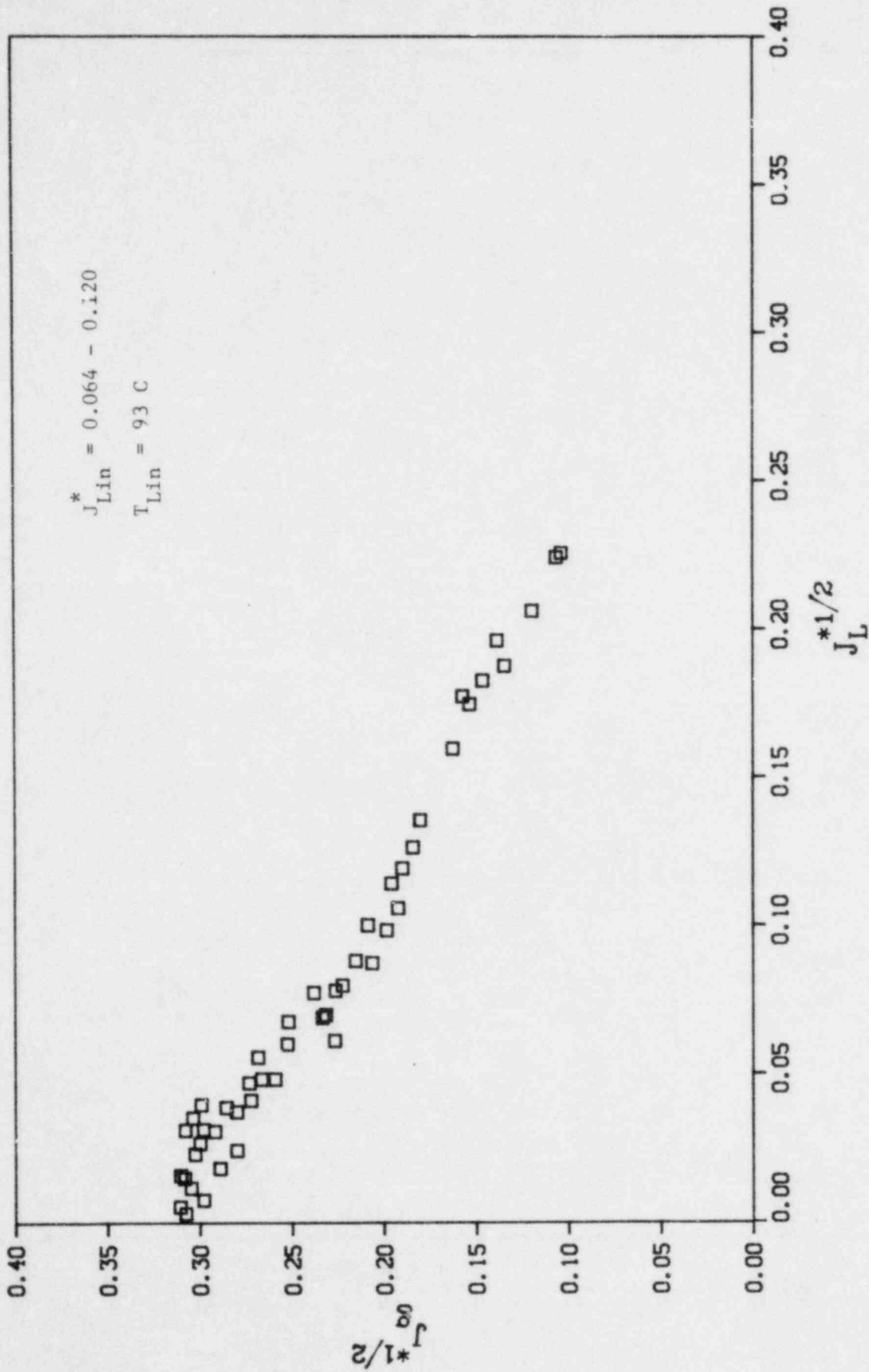


FIGURE 9. DATA OF FIGURE 6 ON $J^{*1/2}$ COORDINATES

TABLE 2. WALLIS CORRELATION PARAMETERS CALCULATED FROM 2/15-SCALE,
AIR-WATER PLENUM FILL TESTS--J* PARAMETERS

J_{Lin}^*	$P_V,$ kPa	$T_{Lin},$ C	m	C
0.064 - 0.120	170	25	0.7256 ± 0.0540	0.2970 ± 0.0079
0.064 - 0.120	190	57	0.9099 ± 0.0572	0.3124 ± 0.0064
0.064 - 0.120	204	93	0.9812 ± 0.0572	0.3154 ± 0.0059

narrow range (typically $25\text{ C} \pm 10\text{ C}$). If the injected ECC water temperature is higher than the inlet air temperature, the air temperature in the vessel can be expected to increase due to air-water heat transfer. The saturation humidity ratio of the air increases with air temperature. Humidity ratio is defined in this case in lb_m of water vapor per lb_m of dry air. Saturation implies the maximum amount of water vapor the air can hold at the ambient temperature and total pressure. The mass flow rate of the gas phase increases as the water evaporates. This additional mass is not taken into account in the present method of calculating the dimensionless air flow rate, J_g^* . Therefore, the additional bypass observed in heated water-air tests could be caused by the effects of ECC water evaporation.

During the series of tests presented in this report an attempt was made to determine if evaporation could cause the temperature dependent effect reported previously. Tests were carried out with air only to calibrate the pressure drop in the exhaust line of the pressure suppression tank as a function of known gas flow rate. The flow coefficient defined by this calibration procedure was used along with the measured pressure drop in the exhaust line during air-water tests to determine air-water vapor mass flow rates out of the suppression tank.

Results from sample calculations are illustrated in Table 3, for tests at three different injected water temperatures. This table includes the injected liquid and air temperatures, T_{Lin} and T_{gin} respectively, the measured air flow rate into the model, W_{gin} , the suppression tank pressure, P_c , and the measured pressure drop in the exhaust line, ΔP_{meas} . The calculated pressure drop for the measured flow rate of dry air at T_{Lin} and T_{gin} is shown as ΔP_{dry} . Similarly, the calculated pressure drop for saturated air at the two temperatures is listed as ΔP_{sat} .

Comparison of the measured and calculated pressure drops indicates that for low liquid temperatures (Test 25256) the measured pressure drop lies in the range calculated for dry air, or in the range of partly saturated air at the liquid temperature. For the intermediate liquid temperature (Test 25270) it is clear that the air must be at least partly saturated at the liquid temperature or possibly fully saturated at some temperature between the air and water injection temperatures. The high liquid injection temperature case shows similar results.

TABLE 3. EFFECTS OF EVAPORATION FOR THREE
INJECTED WATER TEMPERATURES

Test ID	T_{Lin} , T_{gin} , °F	W_{gin} , lb _m /sec	P_c psia	ΔP_{meas} , psid	ΔP_{dry} , psid	ΔP_{sat} , psid	T_{calc} , °F	μ_{calc} , %	W_{gout} , lb _m /sec	J_{gin}^*	J_{gout}^*
25256	73 110	2.29	23.81	9.39	8.98 9.55	9.44 11.08	90	20	2.30	0.090	0.089
25270	137 110	2.28	25.83	11.41	9.73 9.28	13.55 10.77	130	50	2.55	0.087	0.101
25356	197 110	2.34	32.44	18.02	8.75 7.59	92.10 8.81	175	44	2.88	0.082	0.112

The calculated gas temperature, T_{calc} , and the calculated relative humidity, μ_{calc} , are consistent with the measured values of W_{gin} and ΔP_{meas} for the measured exhaust line flow coefficient. The calculated mass flow rate of moist air leaving the suppression tank is shown as W_{gout} . The dimensionless gas flow rates which correspond to W_{gin} and W_{gout} , J_{gin}^* and J_{gout}^* , are also tabulated. Comparison of the J^* values for the three tests illustrates the effect of evaporation of water into the countercurrent flowing air. Comparing the J_{g}^* values determined in the usual way we note that J_{g}^* decreases slightly (due to pressure effects) as the liquid injection temperature is increased. The reverse is true when the effective J_{g}^* values, which account for moisture addition to the air, are compared. For the hot water test the effective J_{g}^* is increased from 0.082 to 0.112. Such an increase is entirely sufficient to compensate the apparent downward shift of penetration curves for air-hot water tests.

It seems quite clear that the dependence of penetration on temperature in air-water tests could be accounted for by using a dimensionless gas flow rate which includes the moisture evaporated from the penetrating liquid. This would be similar to the way in which condensation is treated in analyses of steam-cold water experiments.

Comparison With Earlier Air-Water Data. The overall trends obtained from the 2/15-scale tests are virtually identical to those obtained from 1/15-scale studies. However, Figure 10 shows that the penetration data from the two different scale models do not overlay when they are plotted on J^* coordinates. The 2/15-scale data lie below and to the left of the 1/15-scale data. The 1/15-scale data are from two different test series and appear to be on a single curve. Both these 1/15-scale series were conducted in the plenum fill mode and in identical geometries. In contrast, the 2/15-scale data from two different series form two different curves. The earlier 2/15-scale data (reported in NUREG/CR-0526, BMI-2011, Table A-3) were conducted in the quasi-steady-state mode and without VDM probes inserted in the annulus. These data lie above and to the right of the recent 2/15-scale data which were run in the plenum fill mode with VDM probes in place. The earlier data indicate a higher penetration rate for a given reverse core air flow rate.

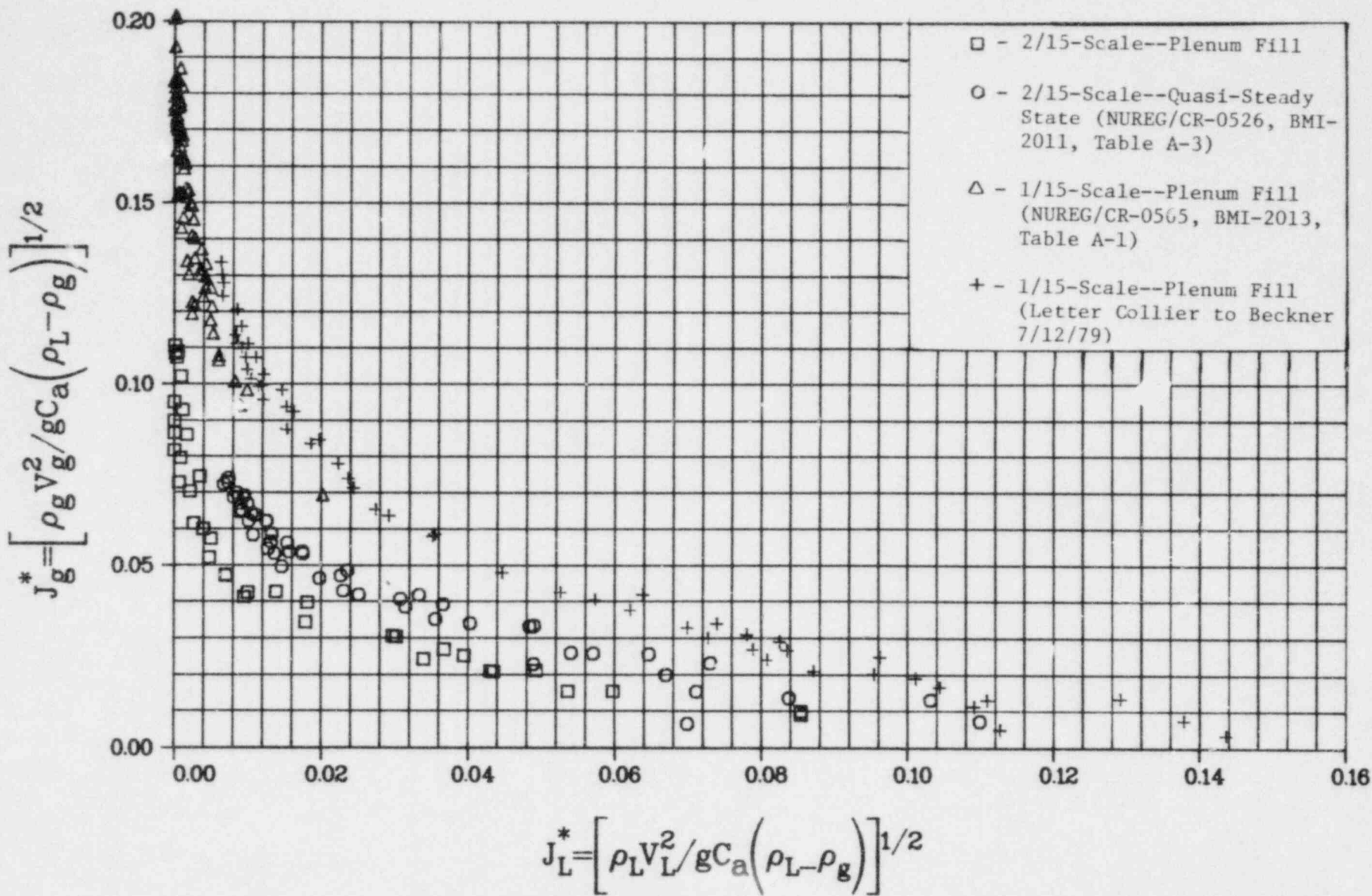


FIGURE 10. COMPARISON OF 1/15 - AND 2/15-SCALE AIR-WATER PENETRATION DATA - $J_{Lin}^* = 0.064 - 0.150$, $T_{Lin} = 25 \text{ C (77 F)}$

When the 2/15-scale data from the two test series were first compared, several possible explanations for the differences in the data sets were investigated:

- 1) Instrument error or miscalibration, particularly of a key instrument such as the gas flow meter, could cause an apparent shift in the penetration curve.
- 2) An error in the data reduction program which converts voltages from the instruments into data in engineering units, and carries out time averages of the data could cause a similar result.
- 3) To obtain complete bypass data for the recent series of 2/15-scale tests an additional air compressor was brought in from an outside source. If the air from this compressor included an excessive amount of oil the surface tension would be changed and could cause the apparent shift in the penetration curve.
- 4) A difference in the lower plenum penetration behavior between the quasi-steady-state and plenum fill test modes might explain the difference.
- 5) A difference in the penetration due to the presence of the VDM probes might also cause the observed behavior.

Review of these possible causes began with recalibration of the key instruments against independent measurements. All were found to be accurate within their previously stated tolerances, with the exception of two of the ECC water turbine flow meters which read approximately 6% low. Since penetration has been shown to be insensitive to injected water flow rate (see Figures 4 through 6) the lower than nominal water injection rate cannot explain the shift in penetration curves.

To investigate the next three possibilities additional tests were conducted using the BCL house air supply only. For these tests, voltages from flow, pressure, and temperature measuring instruments were recorded on strip chart recorders as well as with the data acquisition system. Plenum fill and quasi-steady-state tests were conducted for each air flow. The results of these tests are listed in Table A-1, Tests 25702 to 25729. Voltages converted to engineering units by hand calculation from the strip charts were

identical with the computer results listed in Table A-1. Figure 11 is a plot of these penetration data and shows that the quasi-steady-state and plenum fill test results agree closely. The curves of Figure 11 also overlay well with those of Figure 4, an indication that the data are reproducible and, consequently, the properties such as surface tension were not varied between the tests. Note that the data in Figure 11 do not extend across the whole range of penetration because of the limitations of the BCL house air supply.

To investigate the fifth possibility, the VDM probes were removed from the annulus and replaced with plugs. The results of the air-water tests conducted with the VDM probes removed are plotted in Figures 12 and 13 and the data are listed in Table A-1, Tests 25902 to 26014. In these figures, the data obtained with the VDM probes removed are compared to data from the recent air-water tests which had the VDM probes in the annulus and the earlier 2/15-scale data which were obtained with a smooth annulus. The data taken with the probes removed lie substantially above the data taken with the probes in, indicating that the presence of the VDM probes in the annulus was an important cause of the discrepancy between earlier and current data. We also note that the data taken with the probes removed lie somewhat below the earlier data, indicating that the probes themselves do not account for all the disturbance. In fact, when the probes were removed the 5/8" diameter mounting holes in the vessel were plugged with simple pipe plugs which were not flush with the inner surface of the vessel wall, thus the vessel wall was not smooth even when the probes were removed.

Visual studies of air-water flows at 1/15-scale have shown that the water tends to flow down the annulus walls in films with an air core in the center of the annulus. Bypass occurs when the interfacial momentum exchange is large enough to shear off droplets which are then entrained or when it is high enough to carry a portion of the bulk liquid to the break, possibly through wave interaction. Disturbance of the film surface by probes or mounting holes will cause droplet formation and wave generation at lower gas flow rates than would be seen with a smooth annulus.

The data of Figures 12 and 13 support this view of the physics. When both probes and mounting holes were present, the disturbance of the film was the largest and the penetration at a given gas flow rate was the

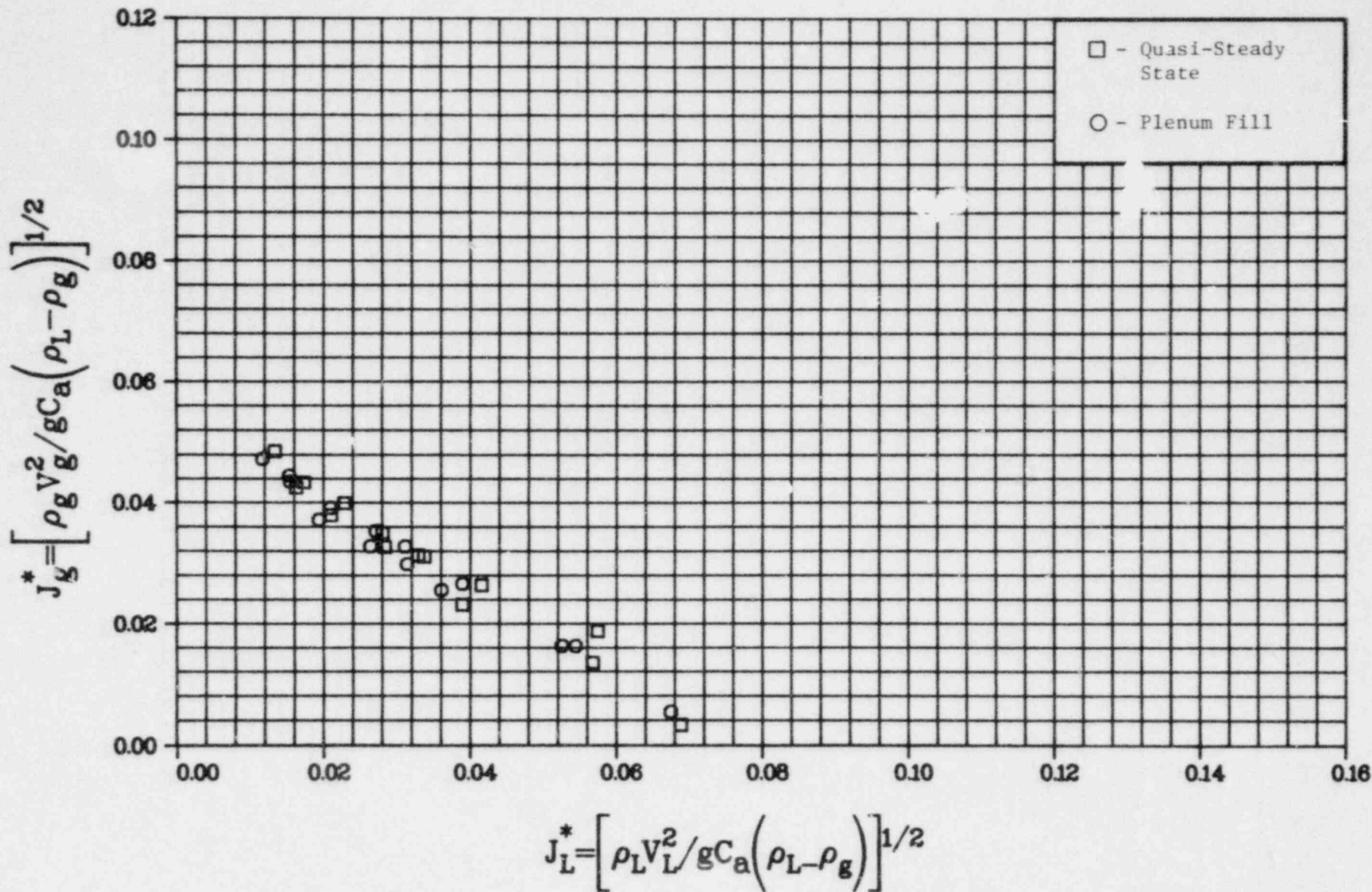


FIGURE 11. COMPARISON OF QUASI-STeady STATE AND PLENUM FILL AIR-WATER PENETRATION DATA OBTAINED WITH $J_{Lin}^* = 0.064$ AND 0.098 AND $T_{Lin} = 27$ C (82 F) - VDM PROBES IN ANNULUS

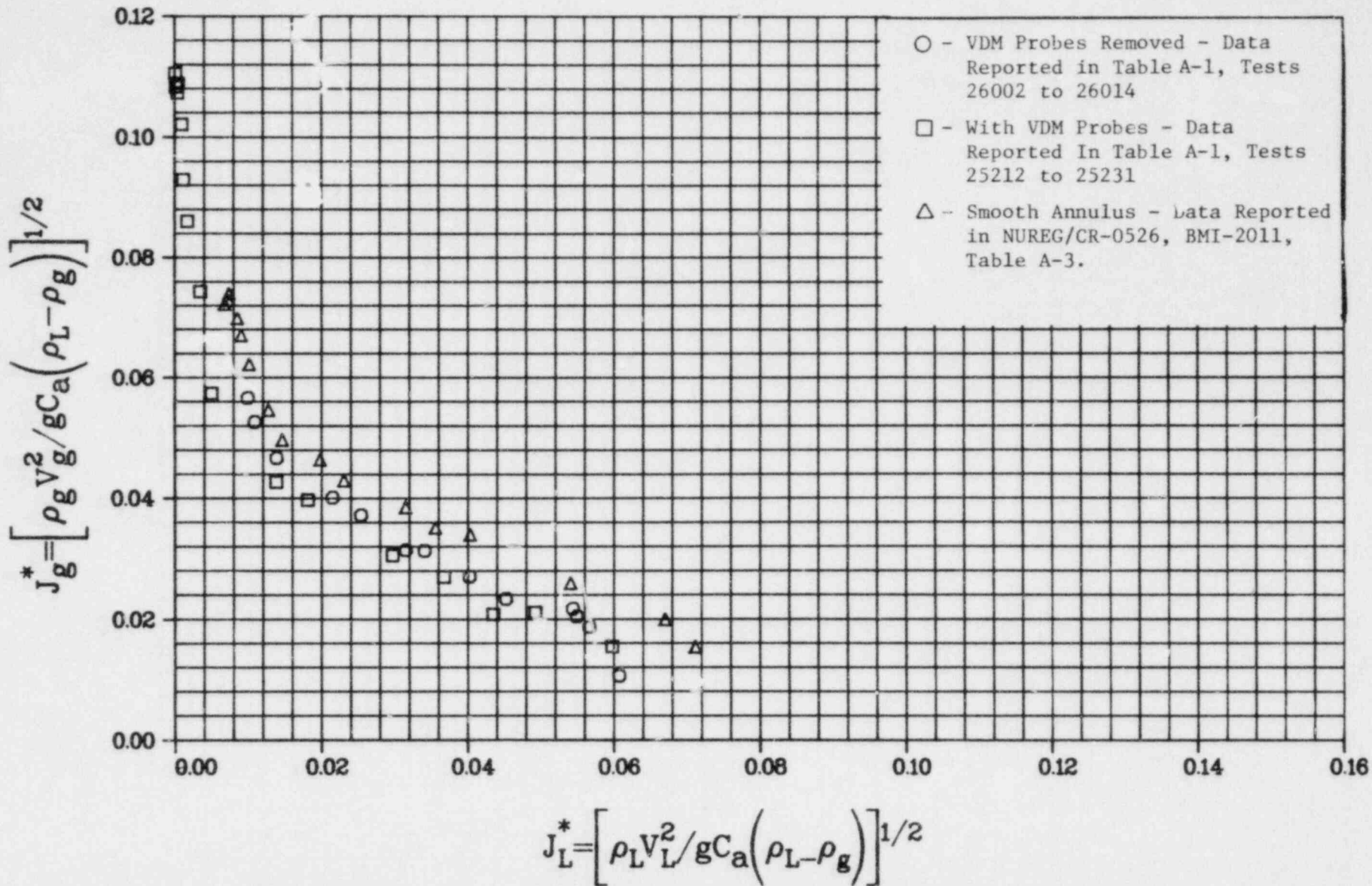


FIGURE 12. COMPARISON OF 2/15-SCALE AIR-WATER PENETRATION DATA OBTAINED WITH AND WITHOUT VDM PROBES IN THE DOWNCOMER ANNULUS - $J_{Lin}^* = 0.064$, $P_V = 153$ kPa (23 psia), $T_{Lin} = 27$ C (80 F)

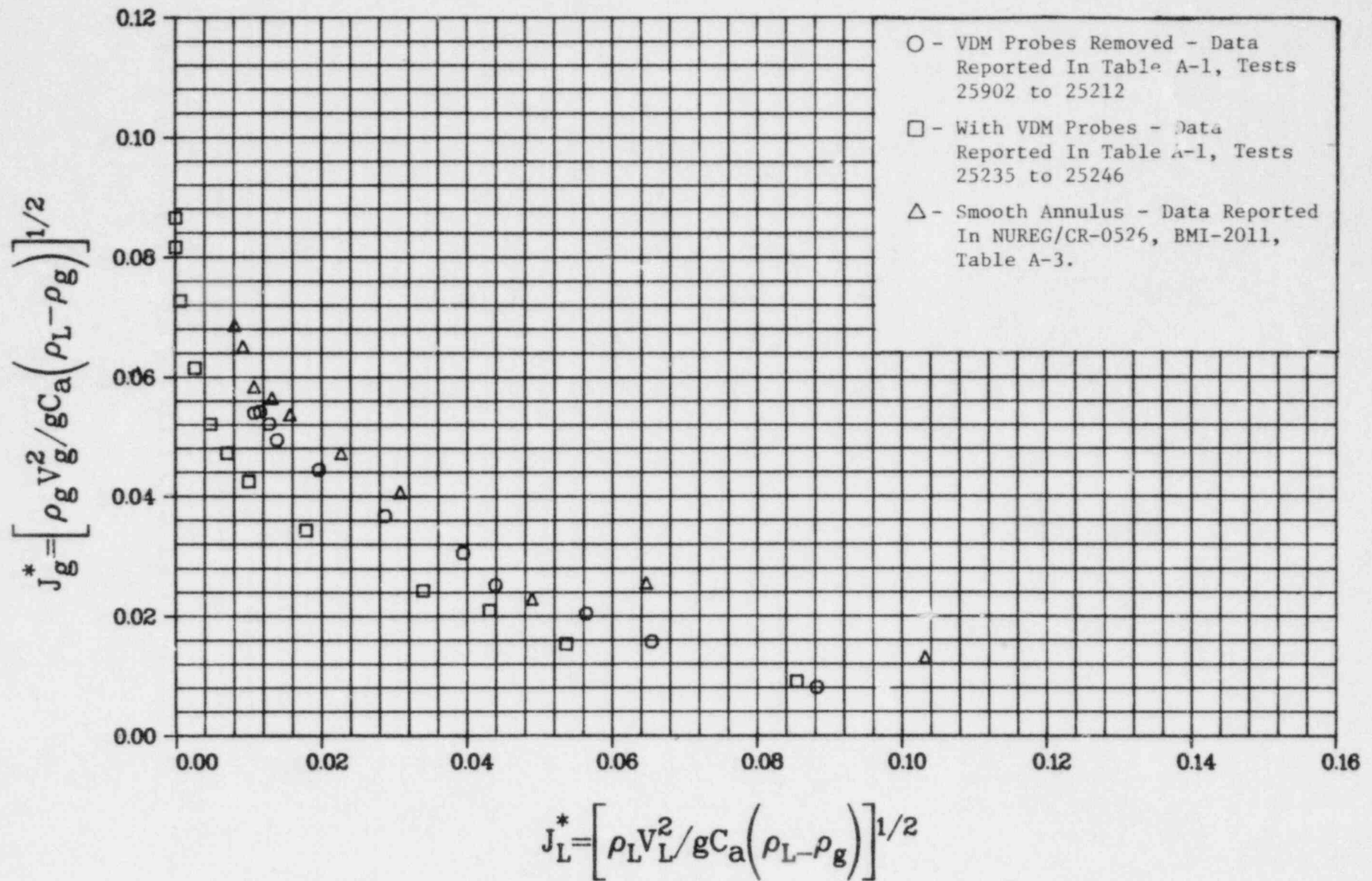


FIGURE 13. COMPARISON OF 2/15-SCALE AIR-WATER PENETRATION DATA OBTAINED WITH AND WITHOUT VDM PROBES IN THE DOWNCOMER ANNULUS - $J_{Lin}^* = 0.098$, $P_V = 153$ kPa (23 psia), AND $T_{Lin}^* = 27$ C (80 F)

least. When the probes were removed and the mounting holes remained the disturbance was less and the penetration at the given gas flow rate increased. Finally, for the earlier data taken with a smooth annulus the disturbance was minimized and the penetration maximized.

The displacement of the penetration curves with VDM probes in place complicates the direct application of the high bypass air-water data, for example, to the determination of the complete bypass point in the absence of condensation. However, a useful application can be made after correcting the data for VDM probe effects. Figures 14 and 15 illustrate this correction. The high bypass data (with VDM probes) and smooth annulus data of Figure 13 are replotted on $J_g^{*1/2}$ coordinates in Figure 14. The NLINMLE program has been used to evaluate m and C for both data sets. The slopes of the straight lines fit to the two data sets are virtually identical (either lies within the confidence interval of the other). The intercept value C for the high bypass data is lower than that of the smooth annulus data.

We can account for the downward shift of the data taken with the probes in place by adding a fixed amount, equal to the difference in the C values for probes in place and smooth annulus cases, to the $J_g^{*1/2}$ value for each point in the high bypass data set. That causes the two data sets to overlay in their common region. This correction thus shifts the data taken at high bypass with VDM probes in place straight up on $J_g^{*1/2}$ coordinates. Figure 15 illustrates the result of such a correction.

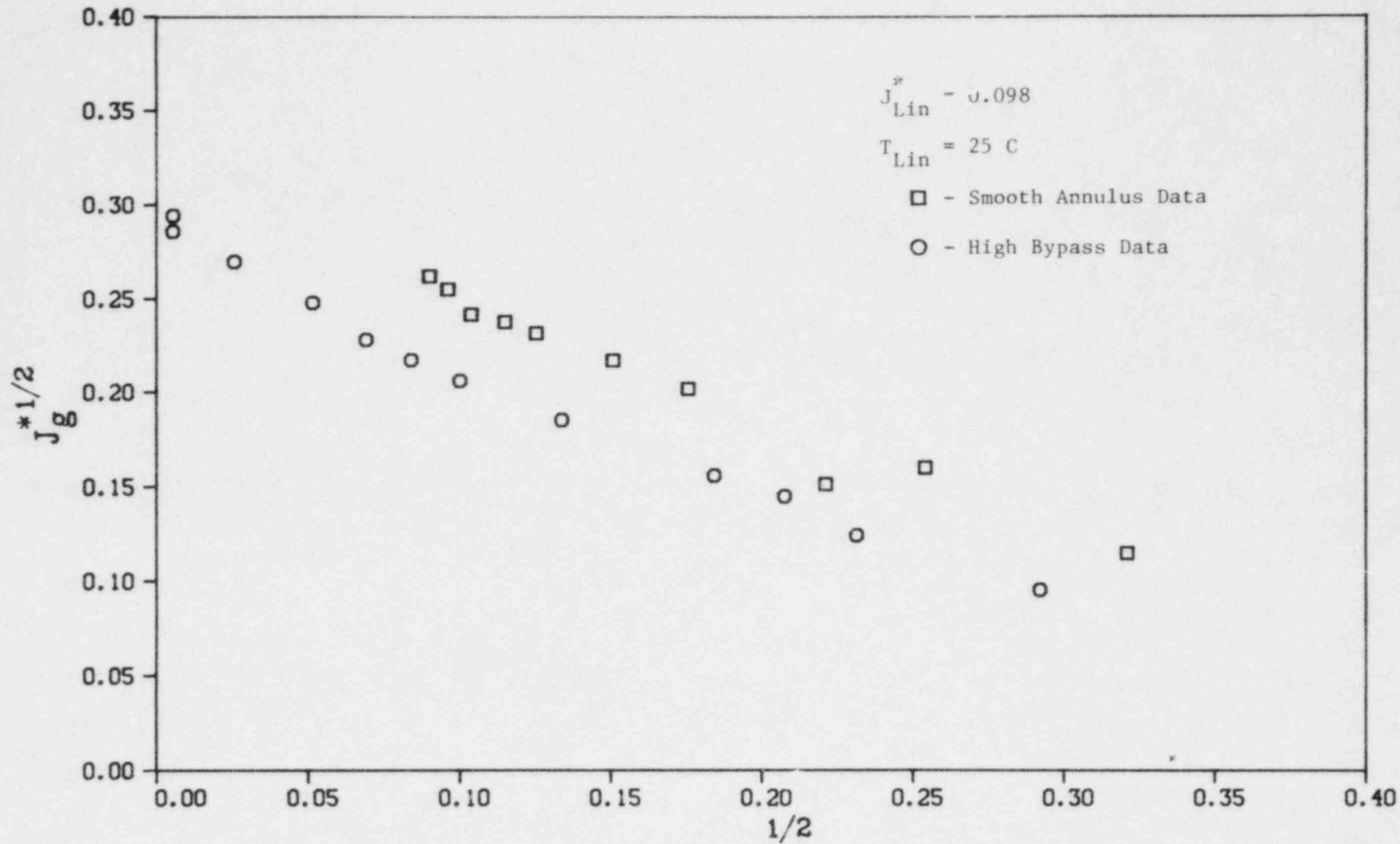


FIGURE 14. COMPARISON OF DATA WITH AND WITHOUT VDM PROBES IN ANNULUS ON $J^{*1/2}$ COORDINATES

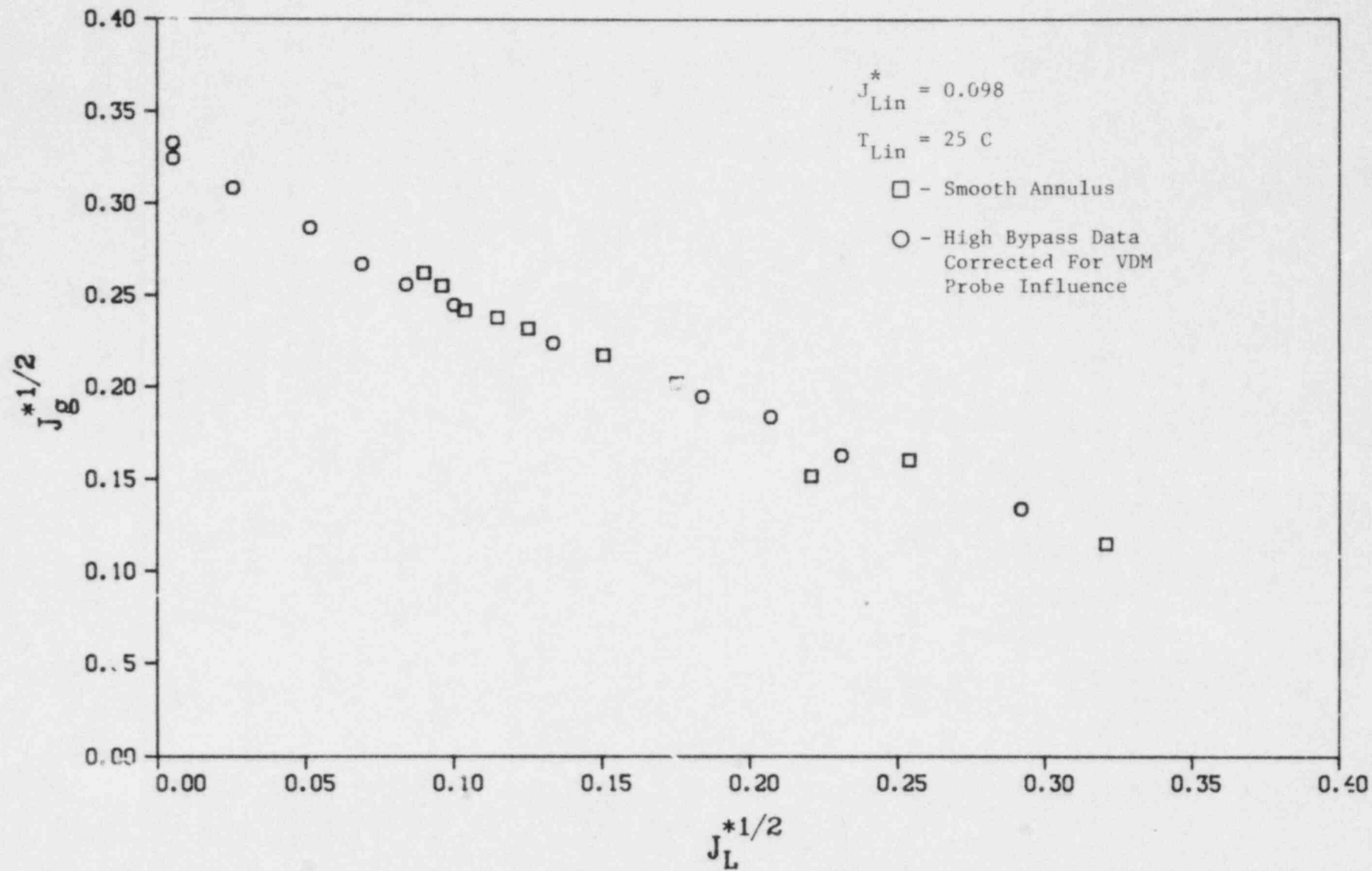


FIGURE 15. PENETRATION DATA CORRECTED FOR VDM PROBE INFLUENCE

Results of Low Subcooling Steam-Water Tests in the 2/15-Scale Model

Nominal operating conditions for low subcooling steam-water penetration studies in the 2/15-scale model with the standard core barrel are given in Table 4. The objective of these tests was to gather plenum fill data at low subcooling conditions. The penetration data are plotted in Figures 16 through 18 and listed in Table A-2.

Pressure, Flow Rate, and Test Mode Effects. Figure 16 presents data obtained with the ECC injection flow rate and water temperature constant and the model pressure as a variable. This figure shows that, at a constant reverse core steam flow rate, the penetration increases with model pressure. The pressure increase causes more steam to condense, thereby decreasing the amount of steam available to cause bypass. Since condensation decreases the effective steam flow, a greater amount of core steam is needed to bypass a given amount of ECC water as pressure is increased.

Figure 17 shows data obtained for three different injection flow rates at constant model pressure and temperature. This figure shows that the amount of steam condensation is directly proportional to the amount of ECC water injected. Therefore, penetration increases as the injection flow rate is increased.

Figure 18 presents a comparison between plenum fill and quasi-steady state penetration data for a constant injection flow rate, model pressure, and water temperature. The two data sets agree quite closely, supporting the argument that there is little difference between quasi-steady state and plenum fill steam-water tests.

The data from the steam-water tests have been analyzed with the NLINMLE program, using a correlation proposed by Beckner, et al⁽²⁾. The correlation parameters are presented in Table 5, and Figures 19 and 20 compare actual data with calculated penetration curves based on the correlation.

VDM Probe Effects. The steam-water data presented up to this point were obtained with VDM probes in the annulus. For steam-water flows, the

TABLE 4. STEAM-WATER PLENUM FILL TEST MATRIX--NOMINAL CONDITIONS

Test No.	Model Pressure kPa	ECC Water Temp., C	ECC Water Injection Flow Rate, gpm	J_{Lin}^*	J_g^*
1	136	99	250	0.064	air flows to span range from full penetration to full bypass
2	306	99	250	0.064	
3	510	99	250	0.064	
4	306	99	380	0.098	
5	306	99	480	0.120	
6*	306	99	250	0.064	

* Tests conducted in quasi-steady state mode

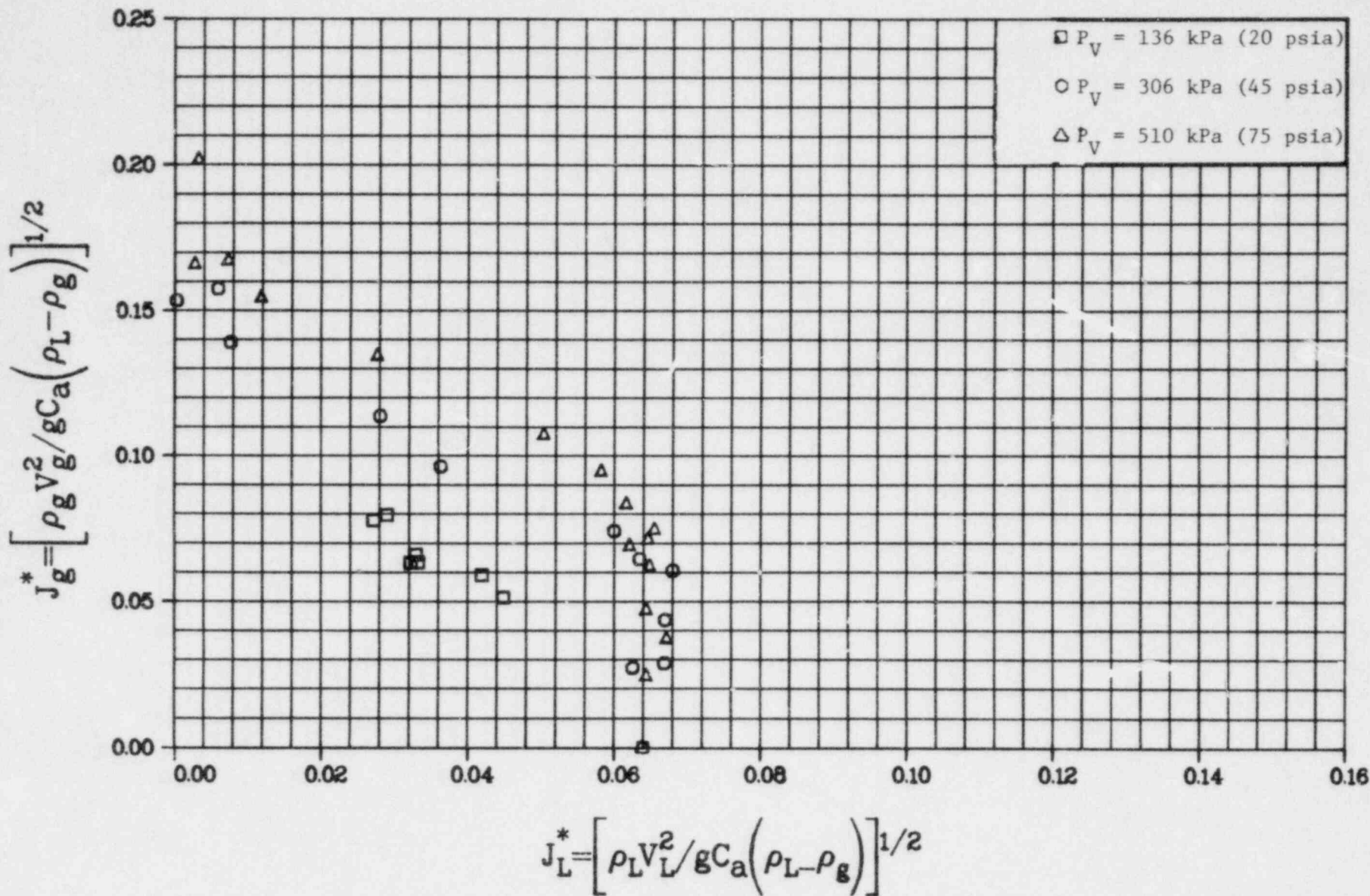


FIGURE 16. STEAM-WATER PLENUM FILL PENETRATION DATA OBTAINED
 WITH $T_{Lin} = 99 \text{ C (210 F)}$ AND $J_{Lin}^* = 0.064$

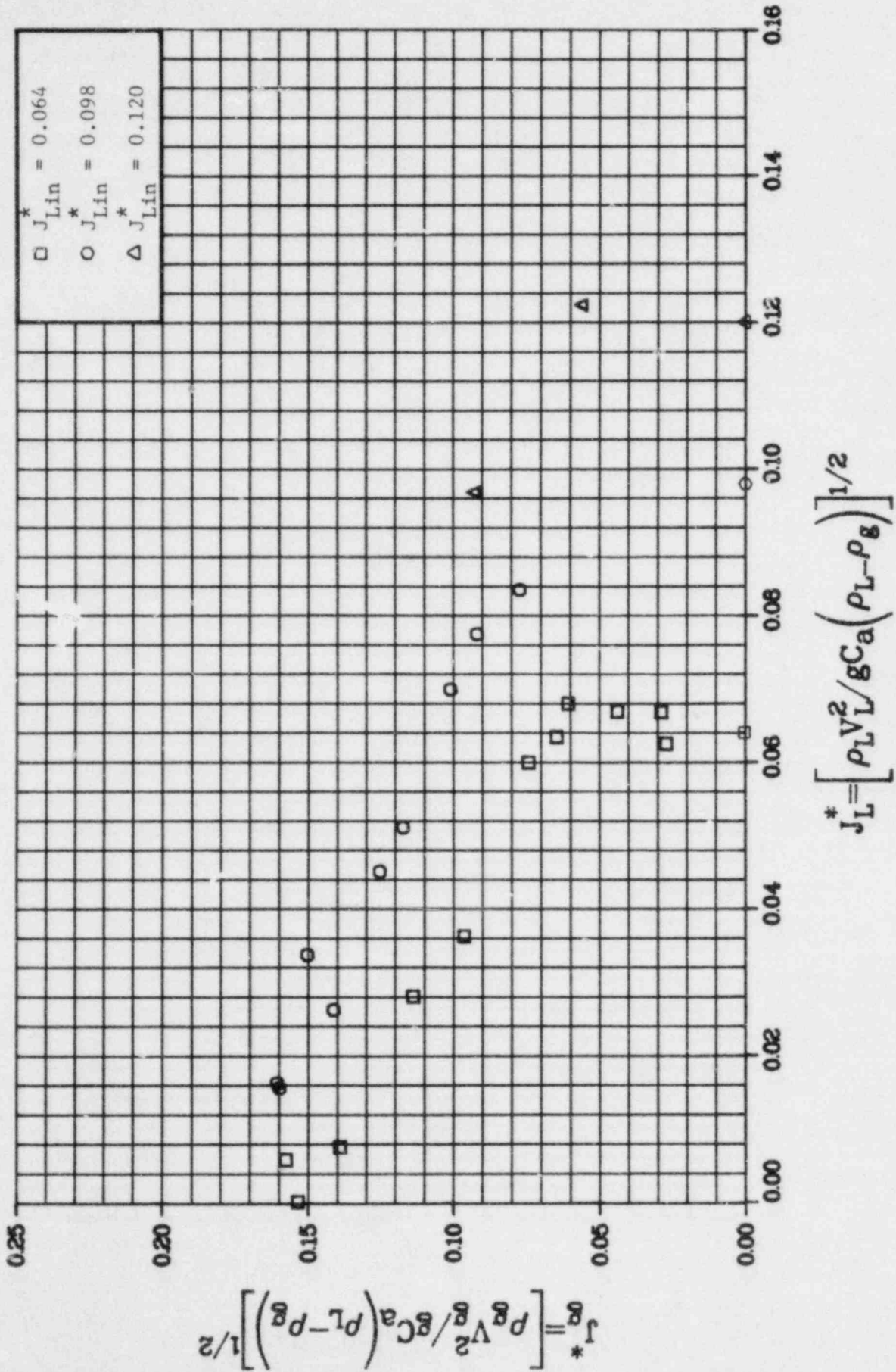


FIGURE 17. STEAM-WATER PLENUM FILL PENETRATION DATA OBTAINED WITH $T_{Lin} = 99$ C (210 F) AND $P_v = 306$ kPa (45 psia)

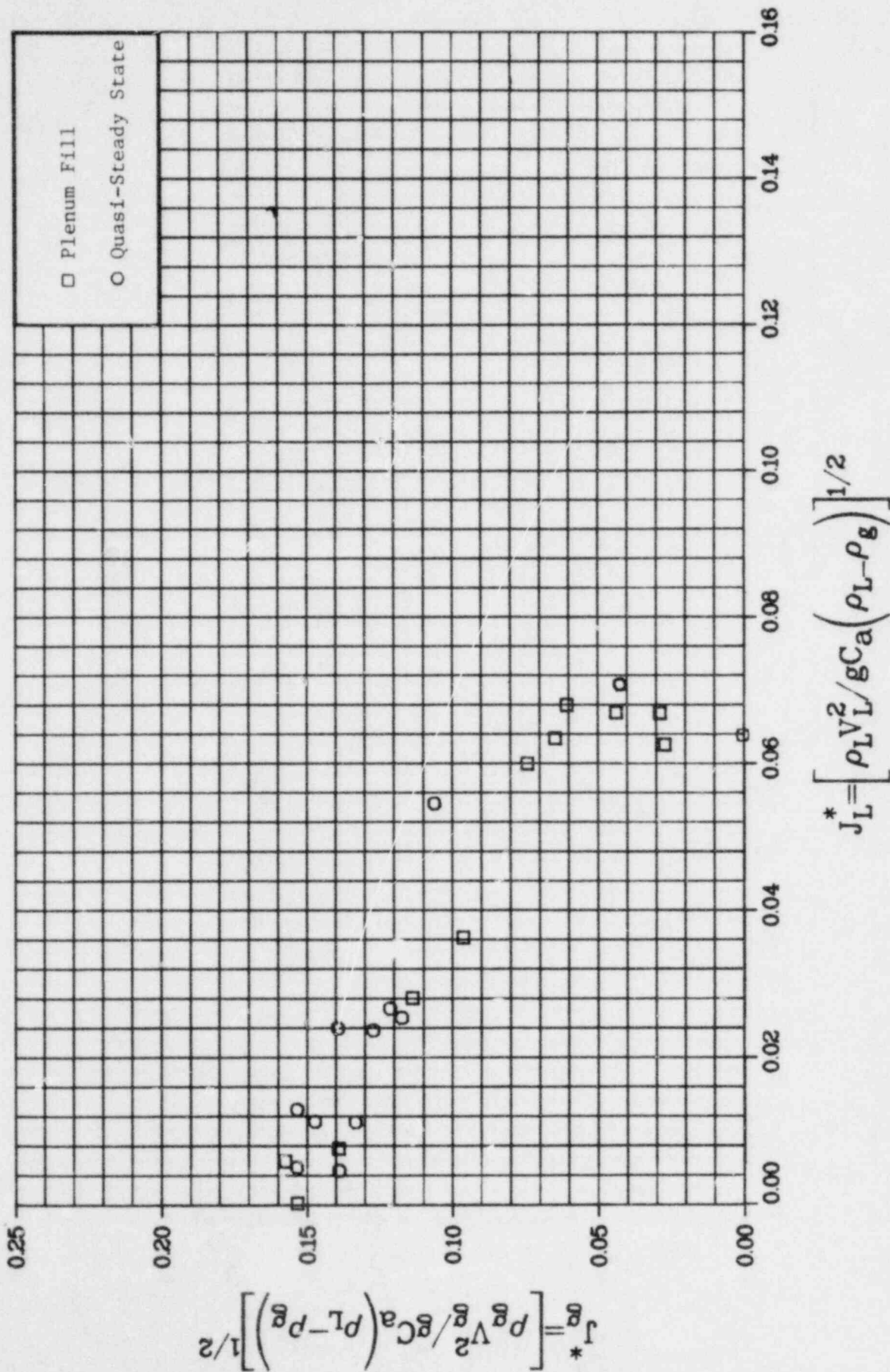


FIGURE 18. COMPARISON OF QUASI-STEADY STATE AND PLENUM FILL STEAM-WATER PENETRATION DATA WITH $J_{Lin}^* = 0.064$, $P_j = 306$ kPa (45 psia) AND $T_{Lin} = 99$ C (210 F)

TABLE 5. CORRELATION PARAMETERS CALCULATED FROM 2/15-SCALE
STEAM-WATER PLENUM FILL TESTS *

J_{Lin}^*	P_V , kPa	T_{Lin} , °C	M	C	F	Z
0.064 - 0.120	136 - 510	99	0.4292 ± 0.1453	0.3033 ± 0.0513	0.8034 ± 0.2180	5.8262 ± 7.809

* Assuming correlation form suggested by Beckner, et al⁽²⁾ :

$$J_g^{*1/2} - F(\lambda J_{Lin}^*)^{1/2} + [M - Z\lambda J_{Lin}^* \exp(-5.5 J_{Lin}^{*1/2})] J_L^{*1/2} = C$$

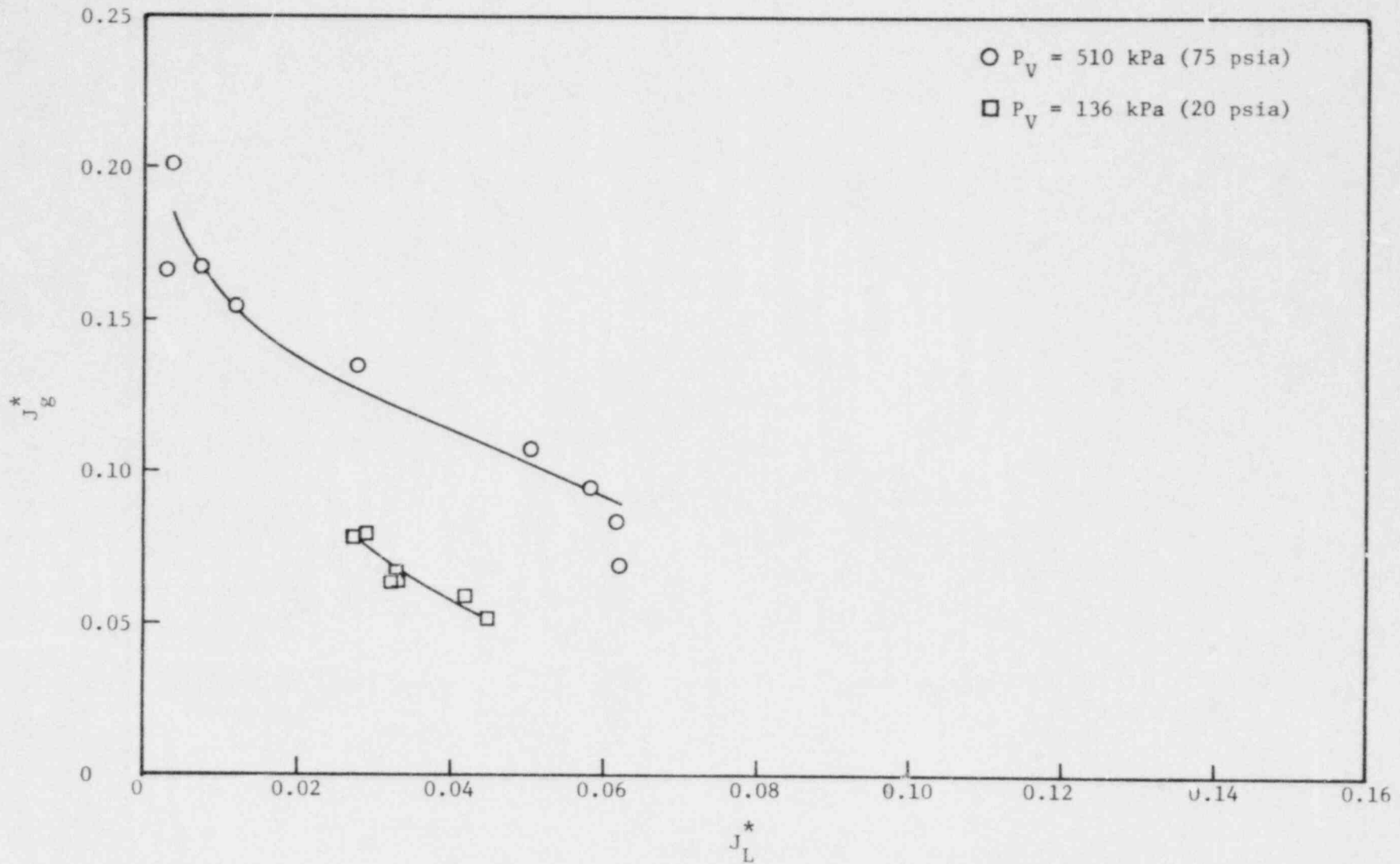


FIGURE 19. COMPARISON OF CORRELATION AND STEAM-WATER PENETRATION DATA
 FOR $J_{Lin}^* = 0.064$ AND $T_{Lin} = 99^\circ\text{C (210}^\circ\text{F)}$

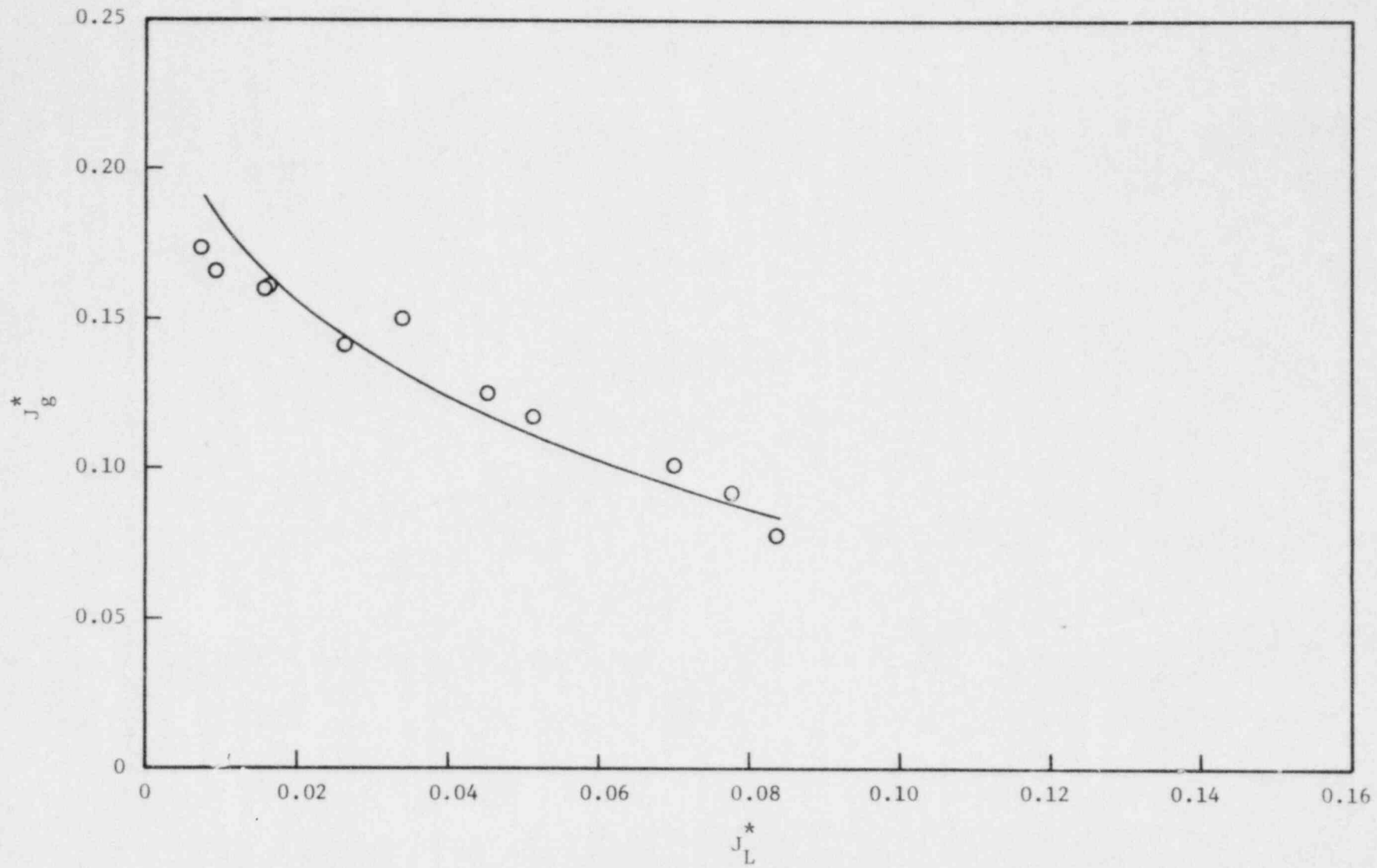


FIGURE 20. COMPARISON OF CORRELATION AND STEAM-WATER PENETRATION DATA
 FOR $J_{Lin}^* = 0.098$, $T_{Lin} = 99^\circ\text{C}$ (210°F), AND $P_V = 306$ kPa (45 psia)

VDM data revealed very chaotic flow conditions in the annulus, unlike the film flows in air-water tests. It was theorized that for steam and water the effect of VDM probes on penetration would be minimal since a stable flow pattern does not exist in the annulus. To verify this, a number of steam-water tests were performed with the VDM probes removed from the annulus. In Figure 21, the results of some of these tests are compared to data obtained with the VDM probes in the annulus. No obvious difference can be observed between the two penetration curves. This suggests that for steam-water flows, the VDM probes do not influence penetration to the extent evident in air-water tests.

Comparison With Earlier Steam-Water Data. In Figures 22, 23, and 24 the data presented in this report are compared to data from the 2/15-scale Model Development Tests (see NUREG/CR-0526, BMI-2011, Table A-1). Those tests were conducted in the quasi-steady state mode, with an oversized break leg. Figure 22 shows penetration data obtained at one injected liquid flow rate and temperature for different model pressures (and, consequently, subcoolings). They are compared to earlier data with similar, but not exactly equivalent, pressures and subcoolings. When new data at 20 psia are compared to older data the effect of subcooling is consistent. Also, comparison of data with similar subcoolings but different pressures show the pressure effect to be similar to that seen previously. Figure 23 is similar to Figure 22, comparing the current tests with higher subcooling tests from the Model Development series. Figure 24 compares data for a variety of pressures and subcoolings at a water injection flow rate of 0.097. Again the trends are consistent.

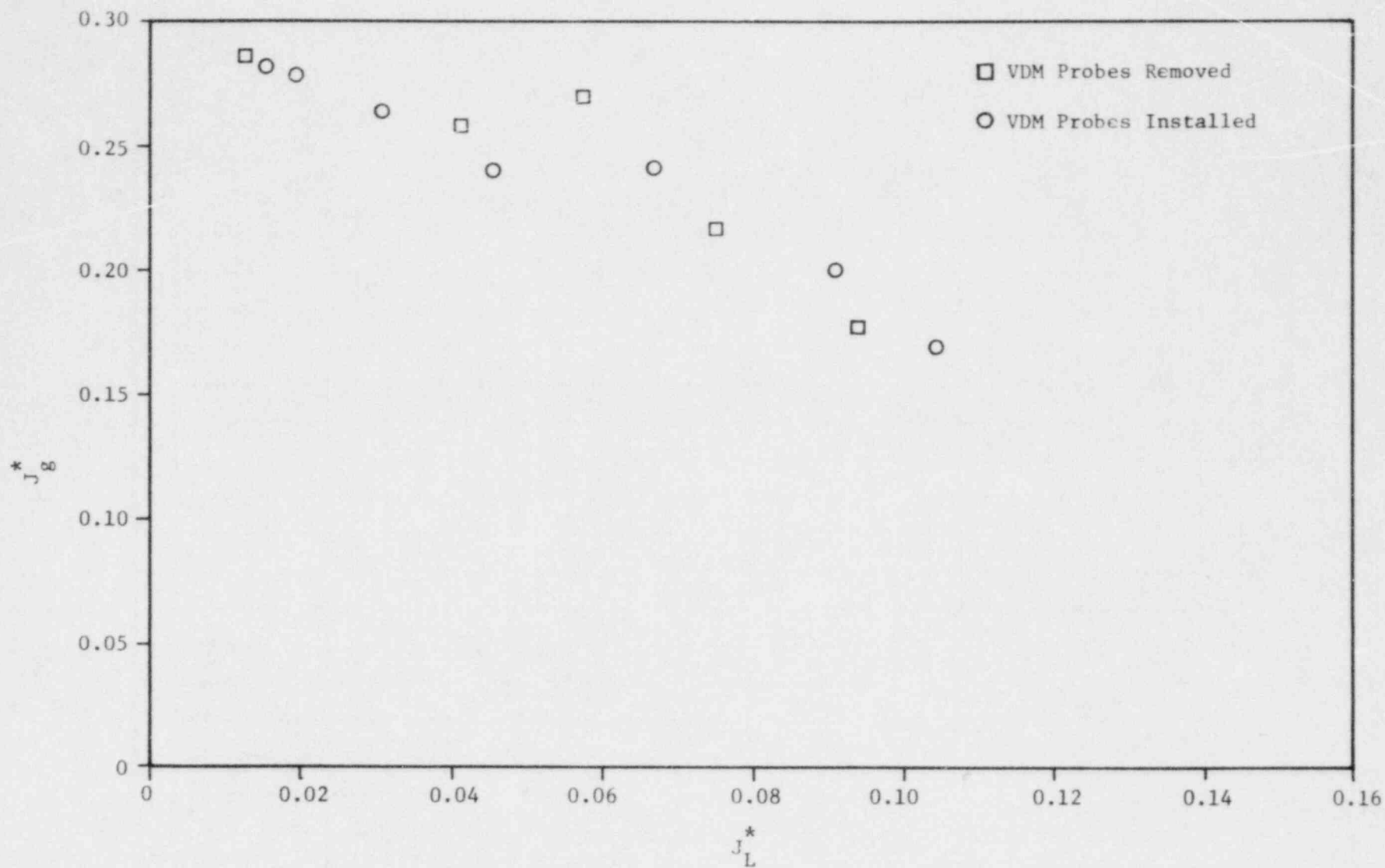


FIGURE 21. COMPARISON OF STEAM-WATER PENETRATION DATA TAKEN WITH AND WITHOUT VDM PROBES IN THE ANNULUS FOR $J_{Lin}^* = 0.098$, $T_{Lin} = 99^\circ\text{C}$ (210°F) $P_V = 306$ kPa (45 psia)

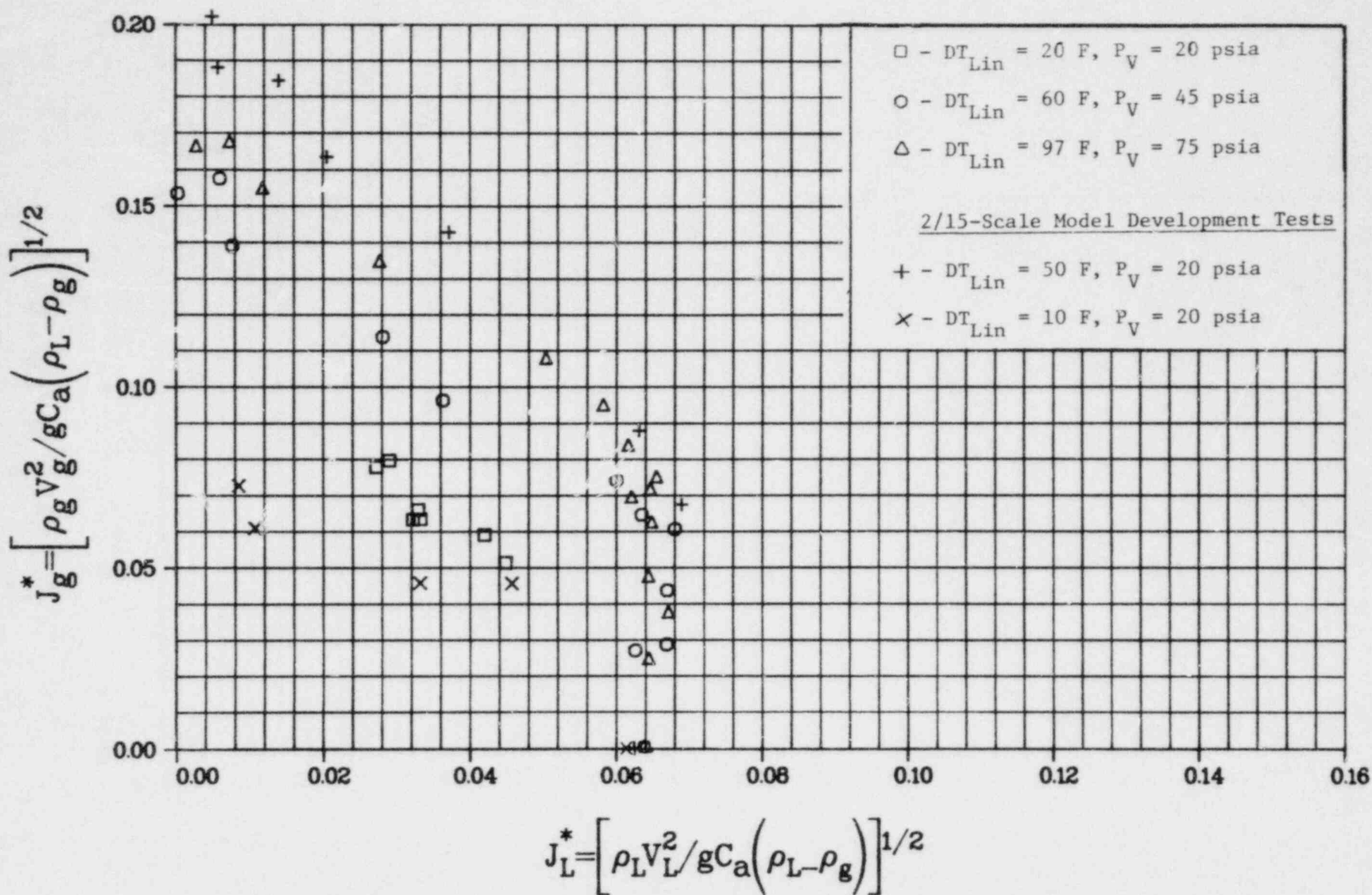


FIGURE 22. COMPARISON OF STEAM-WATER PENETRATION DATA WITH EARLIER RESULTS, $J_{Lin}^* = 0.064$

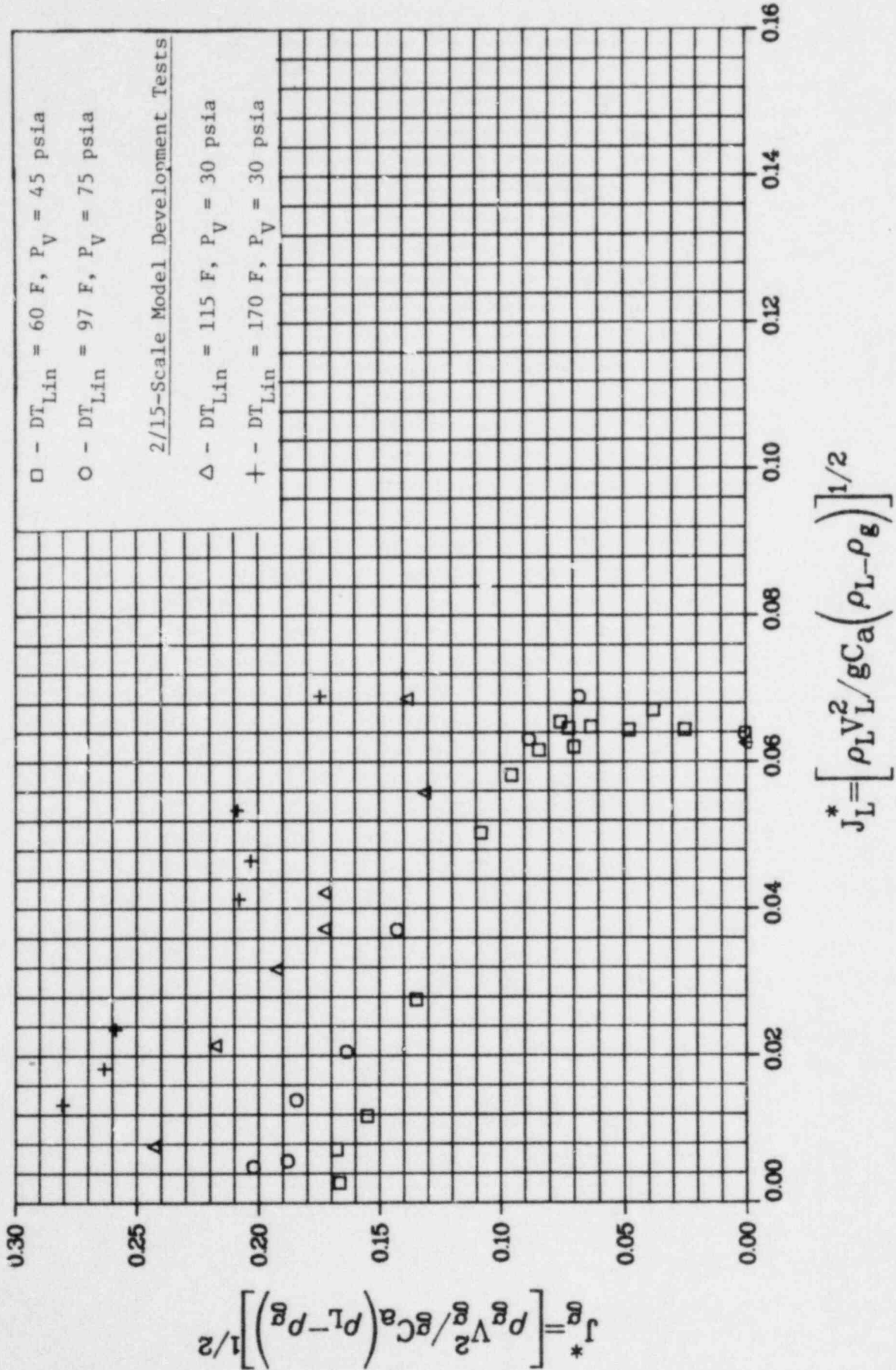


FIGURE 23. COMPARISON OF STEAM-WATER PENETRATION DATA WITH EARLIER RESULTS, $J_{Lin}^* = 0.064$

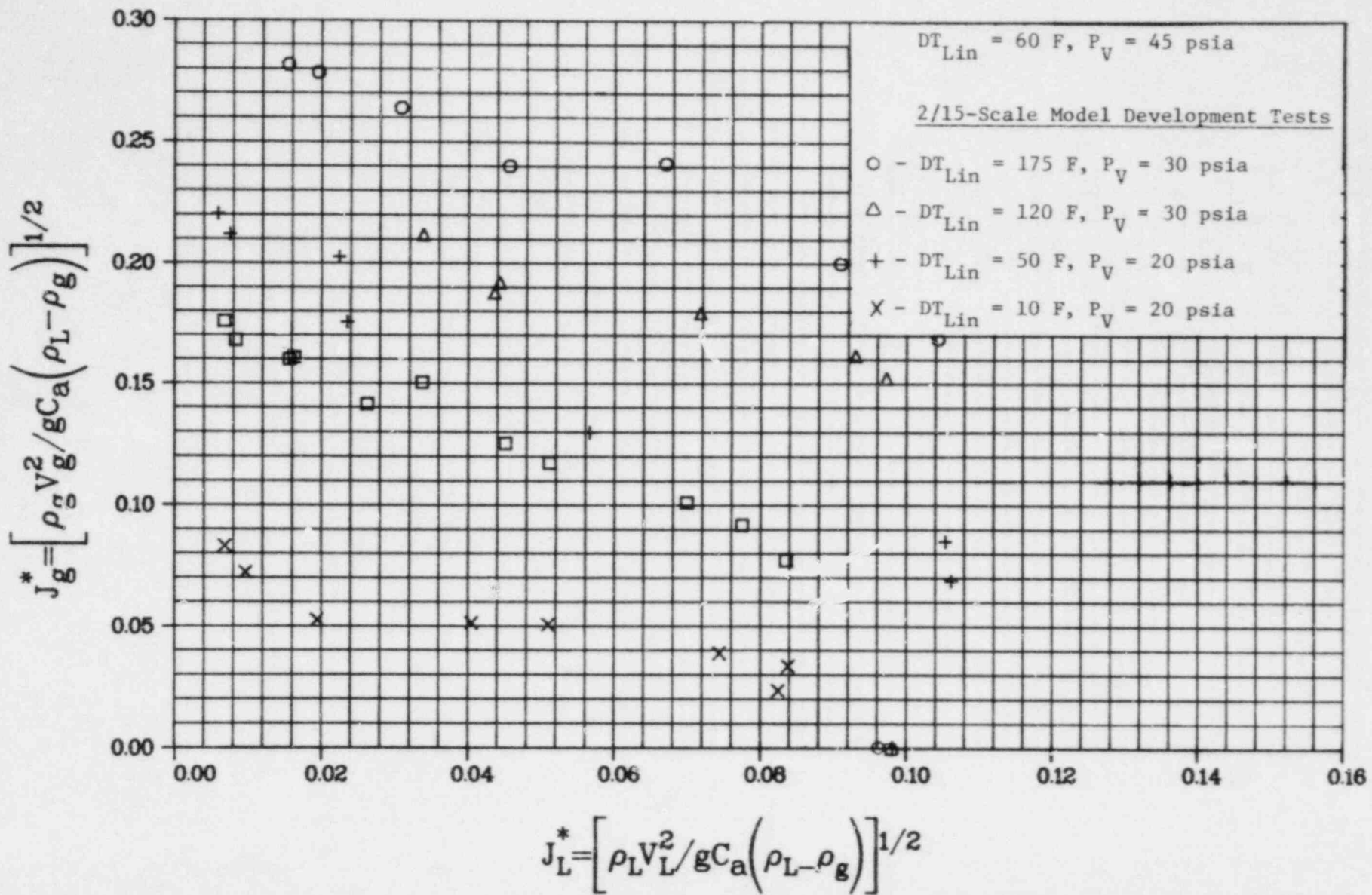


FIGURE 24. COMPARISON OF STEAM-WATER PENETRATION DATA WITH EARLIER RESULTS, $J_{Lin}^* = 0.097$

Continuing Development of a Mechanistic Model
for ECC Penetration

During this quarter, we incorporated the results of the countercurrent condensation study⁽³⁾ into the mechanistic model⁽⁴⁾. It was shown in Reference (3) that the condensation coefficient can be described by the dimensionless temperature:

$$f = \frac{T(L) - T_i}{T_s - T_i}$$

where $T(L)$ and T_i are the liquid temperatures at the end of the core barrel and at the film inlet, respectively. This dimensionless liquid temperature was evaluated during the condensation studies, resulting in the following correlation:

$$f = 1 - \exp \left[-1.34 \times 10^{-4} Re_g^{0.30} Re_\ell^{-0.27} \frac{L}{t} \right]$$

where Re_g and Re_ℓ are the vapor and liquid Reynolds numbers and t is the film thickness at $z = L$. This correlation was developed for the partial bypass region in an inclined rectangular test section. When it is applied to flows in scaled models, a suitable expression is needed for t . This is because the flow geometry in the downcomer is different from that in the inclined rectangular channel. Three dimensional effects, unstable wave growth, and entrance effects are also involved. The best agreement with experiments was given when t was assumed to be linearly dependent on the core barrel length:

$$t = 3.5 \times 10^{-4} L$$

resulting in film thickness of the same order as predicted by the Nusselt equation.

Using the Wallis correlation as a flooding relationship, the following equation is obtained:

$$\left[J_{gc}^* - (f - f_1) J_i^* - f_1 J_{in}^* + Q^* \right]^R + m J_i^{*1/2} = C$$

Calculations using this equation were compared with neutral wall experiments. The steam flux necessary to bypass a given amount of liquid was calculated and compared to experimentally measured values obtained in the 1/15- and 2/15-scale models (Figure 25 and 26). Comparisons to results obtained in the 2/15-scale model with an extended or a short core barrel are shown in Figures 27 and 28 respectively. The relatively good agreement shown indicates that for the range of liquid temperatures and vessel pressures tested the amount of steam condensation in the system is well modeled by the analysis.

It should be noted that the coefficients m and C in the Wallis correlation were evaluated for e_8 geometry from air-water experiments. The different values obtained for these coefficients suggest that the Wallis correlation should not be applied for scaling purposes unless the dependence of m and c on geometry and scale is evaluated.

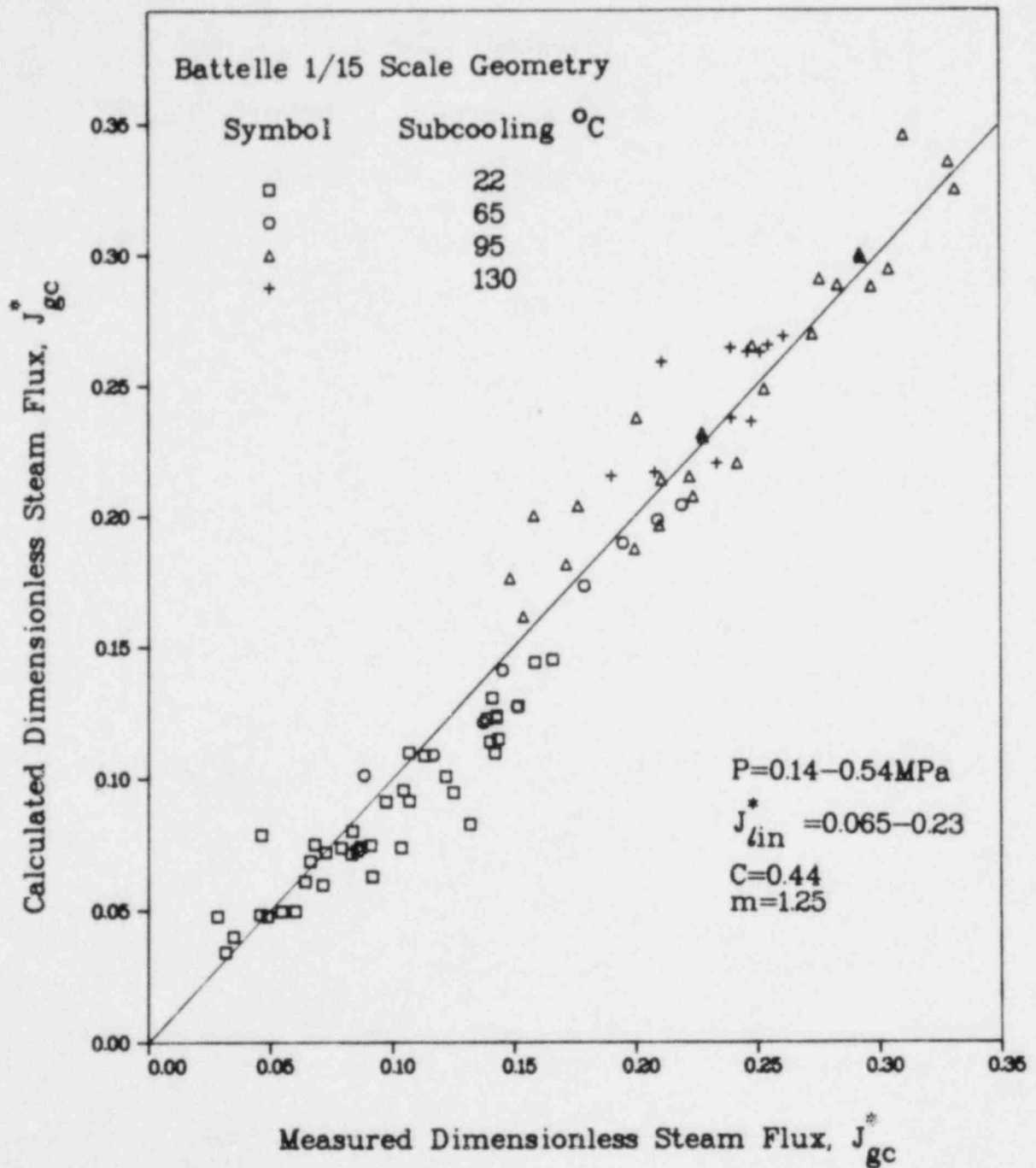


FIGURE 25. COMPARISON OF PREDICTED AND MEASURED J_{gc}^* FOR BATTELLE'S 1/15-SCALE GEOMETRY

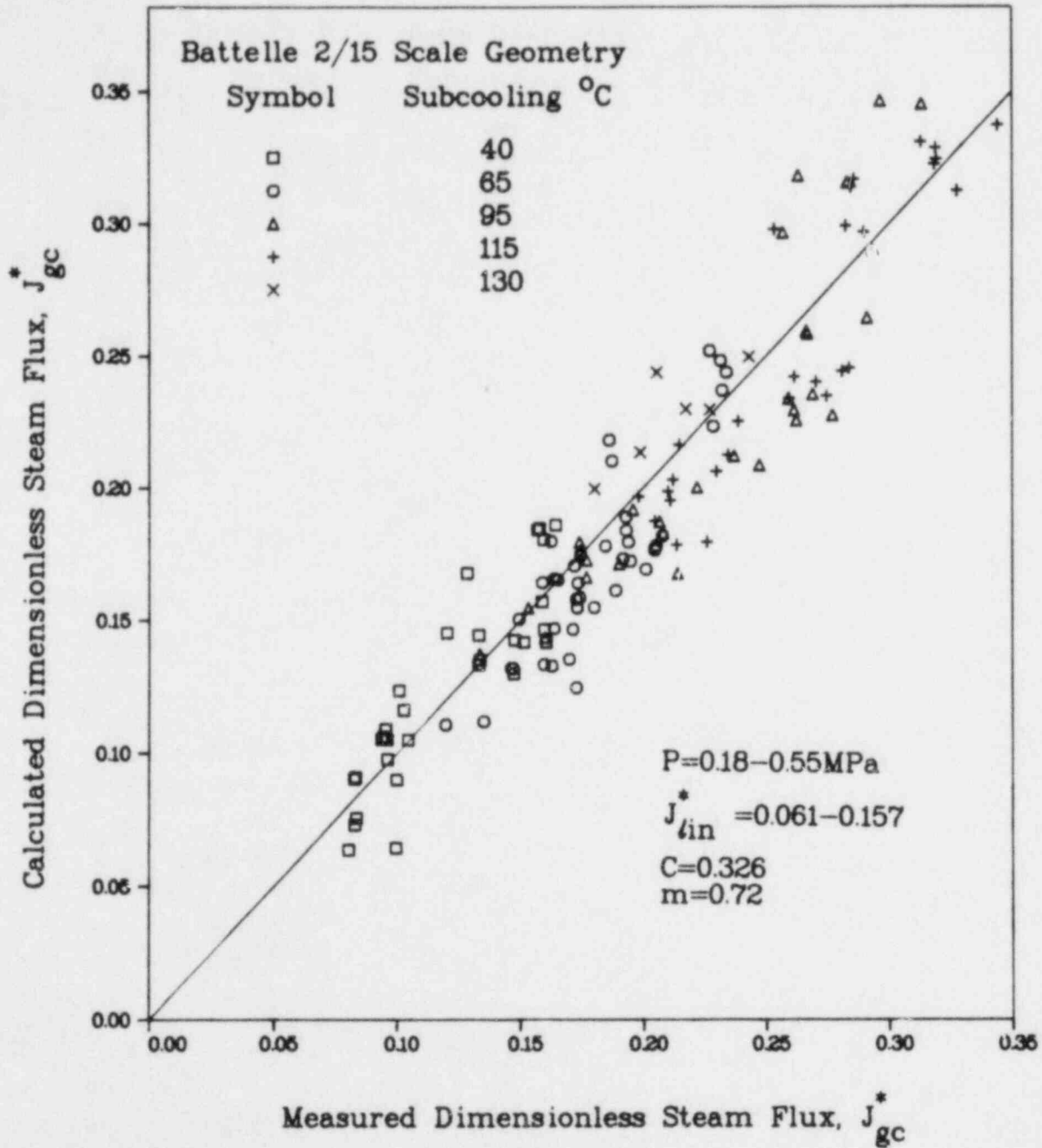


FIGURE 26. COMPARISON OF PREDICTED AND MEASURED J_{gc}^* FOR BATTLE'S 2/15-SCALE GEOMETRY

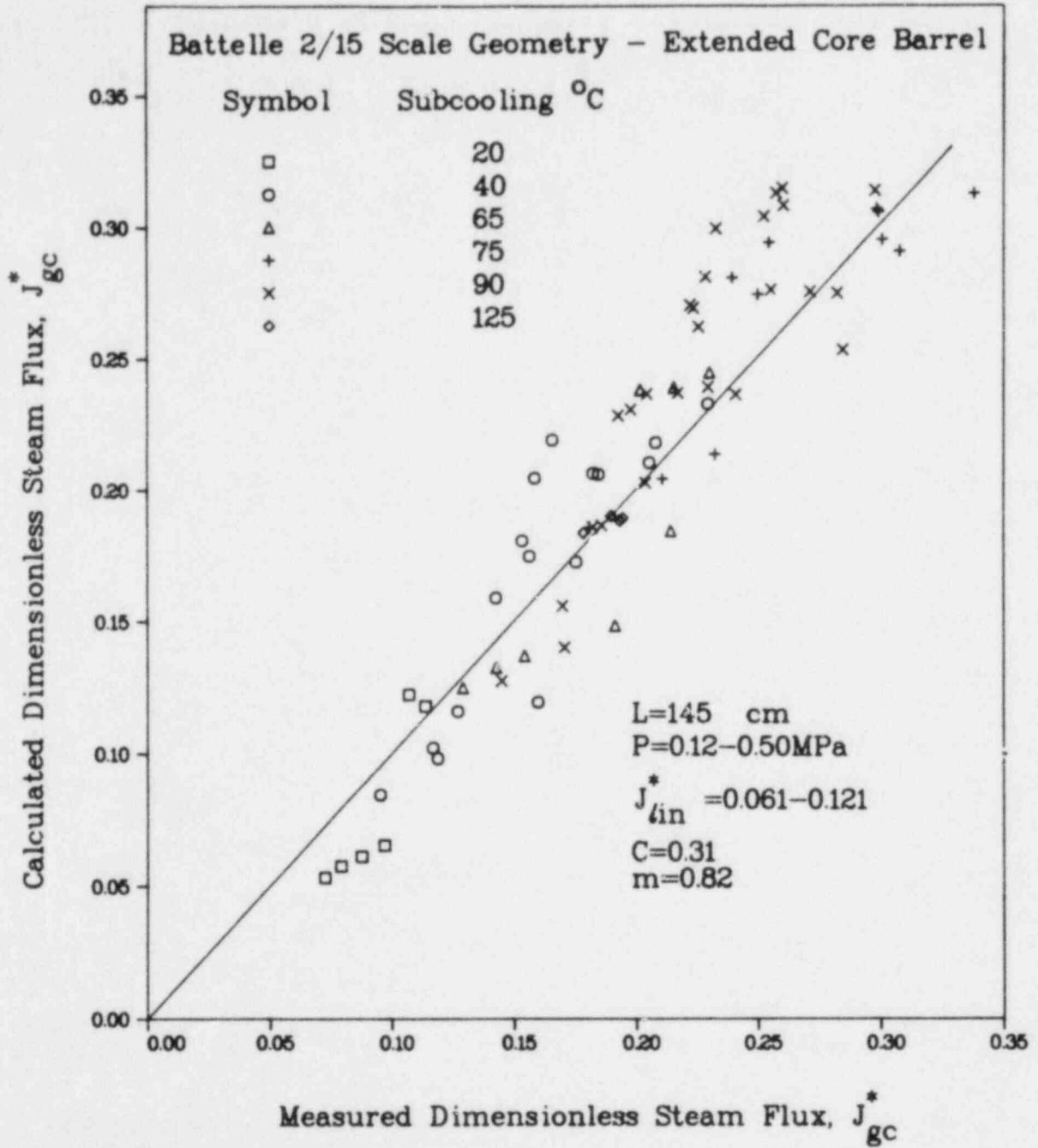


FIGURE 27. COMPARISON OF PREDICTED AND MEASURED J_{gc}^* FOR BATTELLE'S 2/15-SCALE GEOMETRY - EXTENDED CORE BARREL

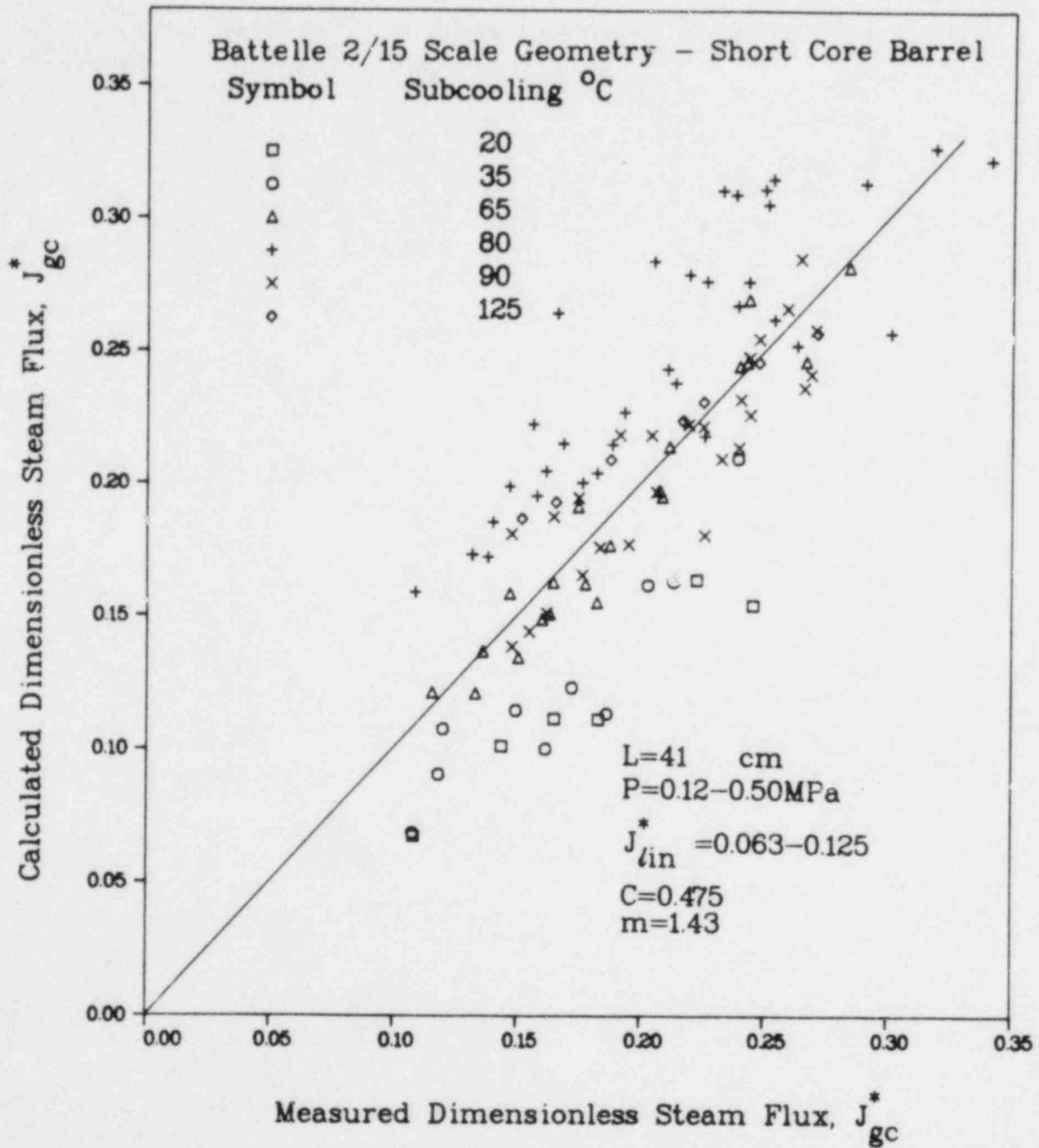


FIGURE 28. COMPARISON OF PREDICTED AND MEASURED J_{gc}^* FOR BATTELLE'S 2/15-SCALE GEOMETRY - SHORT CORE BARREL

TASK 2.0 EXPERIMENTAL TESTING AND DATA REDUCTIONObjectives

The objectives of this task are to:

- (1) Provide experimental data on ECC penetration and lower plenum entrainment using scale models geometrically similar to a four-loop pressurized water reactor. These data should provide a base for establishing a better understanding of the bypass phenomenon in large-scale systems.
- (2) Provide experimental data from small test facilities in support of analytical development programs.
- (3) Provide lead-in information on steam-water interaction phenomena and operational information obtained in smaller scale models for future larger scale experiments.

Work During Quarter

The experimental efforts during this quarter were directed to completion of the installation of the annulus void measurement system and the instrumented spool piece for the break leg, and subsequent check out and acquisition of initial data.

During the first month, the three beam gamma densitometer portion of the instrumented spool piece was received and installed. With this addition the spool piece was complete. It includes a full flow drag disk, a five sensor temperature rake, and a five point Pitot tube rake, in addition to the three beam gamma densitometer. Static pressure and wall temperature are also measured. During the same time period the annulus void distribution measurement (VDM) system was also made operational. This system consists of sensors located throughout the annulus between the pressure vessel and the core barrel and a high speed data acquisition and analysis

system. The annulus sensor array consists of eight rings of probes nearly evenly spaced vertically with each ring containing 12 nearly evenly spaced probes. Each probe contains three sensors spaced across the annulus gap. There are 288 sensor measuring locations in the array. The data acquisition system is programmed to make one scan of the 288 sensors every 10 milliseconds at normal speed or to make one scan every one millisecond. The capacity of the data storage memory is about 4500 scans or frames, which provides for up to 45 seconds of recording during normal operation.

In the second two months of the quarter a series of experimental runs were carried out which had as their objectives check out of the systems, understanding of the various individual and collective data outputs, development of data reduction software, and gathering of the additional and more detailed data that will add to the understanding of the phenomena and behavior of the countercurrent flow of steam and water that would exist in the downcomer and broken leg of a PWR under LOCA conditions.

Plans For Future Work

In the next quarter the studies of annulus and break leg flow with neutral and equilibrium walls that were started in this quarter will be finished, ramped core steam neutral wall tests will be carried out, and steady and ramped core steam hot wall tests will be started.

TASK 3.0 RIL SUPPORT AND TECHNICAL ASSISTANCEObjectives

The objectives of this task are to:

- (1) Prepare a summary technical report, concentrating on scaling, in support of the Research Information Letter on ECC Bypass Research to be issued in FY '79,
- (2) Participate in ECC Bypass Review Group activities as necessary during the program year, and
- (3) Carry out additional technical support as necessary during the program year.

Work During Quarter

During this quarter BCL staff reviewed final material for Research Information Letter #57, "Small Scale ECC Bypass Research Results". This RIL was issued during the quarter.

Plans for Future Work

We will participate in ECC Bypass Review Group activities and carry out additional technical support as required.

TASK 4.0 ACQUISITION AND APPLICATION OF
ADVANCED INSTRUMENTATION

Objectives

The objectives of this task are to:

- (1) Modify the 2/15-scale test facility and install an instrumented spool piece to measure instantaneous two-phase flow conditions in the broken leg, and
- (2) Modify the 2/15-scale test facility and install a system to measure void distribution in the annulus as a function of time.

Work During Quarter

The three beam gamma densitometer for the break leg spool piece was received from INEL and installed in the 2/15-scale facility. The densitometer has been checked out and is in order.

The annulus void distribution measurement (VDM) system was completed and installed during the quarter. Shakedown runs to verify performance of the two systems were carried out.

Plans for Future Work

Acquisition of the advanced instrumentation is now complete. Application of the instrumentation to a wider variety of tests will be carried out next quarter.

PART II

Countercurrent Flooding Flow in Tubes

COUNTERCURRENT FLOODING FLOW IN TUBES

by

J. S. K. Liu

Abstract

The phenomenon of countercurrent flooding has been investigated in 2, 4, and 6 inch I.D. tubes. The experiments were carried out in a typical flooding tube facility in which water is introduced through a porous wall into the test tube. Both steam-water and air-water tests have been performed. A hysteresis effect is clearly indicated in the steam-water flooding data. These experimental data demonstrate that neither the Wallis parameter (J^*) nor the Kutateladze number (K) are completely satisfactory for correlating all the countercurrent flooding data.

Introduction

Countercurrent flow of steam and water may occur in a pressurized water reactor in the event of a loss-of-coolant accident (LOCA). If a cold leg break occurred, steam would flow up the downcomer annulus against the downward flow of emergency core cooling (ECC) water being injected into the reactor vessel. Flooding of the countercurrent steam and water flow might delay the delivery of ECC water to the core, leading to possible overheating of the fuel.

Many experiments have been performed in reduced scale facilities^(5, 6) to investigate the flooding of countercurrent steam-water flow. Thus, scaling laws are required to project the flooding behavior to full reactor scale. However, completely satisfactory scaling laws have not been established at this time and the lack of consistent experimental data at larger scales makes the scaling issue difficult. At least two dimensionless parameters have been developed to scale the available flooding data. These are K , the

Kutateladze number, and J^* , the dimensionless volumetric flow rate, which appears in the Wallis flooding correlation⁽⁷⁾,

$$J_g^{*1/2} + mJ_L^{*1/2} = C$$

These two parameters were mainly developed from flooding data obtained in tube geometries. For small diameter tubes and narrow annuli the Wallis correlation generally represents the experimental flooding data reasonably well. Flooding in large diameter tubes is not well correlated by the Wallis equation, however. It appears that K may be a more appropriate parameter for correlating large tube data. In an extensive study of available air-water flooding data of tube geometries⁽⁸⁾ it was concluded that there is a transition from J^* scaling, which implies that the flooding velocity is size dependent; to K scaling, which indicates that the flooding velocity is independent of size. This transition is a gradual one, and a transition regime for tube diameter of 2 to 6 inches was suggested.

Detailed comparison of experimental data obtained in Battelle Columbus Laboratories' (BCL) 1/15- and 2/15-scale simulated reactor vessels showed that neither J^* nor K is an entirely satisfactory scaling parameter. A slightly more general dimensionless group, I^* , was suggested as a scaling parameter⁽⁹⁾. This I^* parameter may be thought of as a combination of the J^* and K approaches.

The general agreement between tubes and annuli for air-water tests at comparable small scales indicated that a similar agreement at larger scales may be possible. The transition in scaling parameters for air-water scaling in simple tube geometries has important implications for scaling of flooding with more complicated flows in more complicated geometries. The systematic investigation of flooding behavior in tubes would serve to indicate trends in flooding behavior in more complicated reactor-like geometries.

The purposes of this study are: to provide a series of systematic and consistent experimental data over a wide range of scale for both air-water and steam-water flooding flows in tubes to evaluate the effect of physical tube size on flooding, both in steam-water and air-water flows; to investigate differences in behavior between steam-water and air-water in tube geometries, and hopefully, to provide a basis for understanding the differences in steam-water and air-water experiments in reactor-like geometries.

Recent Work on Countercurrent Flooding in Tubes

Countercurrent gas-liquid flow has received extensive experimental investigation in recent years. Hewitt⁽¹⁰⁾ investigated flooding in the countercurrent flow of air-liquid mixtures in vertical and inclined tubes. He found that the effect of tube length was small. The liquid viscosity appeared to have only a small effect on the flooding velocity within the range tested but flooding velocity appeared to decrease significantly with decreasing surface tension. The inclination angle of the tube had a dramatic effect on flooding velocity. Richter and Lovell⁽¹¹⁾ carried out air-water flooding tests in tubes with diameters of 6 and 10 inches. The Wallis correlation in its present form did not fit their experimental data very well, particularly under conditions of high-gas and low-liquid flow. Their work generally confirmed the experimental results of Pushkina and Sorokin⁽¹²⁾.

Wallis, Richter and Bharathan⁽¹³⁾ also studied the air-water countercurrent flow characteristics in 1- and 2-inch-diameter vertical tubes. Liquid fraction measurements indicated that their countercurrent flow could be divided into three regions based on the relative magnitudes of the interfacial and wall shear stresses. A simple theory was proposed to model countercurrent flow within a tube. Dukler and Smith⁽¹⁴⁾ studied air-water flooding in a 2-inch-diameter tube. They found that the onset of flooding was associated with the onset of entrainment. Their data was also well correlated by the Wallis correlation.

In comparison to air-water results, steam-water flooding data are rather meager. Fair and Schrock⁽¹⁵⁾ investigated the flooding of steam-water in a 1.99-cm-diameter tube qualitatively. The flow patterns were generally characterized as oscillatory or transient. However, no quantitative data was reported. De Sieres⁽¹⁶⁾ performed a study of steam-water countercurrent flow in a 2-inch-diameter tube. When he plotted the dimensionless gas flow rate against the dimensionless liquid flow rate he found hysteresis which generally can be explained by condensation and interphase heat transfer.

Tien and Liu⁽¹⁷⁾ recently published a survey on countercurrent flooding covering a total of 56 references. A number of these dealt with flooding in small tubes.

Test Apparatus, Instrumentation, and Test Procedure

There has been a clear need for consistent experimental data obtained with steam-water as well as air-water in larger diameter tubes. Steam, air and water supplies, as well as the necessary control systems, instrumentation, and data acquisition system (DAS) were available in conjunction with the BCL 1/15-scale model experimental facility. A test stand which can accommodate tubes of several different diameters was constructed.

Test Apparatus

A schematic diagram of the experimental equipment is shown in Figure 29.

The apparatus includes the tubular test section, liquid and gas injectors, and two tanks to collect the penetrated and bypassed water. The test section is a tube approximately 96 inches long with a porous wall liquid injection section located approximately 69 inches above the bottom of the tube. The lower end of the test section extends about 6 inches into the lower tank. It is bell-mouthed to carry the penetrating liquid film smoothly away from the injected gas stream. The upper end of the tube is cut squarely and smoothly, and extends about 12 inches into the upper tank. All components of the facility were designed to accommodate tubes ranging from 2 to 10 inches in diameter.

To date we have carried out experiments in 2- and 4-inch diameter tubes made of Lexan polycarbonate, and in a 6-inch-diameter brass tube. This tube was well insulated during all tests. If desired, the test section could be modified easily for top flooding liquid injection or simulation of other specific geometries, such as the Semiscale external downcomer.

Water is injected through a 6-inch-long porous walled section surrounded by an annular "can". The porous section was made by overlapping fine mesh screen to 1/2-inch thickness and soldering the resulting cylinder to flanges which were carefully machined to assure a smooth transition from the injector to the test section. The injector was designed to accommodate high flow rates and to create a smooth liquid film in the test section. (Smooth films were observed for flow rates as high as 100 gpm in the 6-inch tube.) Since the pressure drop in the porous section is small the annular

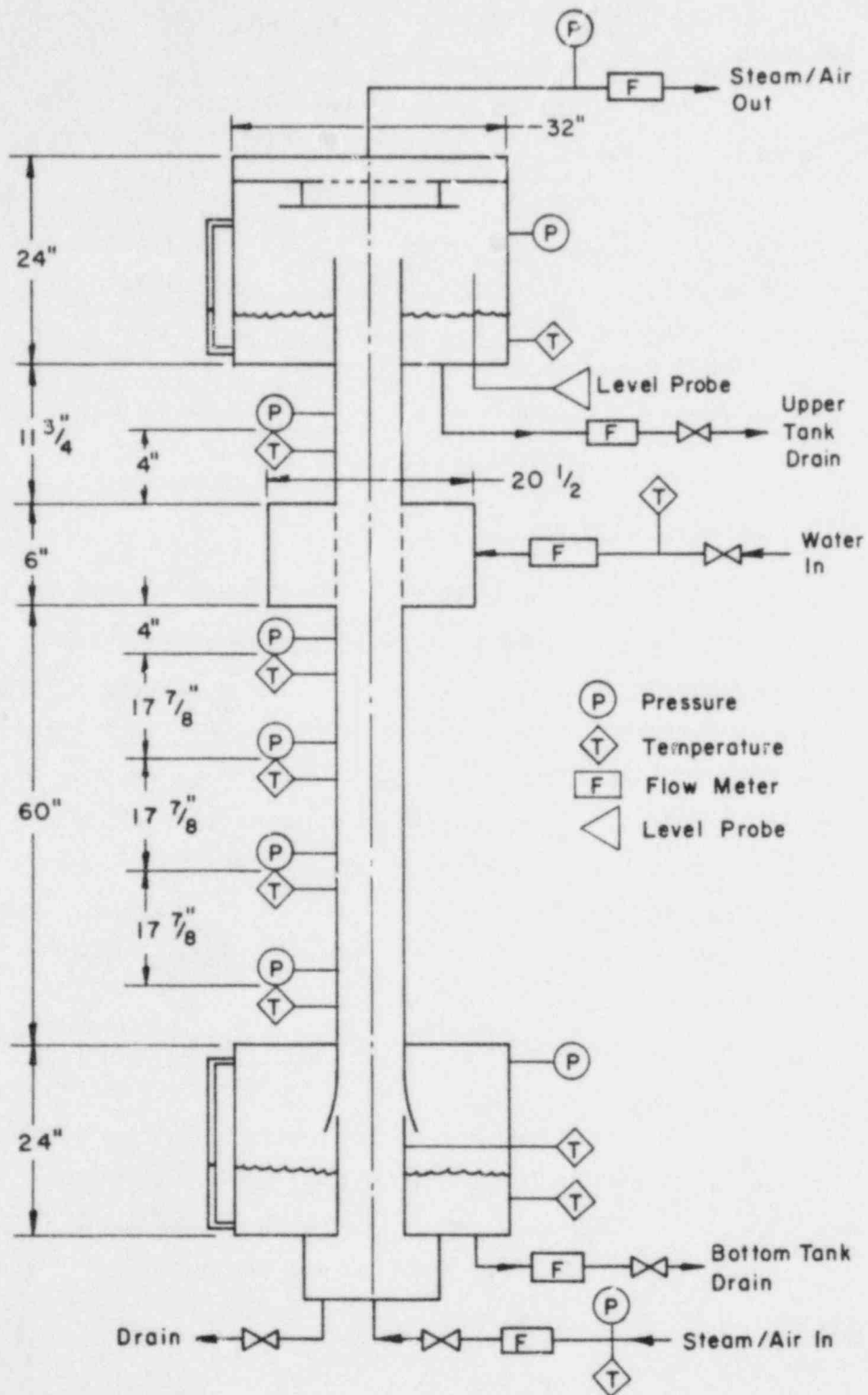


FIGURE 29. SCHEMATIC SKETCH OF TEST FACILITY

can is not always filled and a free surface may exist in the injector. Possible side effects of this will be discussed in more detail in later sections of the report.

Steam or air is introduced through a chamber in the bottom of the lower tank. The gas passes through a perforated plate into an injection tube with the same inside diameter as the test section. The injection tube minimizes contact between the injected gas and the penetrated liquid in the lower tank.

Both the upper and lower tanks are rolled steel, with an inside diameter of 32 inches and a height of 24 inches. A simple separator in the upper tank prevents water from entering the gas exhaust line. This line is connected to the 1/15-scale containment vessel, where cold water sprays can be used to condense the exhaust steam as necessary.

Instrumentation

Wall static pressure and liquid film temperature in the test section are measured at four stations below, and one above, the water injector. The gas inlet temperature is measured at the exit of the injection tube.

The pressure and water temperature in both the upper and lower tanks are also measured. Liquid level in the tanks is visually monitored with sight glasses. The level in the upper tank is measured continuously with a conductivity probe.

The flow rates of the injected gas, injected water, lower tank water drain, upper tank water drain and upper tank gas exhaust are all measured with turbine flow meters. The injected gas pressure and temperature, injected water temperature and exhaust gas pressure are measured at the flow meters to facilitate conversion of volumetric flow rates to mass flow rates.

All temperatures are measured with stainless steel sheathed chromel/alumel thermocouples. Pressures are measured with diaphragm type pressure transducers.

Output from all instruments is passed through signal conditioners to the minicomputer-based data acquisition system, which has a scan rate of approximately 10 kHz and a scan repeat rate of 50 Hz. Data are recorded on magnetic tape and subsequently processed on the BCL computer system.

Test Procedure

Tests are most frequently run in a quasi-steady mode, with fixed gas and liquid supply flow rates. However, a few slow transient tests have been carried out. In the quasi-steady mode water is injected at a fixed flow rate after it is preheated to the desired temperature in the supply tank. Gas flow is then initiated at the preselected value. Choked flow is maintained at the gas supply control valve to minimize the effect of test section fluctuations on the gas flow rate.

After flow adjustment transients die out, the DAS is started and the instrument readings are recorded. Typical runs range from 30 seconds to 4 minutes.

In the tests reported here the liquid level in the lower tank was allowed to vary during a run, but the level was returned to its initial position before stopping the DAS. This was done by throttling the lower tank drain valve.

Experimental Results

Visual Observations

Visual observations were made for air-water flows to confirm that the behavior of the present facility is similar to that seen by previous investigators; and for steam-water flows to help understand the flooding phenomenon in condensing two-phase systems. In general, the steam-water results were similar to those seen for air-water flows, although the steam-water response was much more violent and chaotic. The overall trends in system behavior were similar to those described by Bharathan, et al⁽¹⁸⁾, or Tien, et al⁽¹⁹⁾.

The tests were begun by establishing a smooth liquid film flow (at the specified flow rate) without gas flow. The gas flow rate was then increased in steps and observations made. For both air-water and steam-water flows the film surface became rippled, and was increasingly disturbed as the gas flow was increased.

Continued increase in the gas flow rate caused small droplets to form which then drifted in the upflowing gas stream. For low water flow rates the droplets floated in the injector section; at high water flow rates the droplets drifted in the lower part of the tube. The countercurrent flow at this point was quite unstable and small disturbances (such as adjusting a drain valve) could cause flooding to occur.

For slightly higher gas flow rates, roll waves developed in the lower portion of the tube and propagated rapidly up toward the injector, causing flooding. After flooding occurred the liquid flowed down in a thin film, at a reduced rate. The flow above the injector was in the churn-turbulent regime.

Further increase in the gas flow rate increased the roll wave frequency and caused reflection of those waves downward from the injector. Additional increase in the gas flow dried out the tube. The flow rate at which dryout occurred was significantly higher than that which initiated flooding.

The major difference between steam-water and air-water flooding flow would be due to interphase heat transfer in steam-water flow. For steam-water flow, flashing and sudden condensation of steam was observed at high steam flow rates. Snapping sounds, characteristic of rapid condensation, were clearly heard. Intermittent water penetration (slug delivery) occurred in the 6-inch I.D. tube at higher water flow rates.

The system pressure behavior for steam-water flows was distinct from that seen for air-water flows, as shown in Figure 30. For low gas flow rates the pressure was steady and near atmospheric (Figure 30, top). As the gas flow rate was increased beyond the value which caused flooding for air-water flows the average pressure increased (Figure 30, middle), but fluctuations in the pressure remained small. For steam-water flows under similar conditions (Figure 30, bottom) rather large pressure oscillations were observed. With a fundamental frequency of roughly 1.0 Hz.

Flooding Test Results

Experimental results are listed in Appendix B (Table B-1, air-water, and B-2, steam-water). It is convenient to review the data by plotting it in

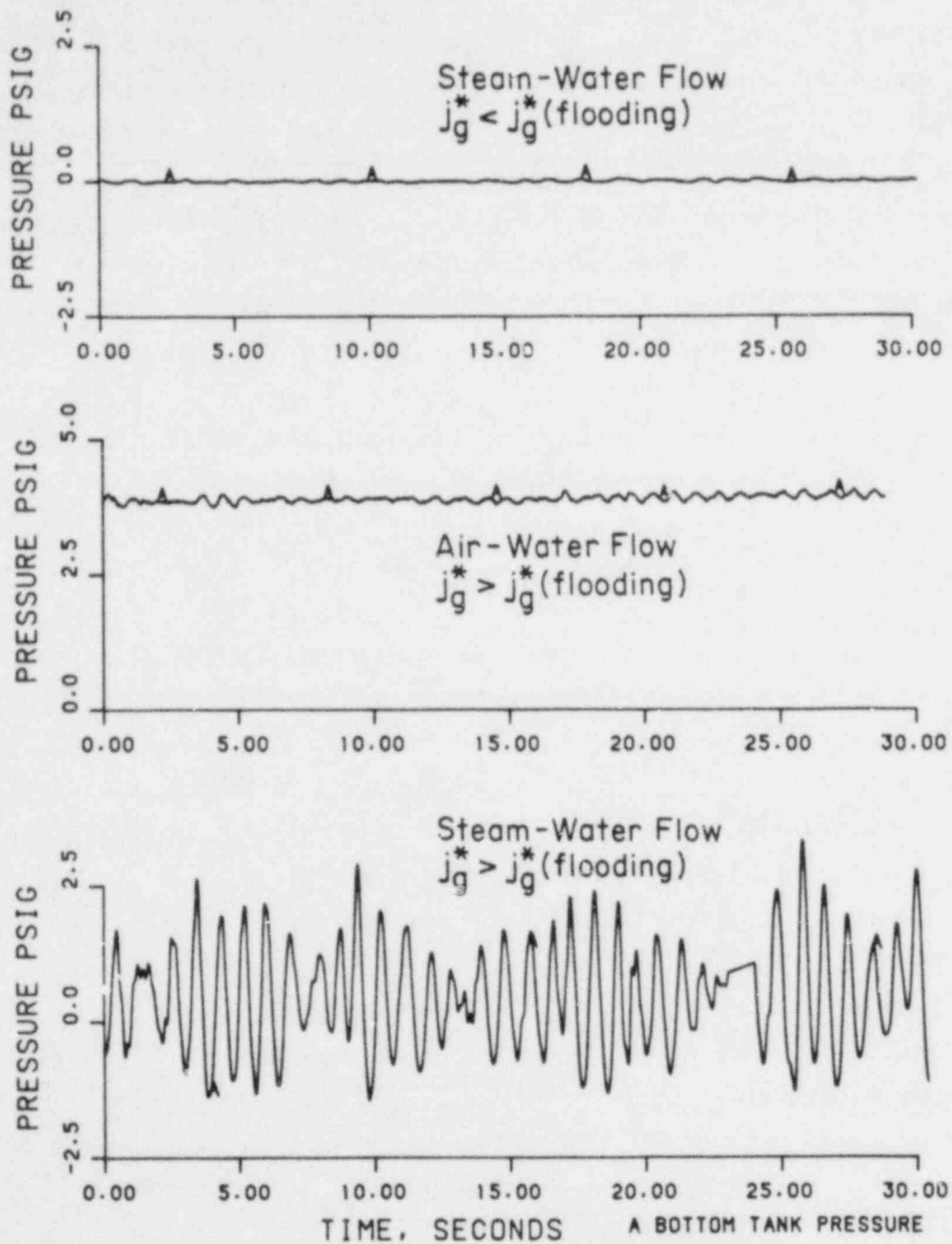


FIGURE 30. LOWER TANK PRESSURE FOR THREE COUNTERCURRENT FLOWS WITH $T_W = 21^\circ\text{C}$

terms of the common dimensionless groups J_g^* and J_l^* . The mode of operation indicates that the data were obtained while increasing or decreasing the gas flow. Figure 31 and Figure 32 illustrate countercurrent air-water flow flooding in the 2-inch diameter tube for 70°F and 140°F inlet water, respectively. Similar flooding data for 4- and 6-inch diameter tubes are shown in Figures 33-36. Cross plots of data at the same nominal inlet flow rates and temperatures for different tube sizes are shown in Figures 37-40. Figures 41-44 show the same data, plotted in terms of the Kutateladze number, K .

Similar results for steam-water tests are shown in Figures 45-58, in order similar to that of the air-water results.

Comparison with Previous Data

It is of interest to compare the present results with the available data. Figure 59 illustrates the comparison of present data to that of Richter and Lovell⁽¹¹⁾ for a 2-inch diameter tube. The present data lie somewhat below that of Richter and Lovell, and thus may not be correlated with the same parameters in the Wallis correlation. This may be attributed to the present inlet water injector design. The 6-inch tube data generally agree with that of Richter and Lovell, as shown in Figure 60.

Figures 37 and 39 indicate that air-water flooding velocities for low injected water flow rates can be correlated reasonably well by J^* (although the functional relationship may or may not be in the form of the Wallis correlation). However, J^* does not scale the flooding velocities for larger inlet water flow rates, as shown in Figures 38 and 40. We suspected that the deviation was due to larger convective mass transfer at higher flow rates, however, the temperatures measured along the test section did not support this hypothesis. The Kutateladze number, K , can represent the data reasonably well for these larger flow rates, as shown in Figures 42 and 44.

For steam-water flows, the same trend can be seen in Figures 51-54. For 2-inch and 4-inch diameter tubes, the flooding flows can generally be characterized by delivery-non-delivery (on-off) behavior. Partial penetration is observed only for the 6-inch diameter tube under certain operating conditions,

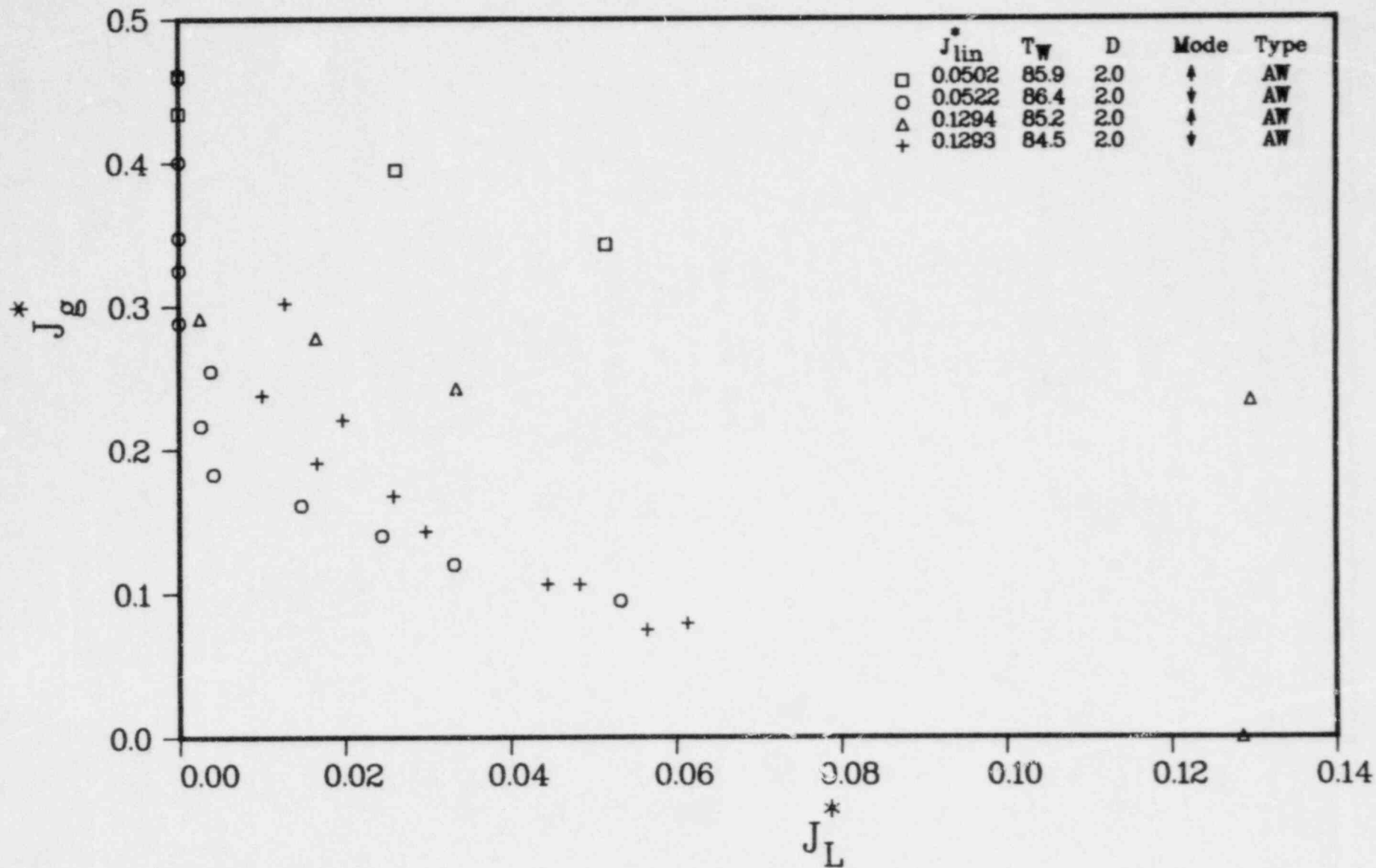


FIGURE 31. FLOODING VELOCITIES FOR AIR-WATER FLOWS IN 2-INCH DIAMETER TUBE WITH $T_W = 85^\circ\text{F}$

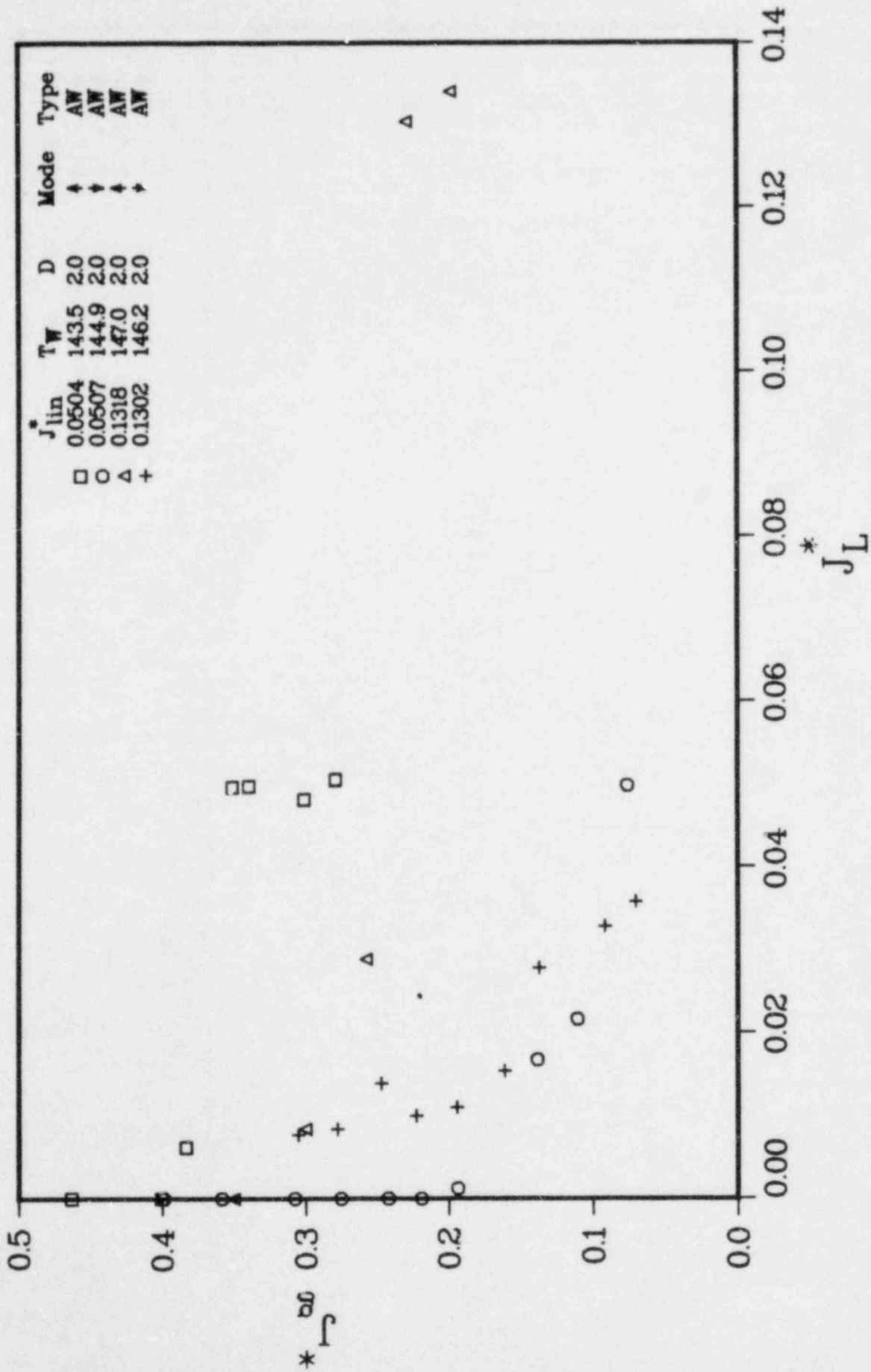


FIGURE 32. FLOODING VELOCITIES FOR AIR-WATER FLOWS IN 2-INCH DIAMETER TUBE WITH $T_w = 140^\circ F$

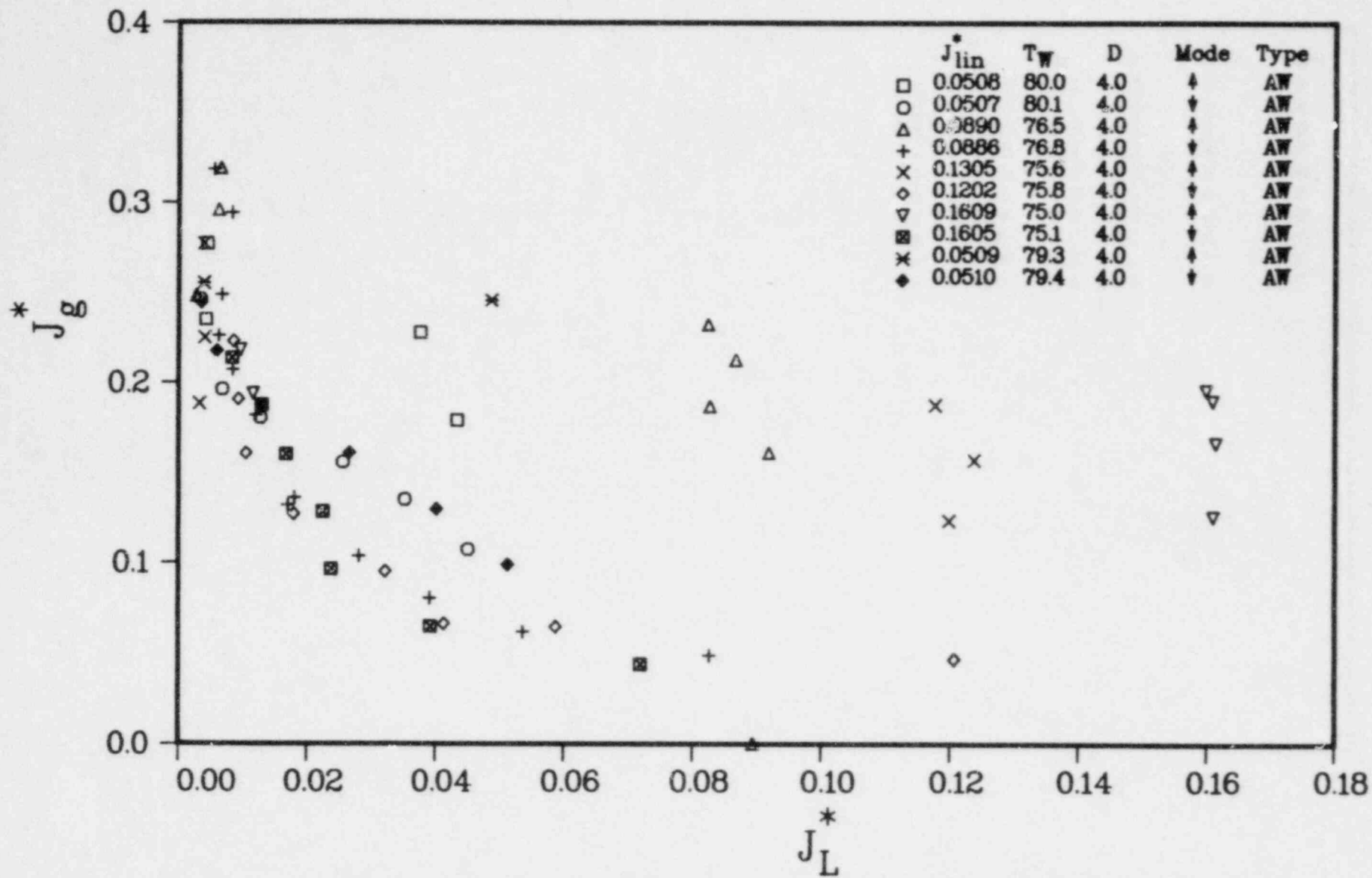


FIGURE 33. FLOODING VELOCITIES FOR AIR-WATER FLOWS IN 4-INCH DIAMETER TUBE WITH $T_W = 75^\circ\text{F}$

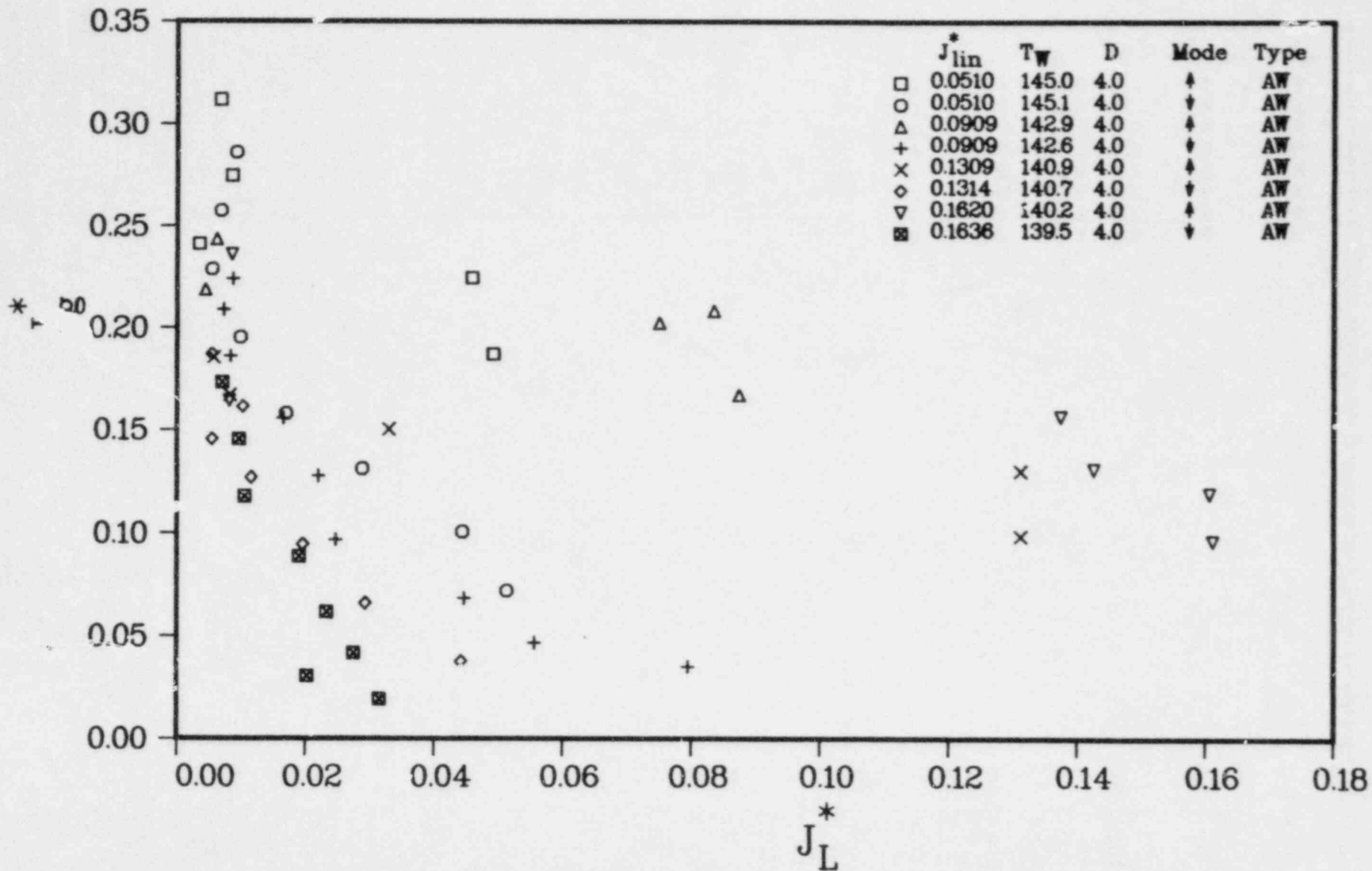


FIGURE 34. FLOODING VELOCITIES FOR AIR-WATER FLOWS IN 4-INCH DIAMETER TUBE WITH $T_W = 140^\circ\text{F}$

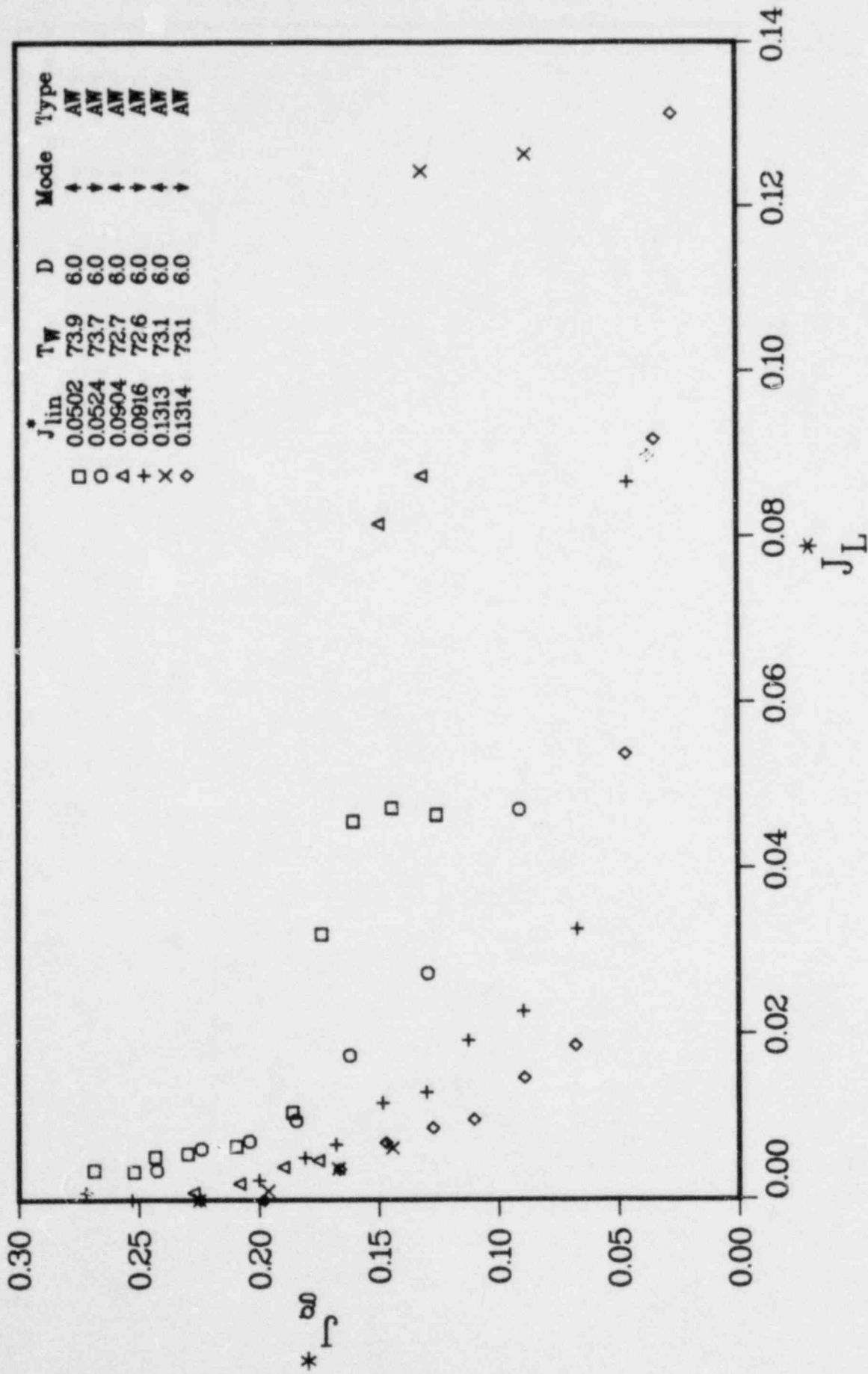


FIGURE 35. FLOODING VELOCITIES FOR AIR-WATER FLOWS IN 6-INCH DIAMETER TUBE WITH $T_W = 75^\circ F$

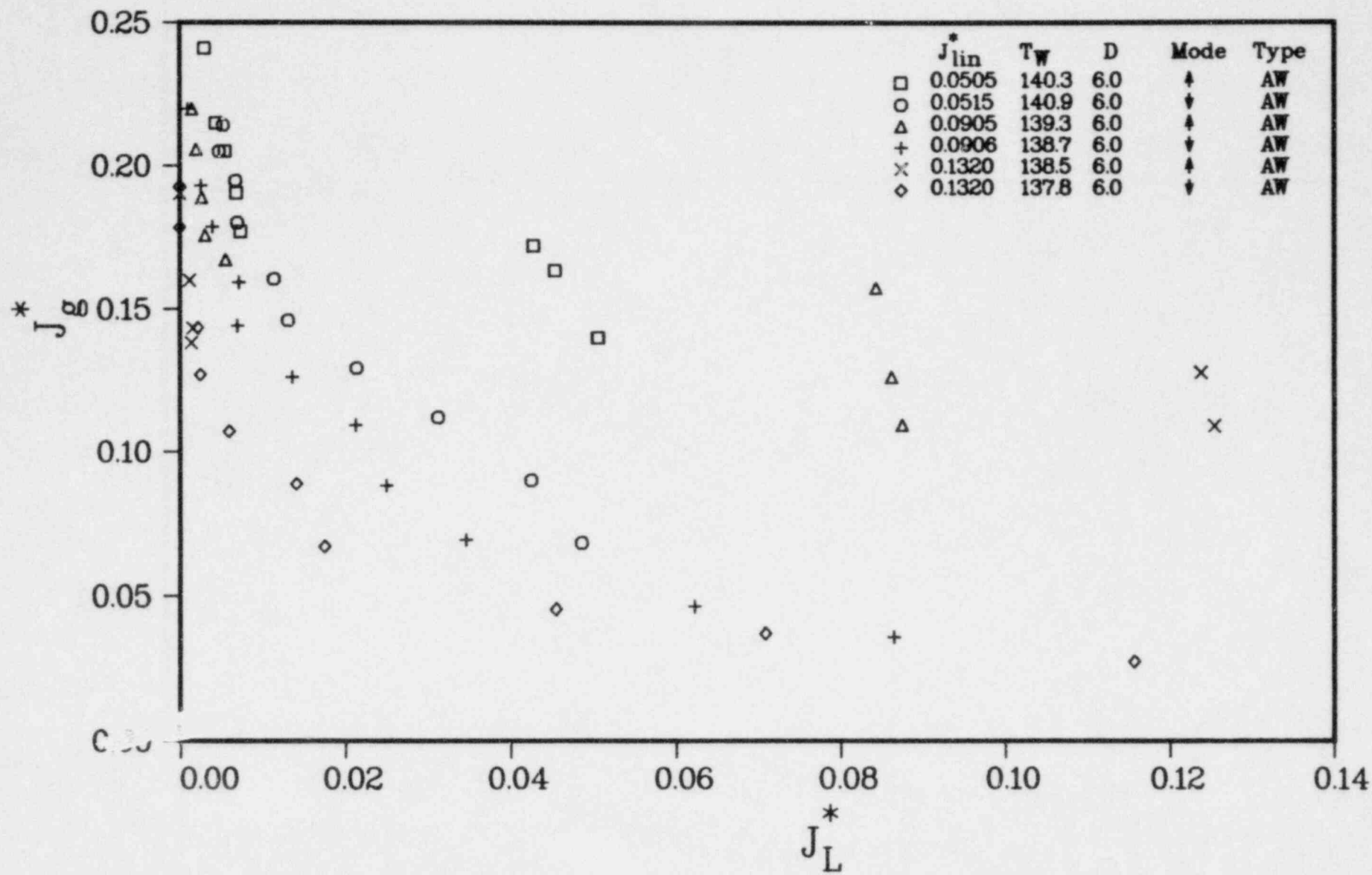


FIGURE 36. FLOODING VELOCITIES FOR AIR-WATER FLOWS IN 6-INCH DIAMETER TUBE WITH $T_W = 140^\circ\text{F}$

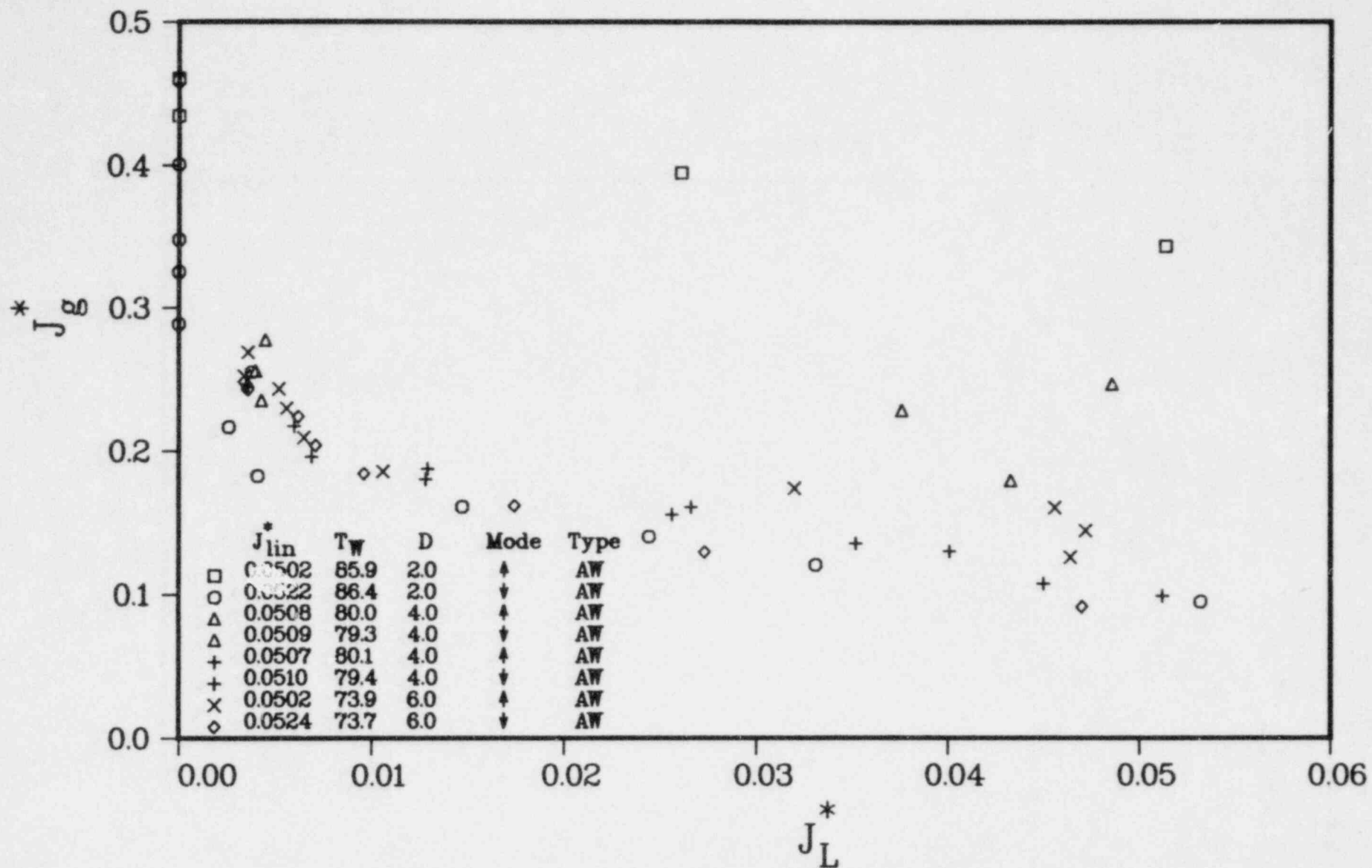


FIGURE 37. VARIATION OF FLOODING VELOCITIES AS A FUNCTION OF TUBE DIAMETER FOR AIR-WATER FLOWS WITH $T_w = 80^\circ\text{F}$ AND $J_{LIN}^* = 0.05$

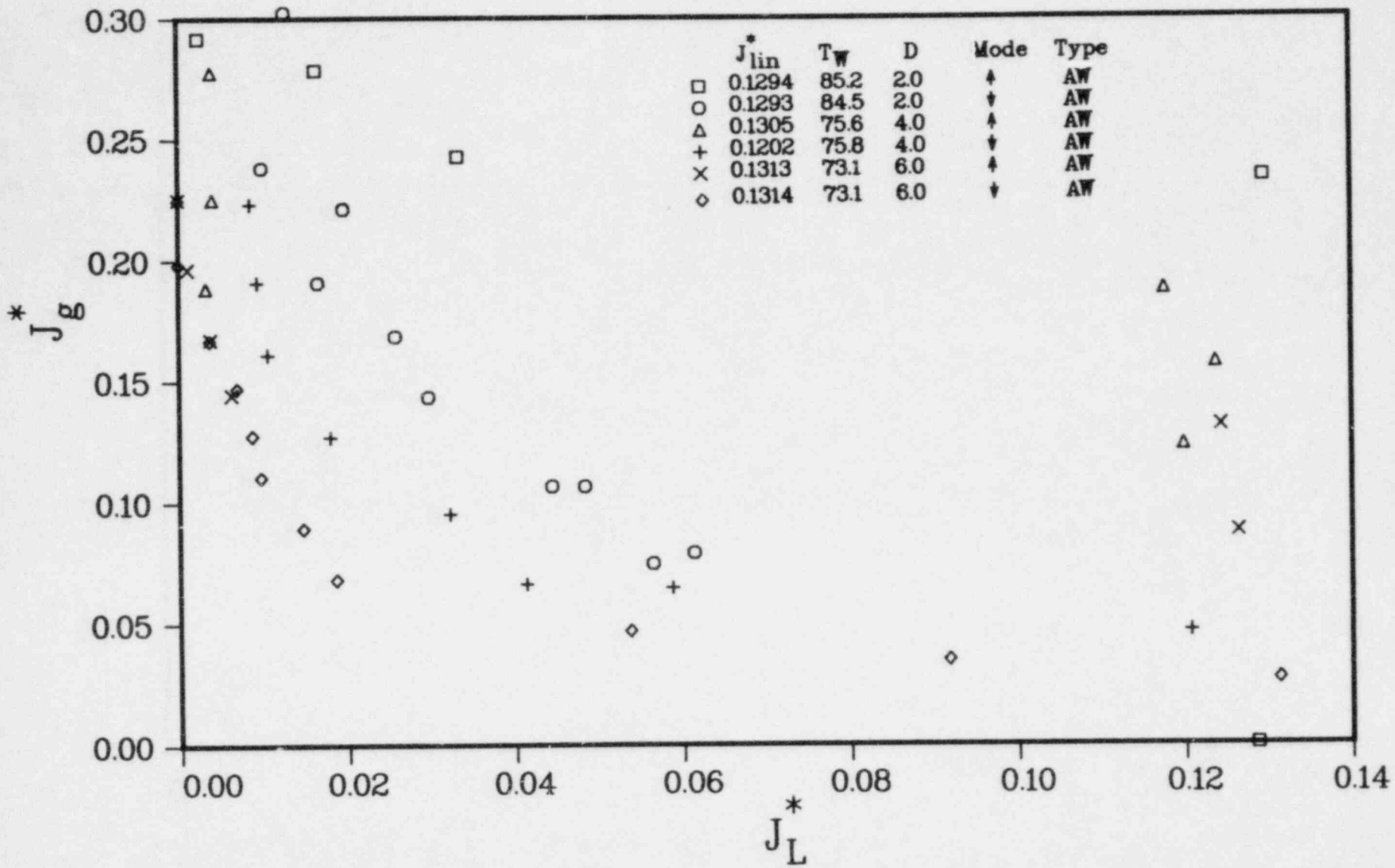


FIGURE 38. VARIATION OF FLOODING VELOCITIES AS A FUNCTION OF TUBE DIAMETER FOR AIR-WATER FLOWS WITH $T_W = 80^\circ\text{F}$ AND $J_{LIN}^* = 0.125$

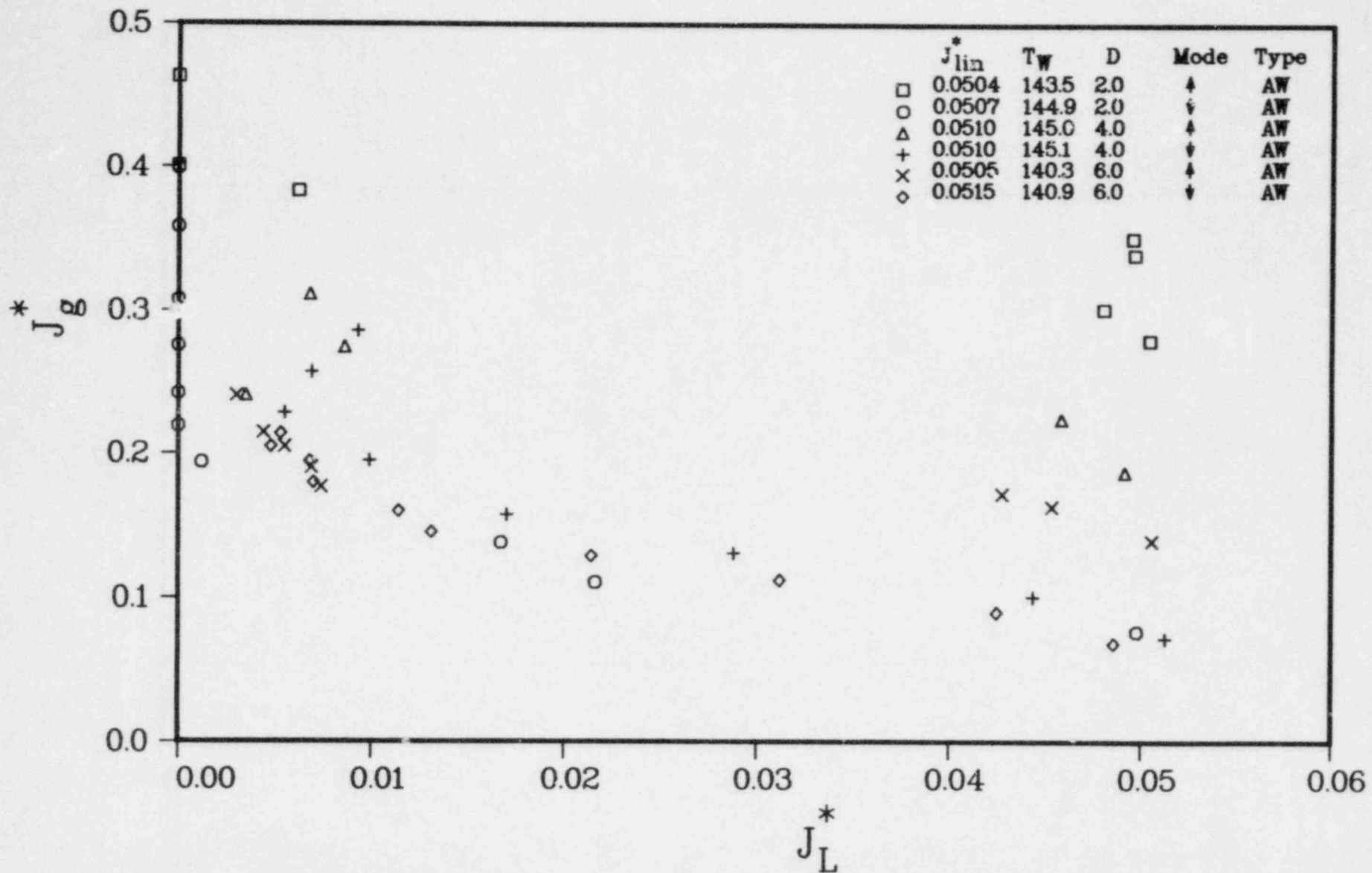


FIGURE 39. VARIATION OF FLOODING VELOCITIES AS A FUNCTION OF TUBE DIAMETER FOR AIR-WATER FLOWS WITH $T_W = 140^\circ\text{F}$ AND $J_{LIN}^* = 0.05$

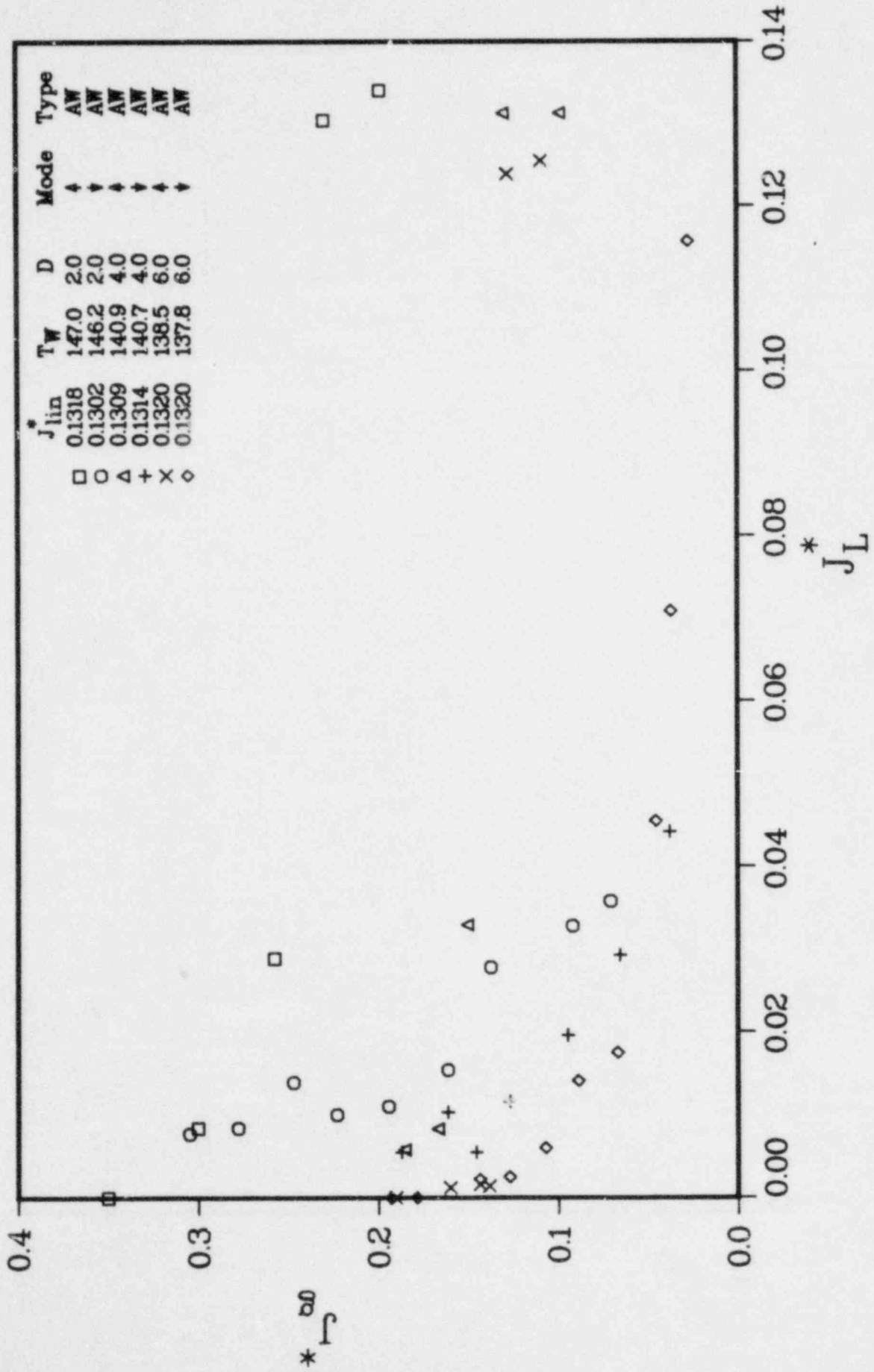


FIGURE 40. VARIATION OF FLOODING VELOCITIES AS A FUNCTION OF TUBE DIAMETER FOR AIR-WATER FLOWS WITH $T_W = 140^\circ F$ AND $J_{LIN}^* = 0.125$

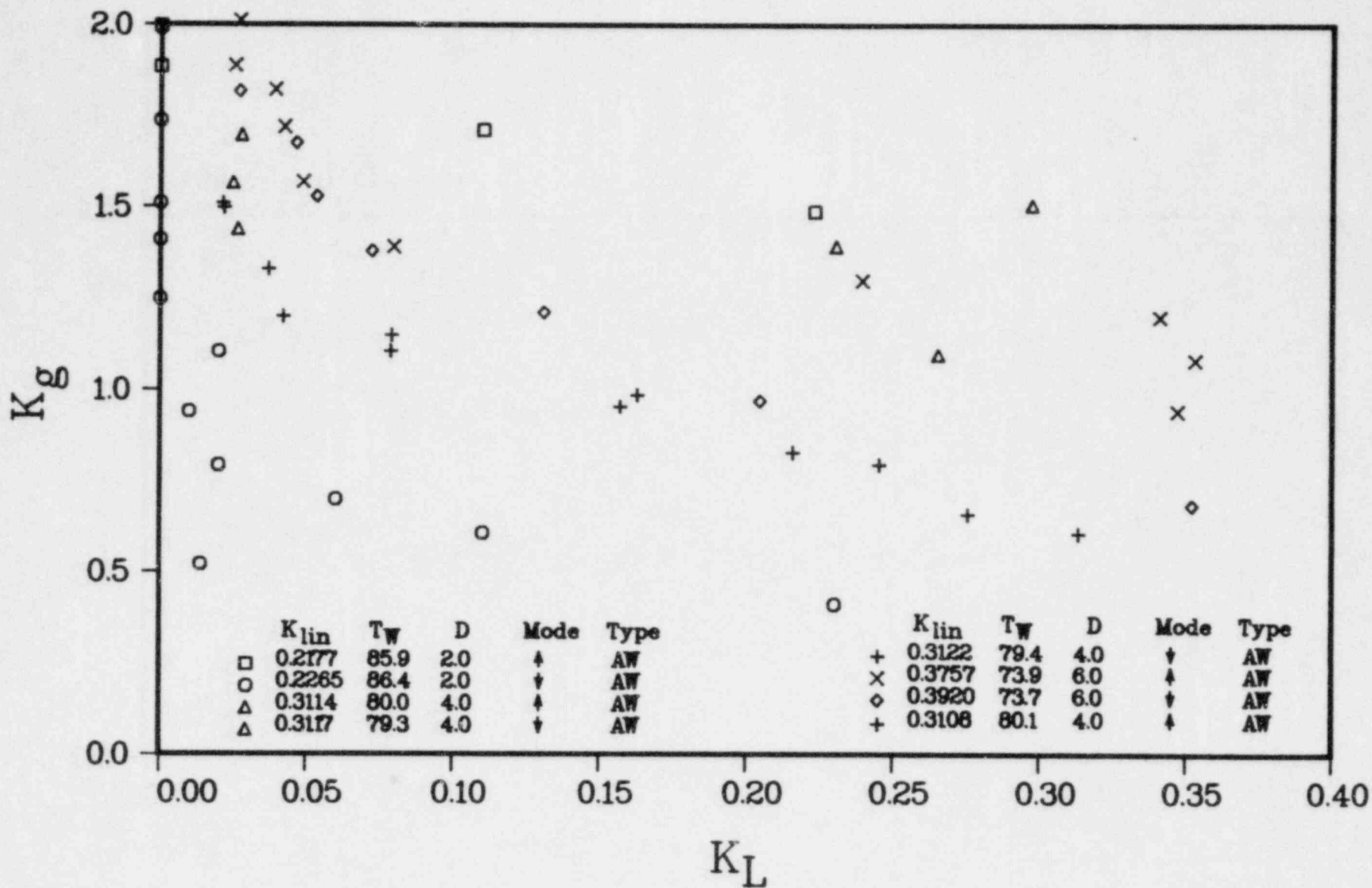


FIGURE 41. VARIATION OF FLOODING VELOCITIES AS A FUNCTION OF TUBE DIAMETER FOR AIR-WATER FLOWS WITH $T_W = 80^\circ\text{F}$

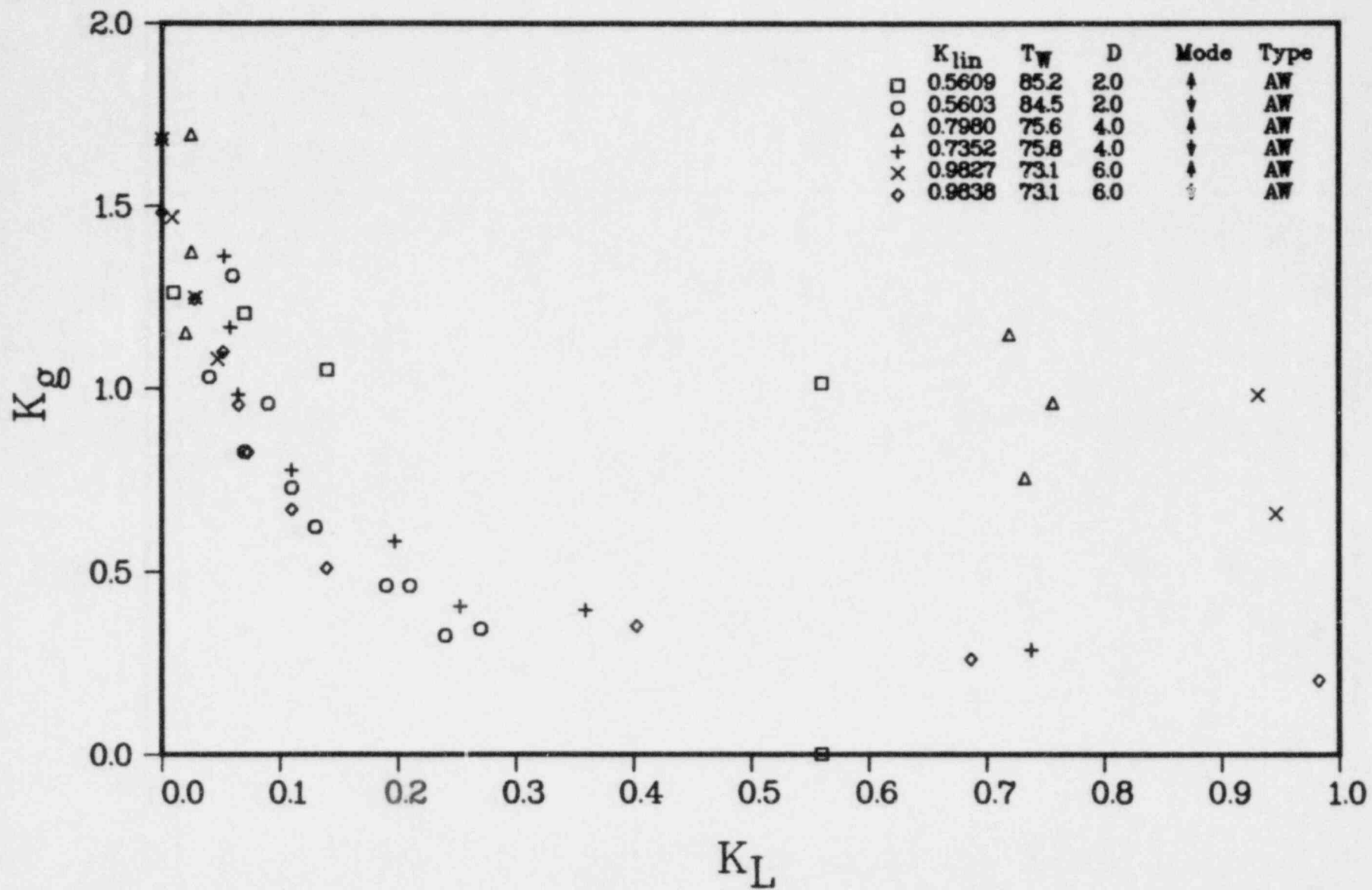


FIGURE 42. VARIATION OF FLOODING VELOCITIES AS A FUNCTION OF TUBE DIAMETER FOR AIR-WATER FLOWS WITH $T_W = 30^\circ\text{F}$

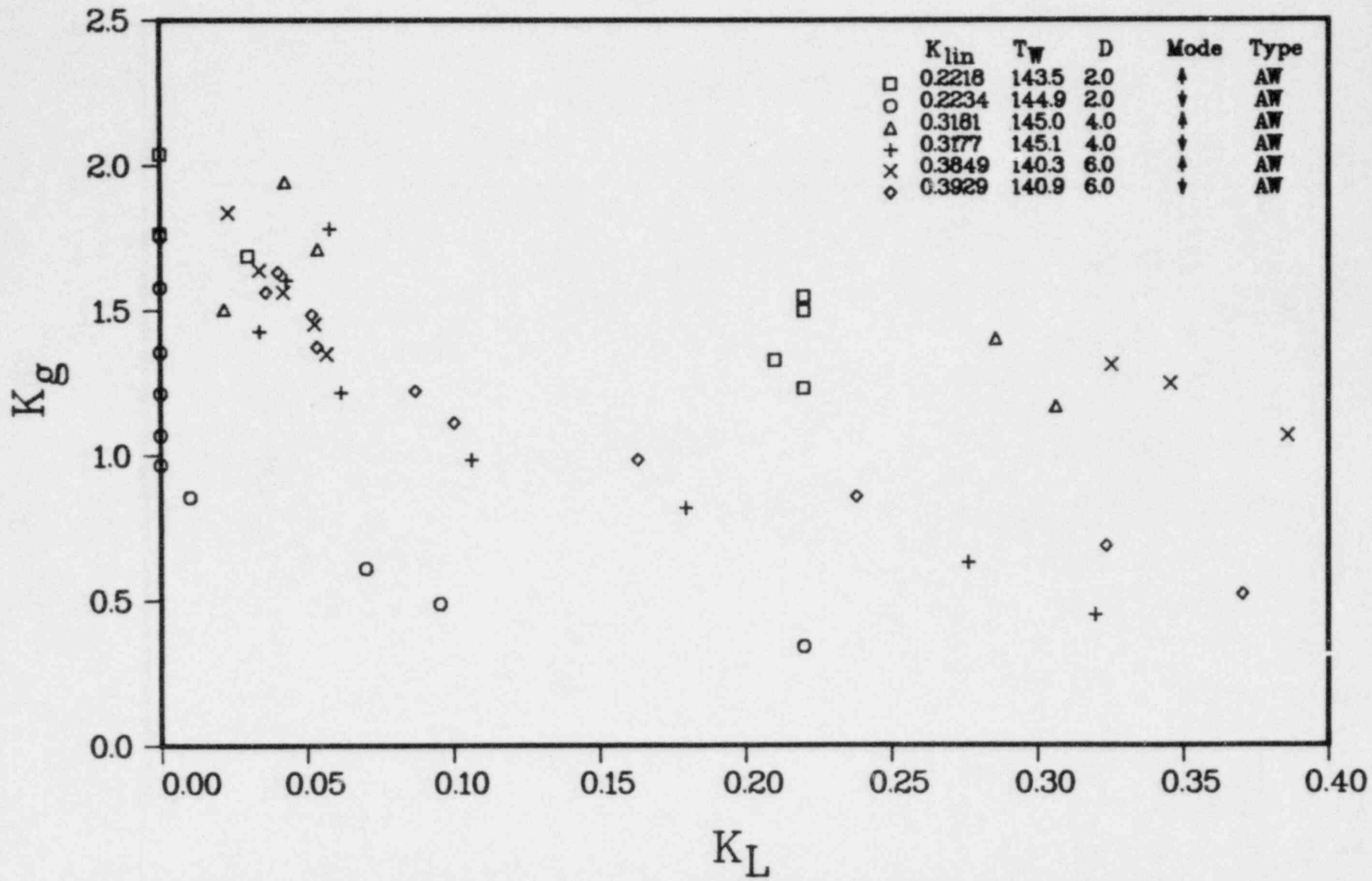


FIGURE 43. VARIATION OF FLOODING VELOCITIES AS A FUNCTION OF TUBE DIAMETER FOR AIR-WATER FLOWS WITH $T_W = 140^\circ\text{F}$

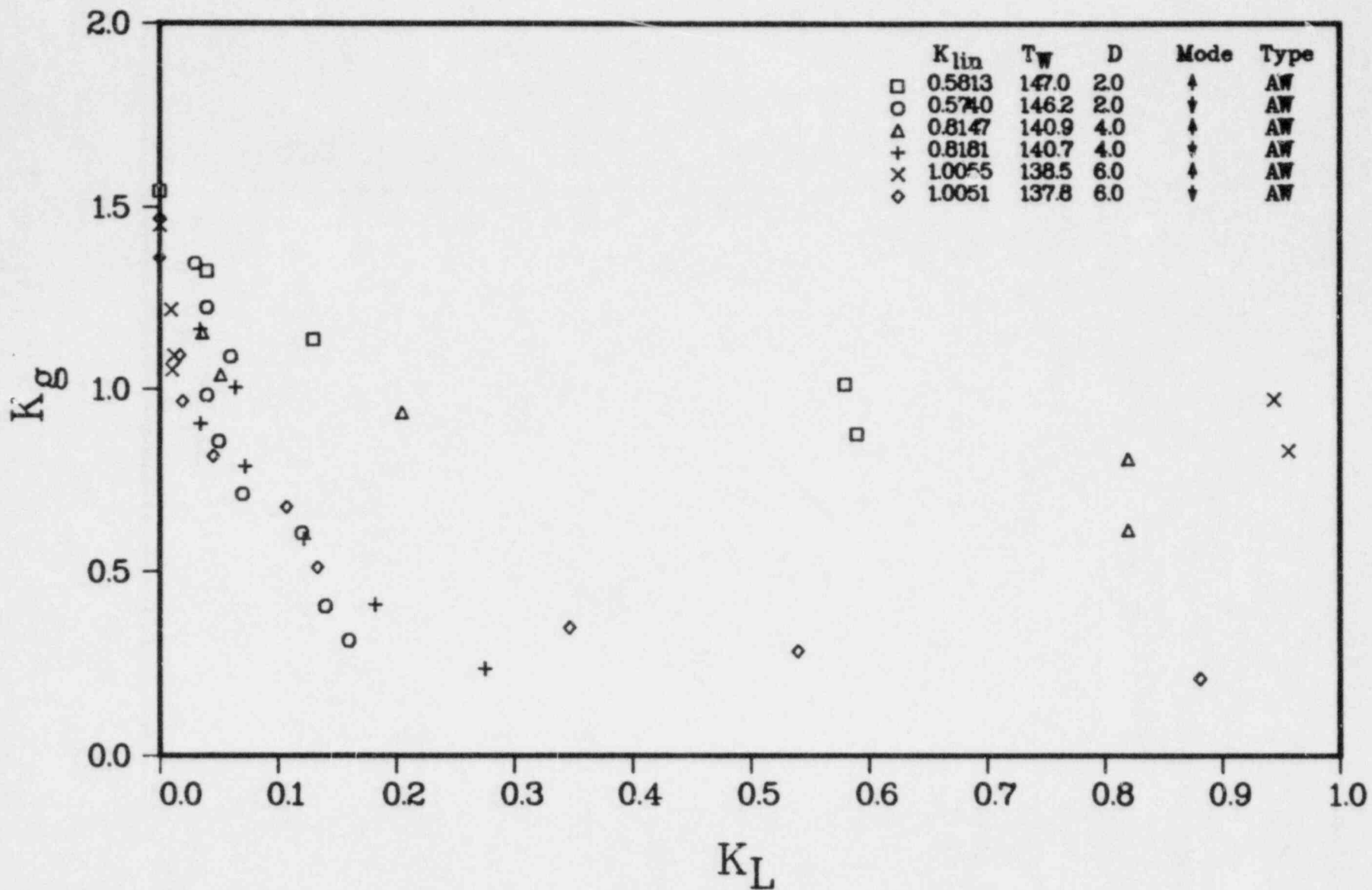


FIGURE 44. VARIATION OF FLOODING VELOCITIES AS A FUNCTION OF TUBE DIAMETER FOR AIR-WATER FLOWS WITH $T_W = 140^\circ\text{F}$

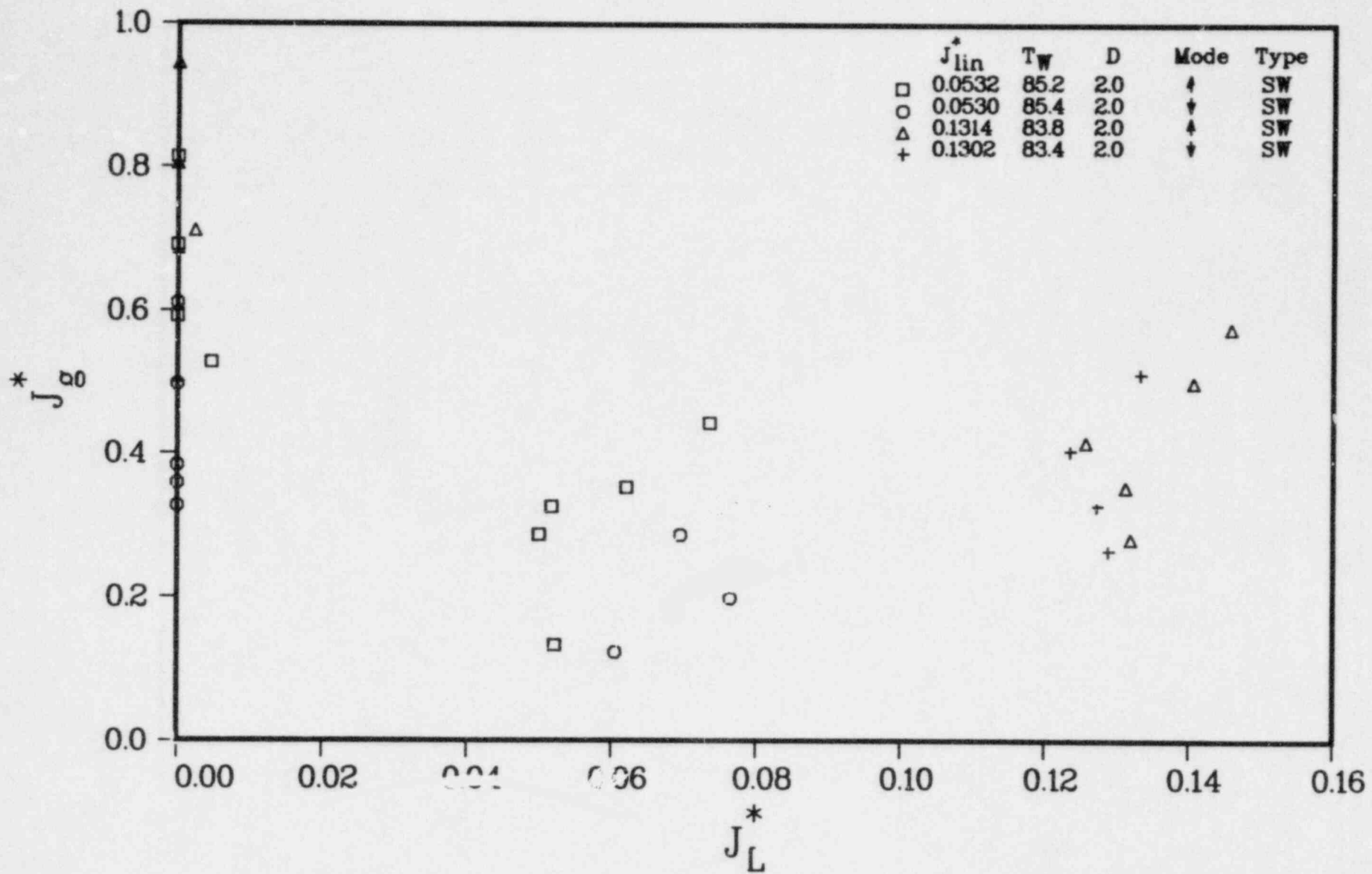


FIGURE 45. FLOODING VELOCITIES FOR STEAM-WATER FLOWS IN 2-INCH DIAMETER TUBE WITH $T_W = 85^\circ\text{F}$

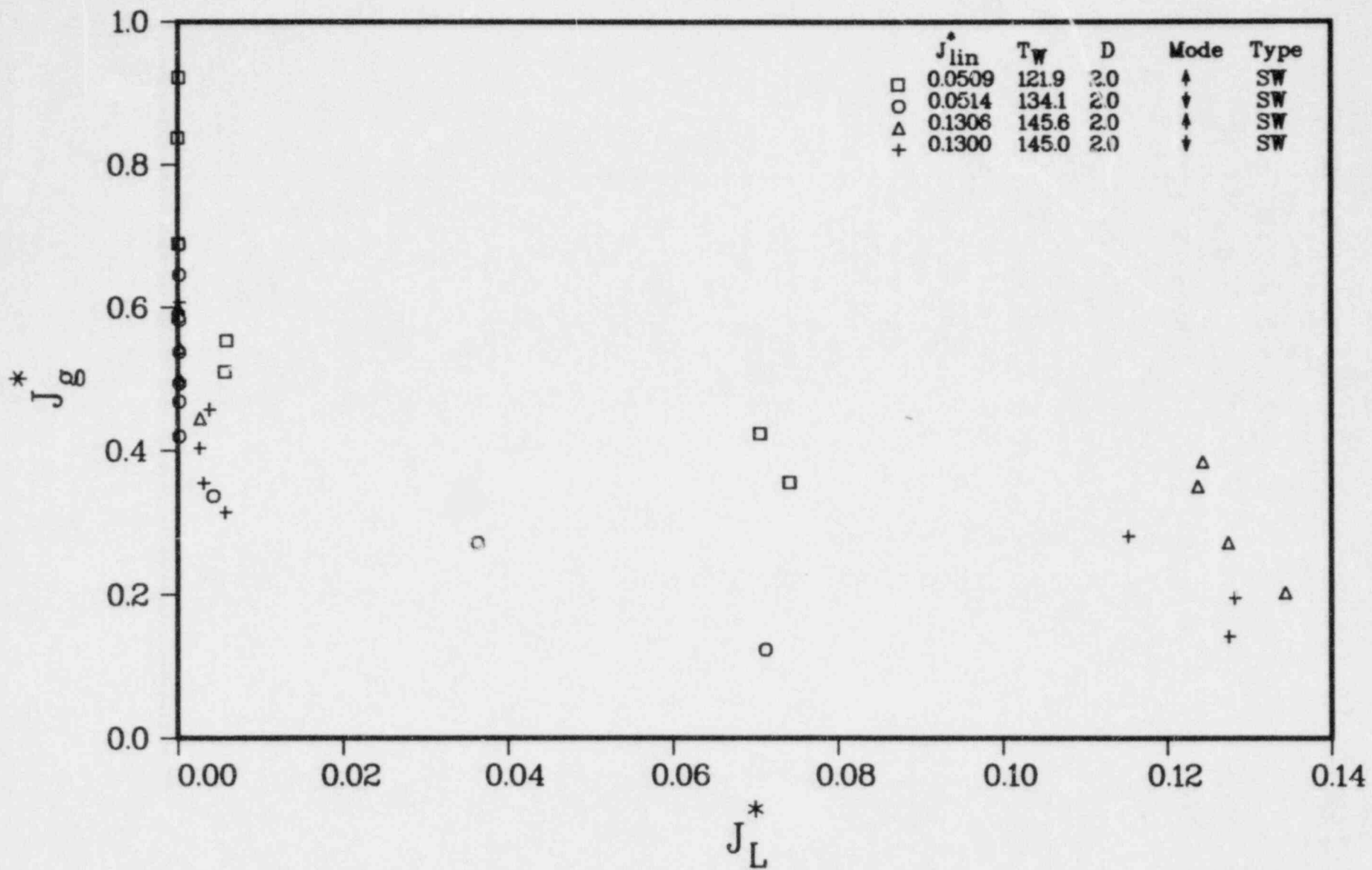


FIGURE 46. FLOODING VELOCITIES FOR STEAM-WATER FLOWS IN 2-INCH DIAMETER TUBE WITH $T_W = 140^\circ\text{F}$

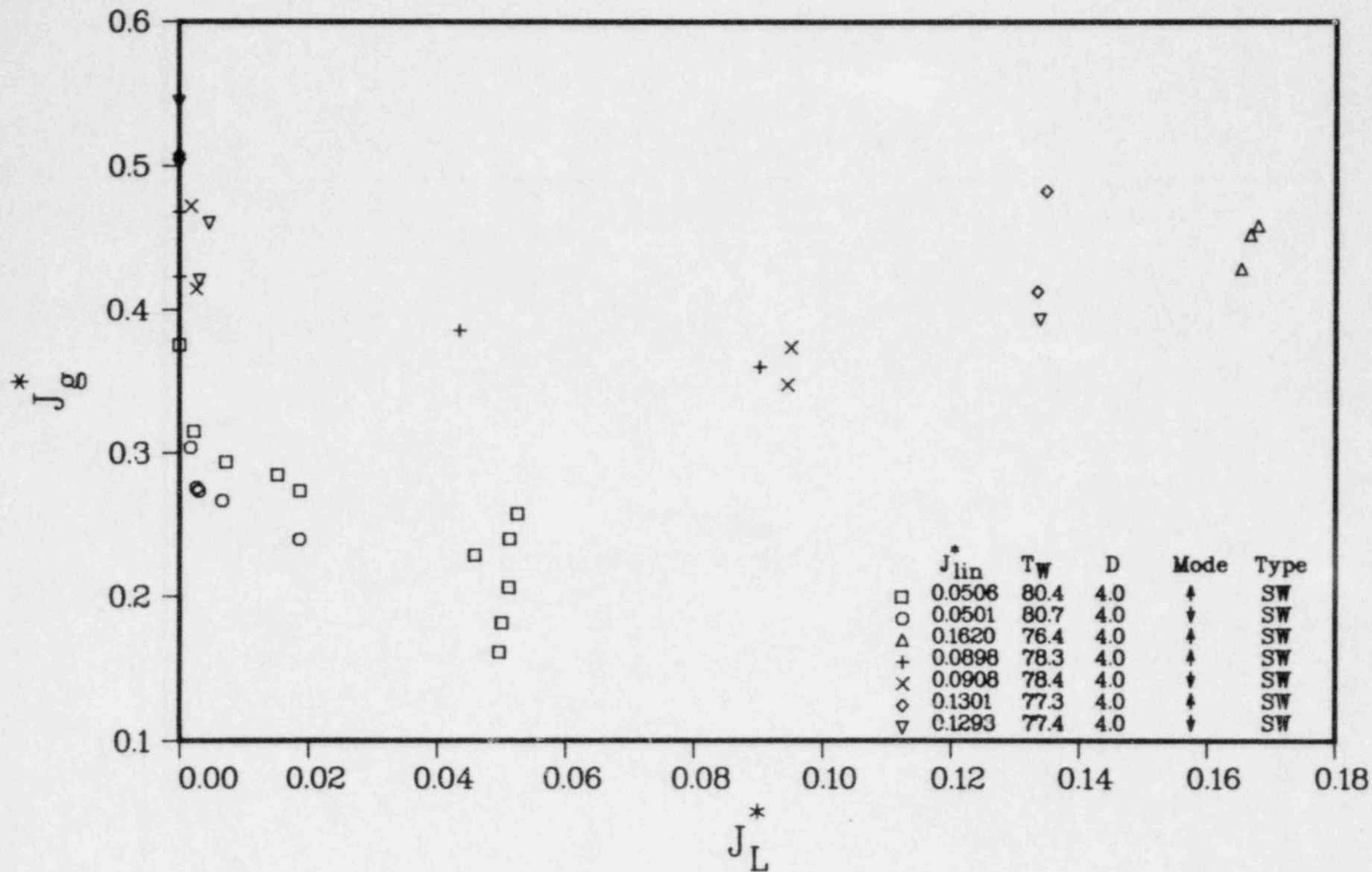


FIGURE 47. FLOODING VELOCITIES FOR STEAM-WATER FLOWS IN 4-INCH DIAMETER TUBE WITH $T_W = 80^\circ\text{F}$

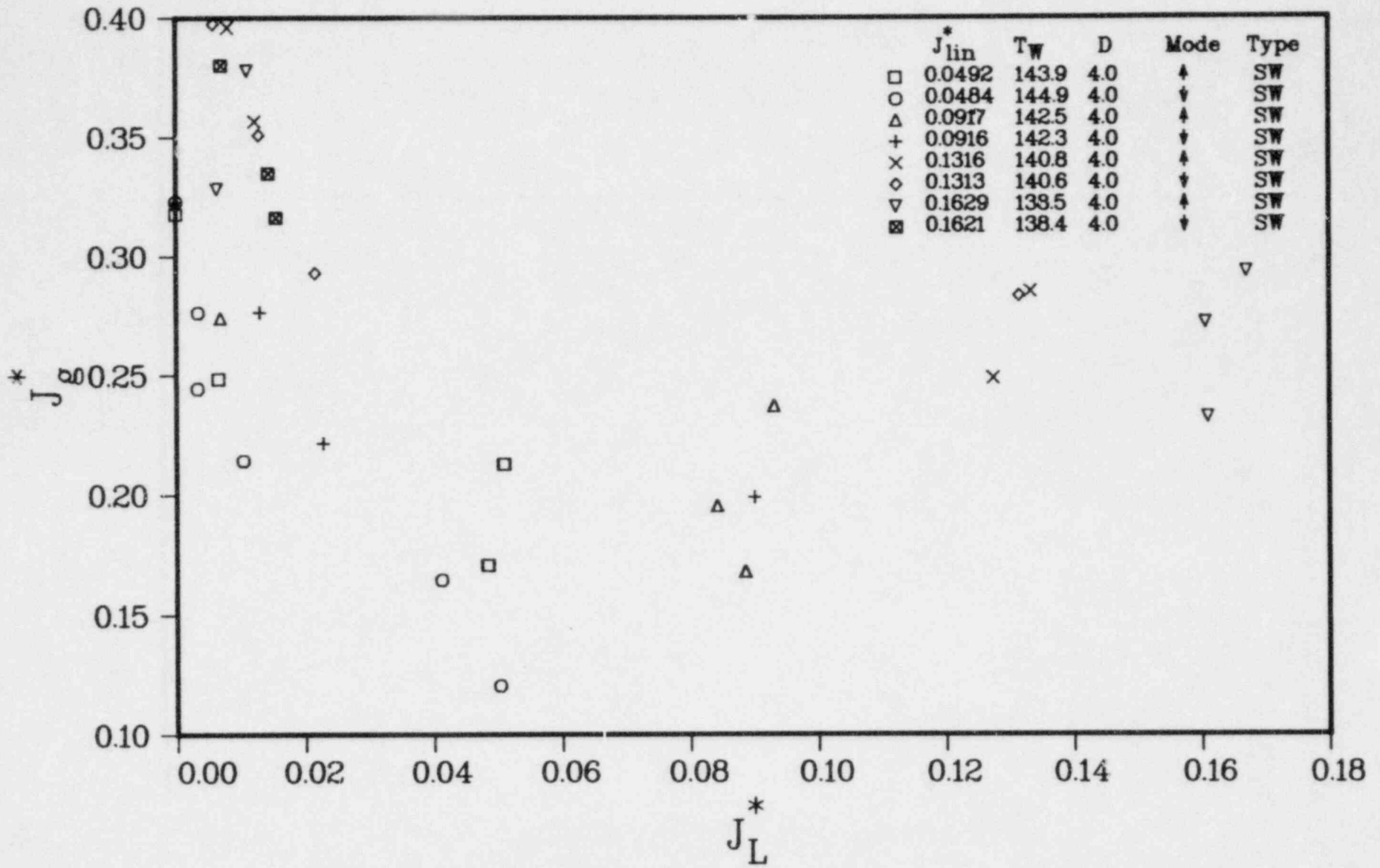


FIGURE 48. FLOODING VELOCITIES FOR STEAM-WATER FLOWS IN 4-INCH DIAMETER TUBE WITH $T_W = 140^\circ\text{F}$

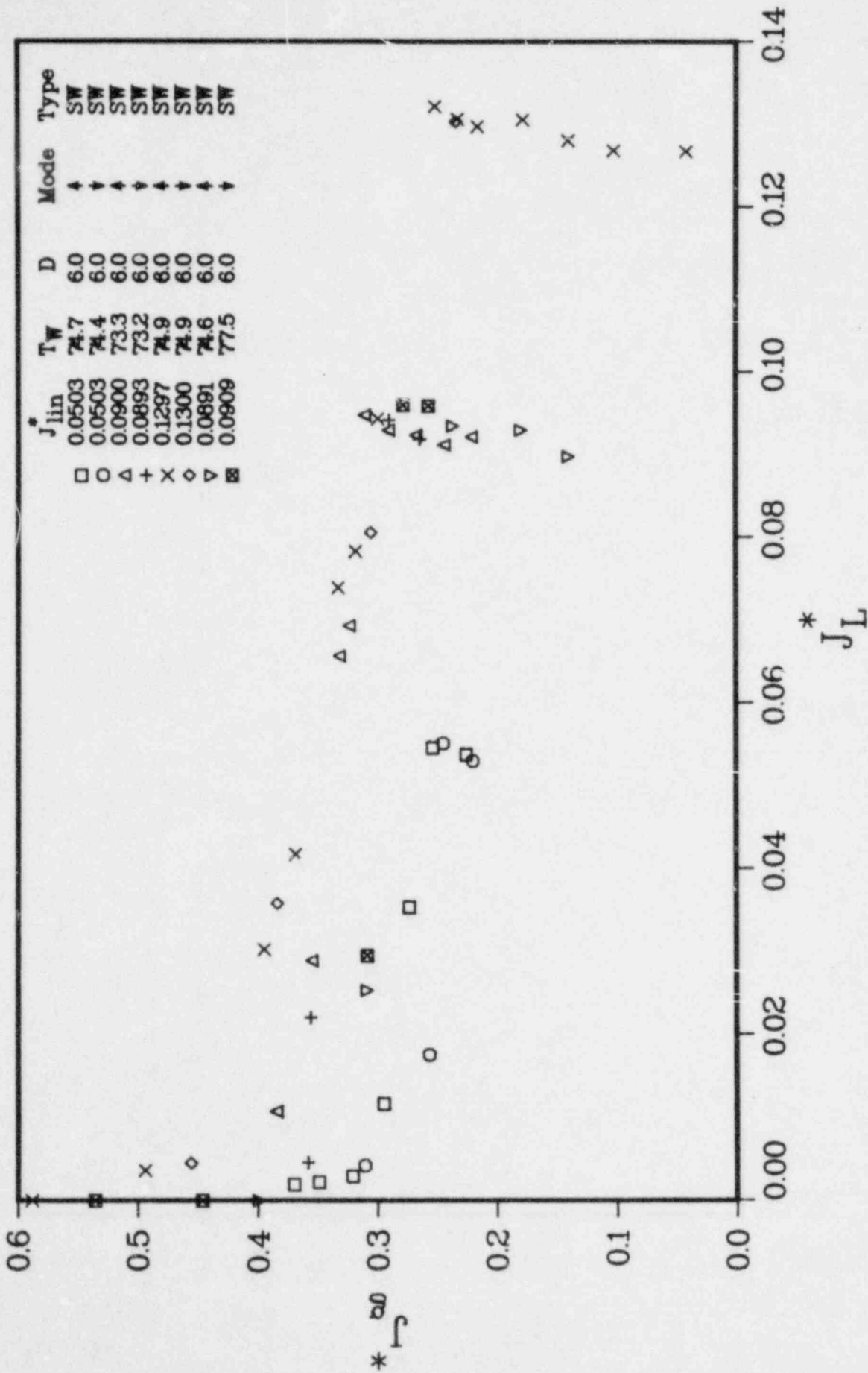


FIGURE 49. FLOODING VELOCITIES FOR STEAM-WATER FLOWS IN 6-INCH DIAMETER TUBE WITH $T_W = 75^\circ F$

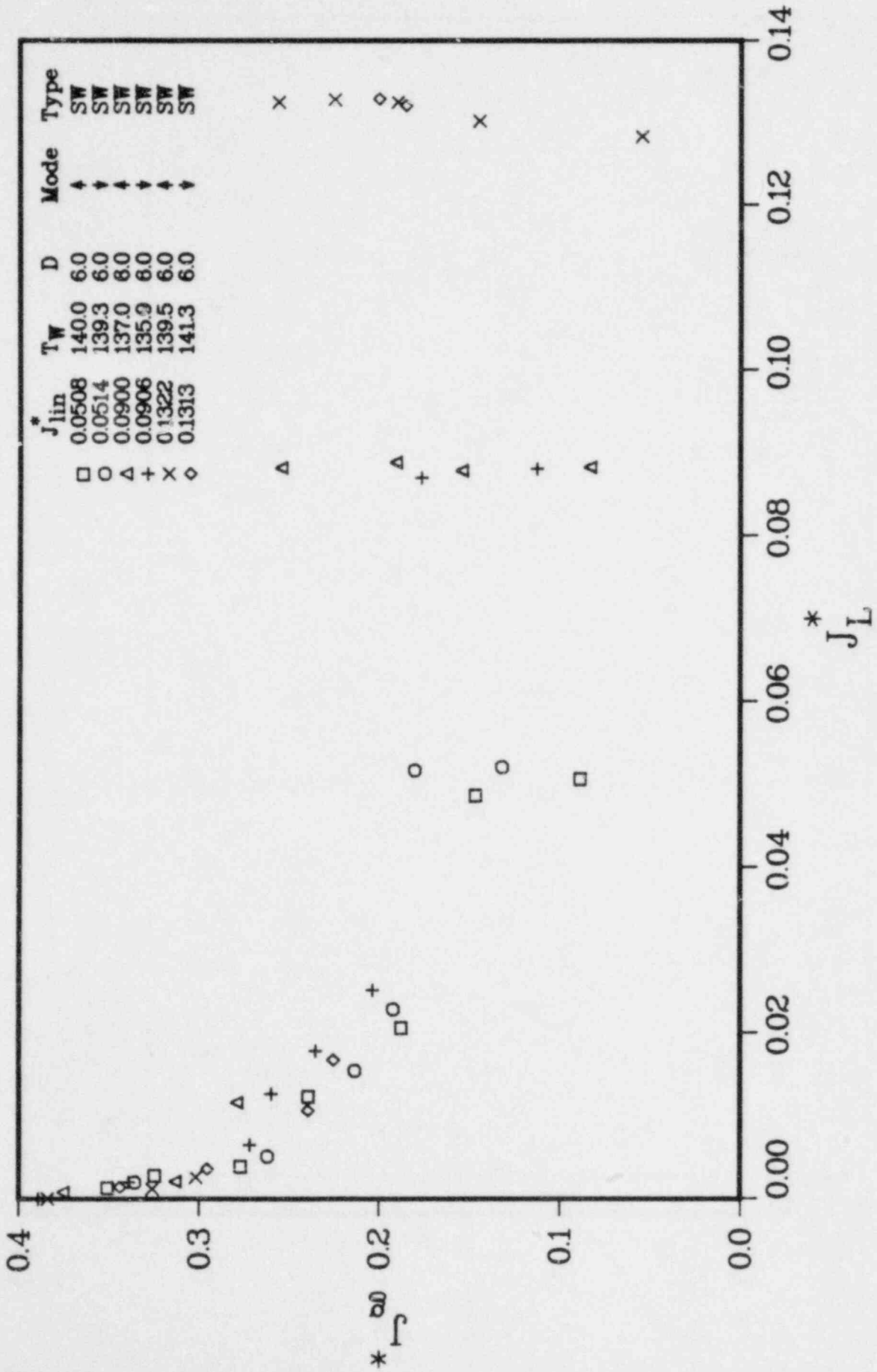


FIGURE 50. FLOODING VELOCITIES FOR STEAM-WATER FLOWS IN 6-INCH DIAMETER TUBE WITH $T_M = 140^\circ F$

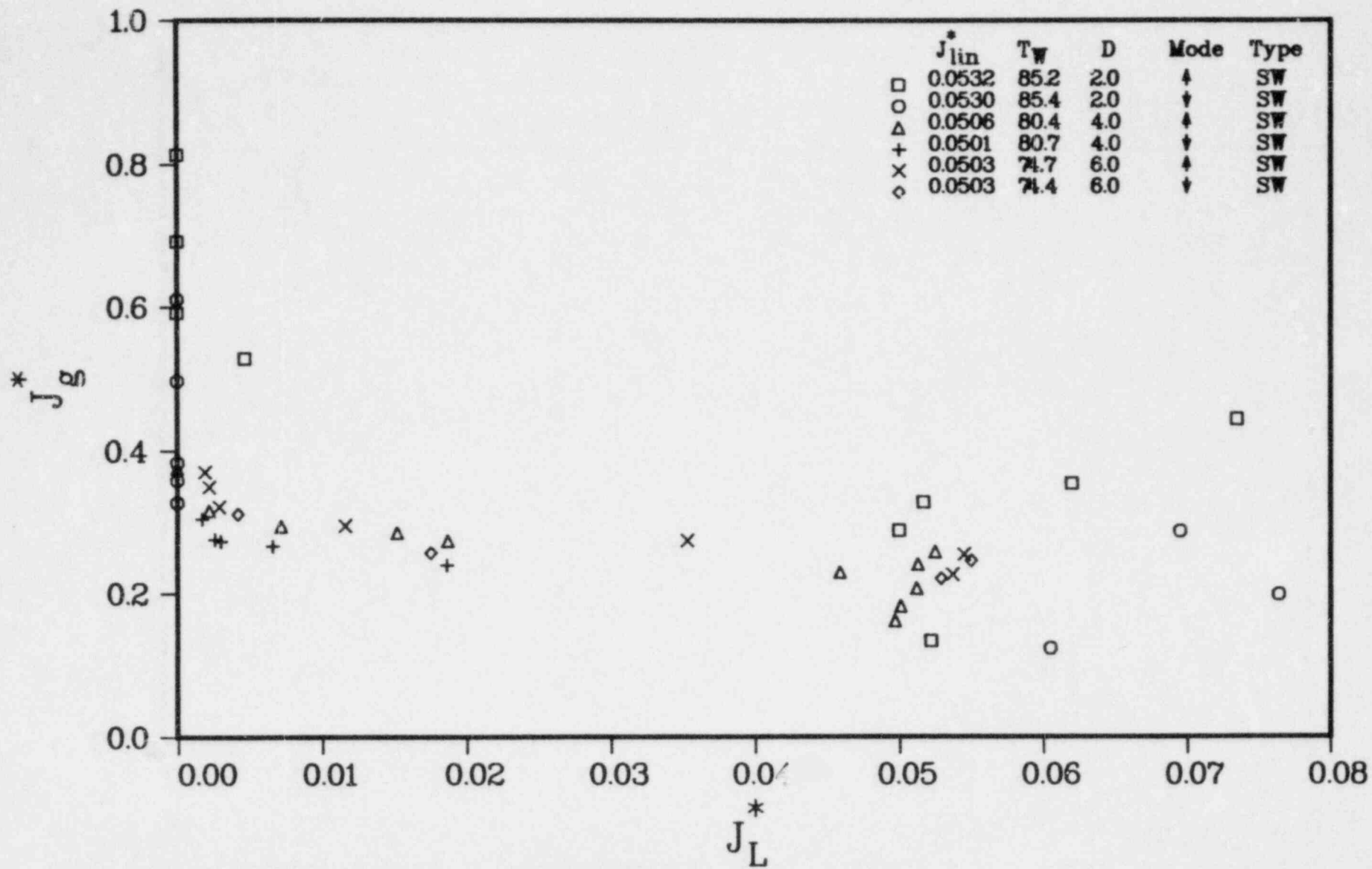


FIGURE 51. VARIATION OF FLOODING VELOCITIES AS A FUNCTION OF DIAMETER FOR STEAM-WATER FLOWS WITH $T_W = 80^\circ\text{F}$ AND $J_{LIN}^* = 0.05$

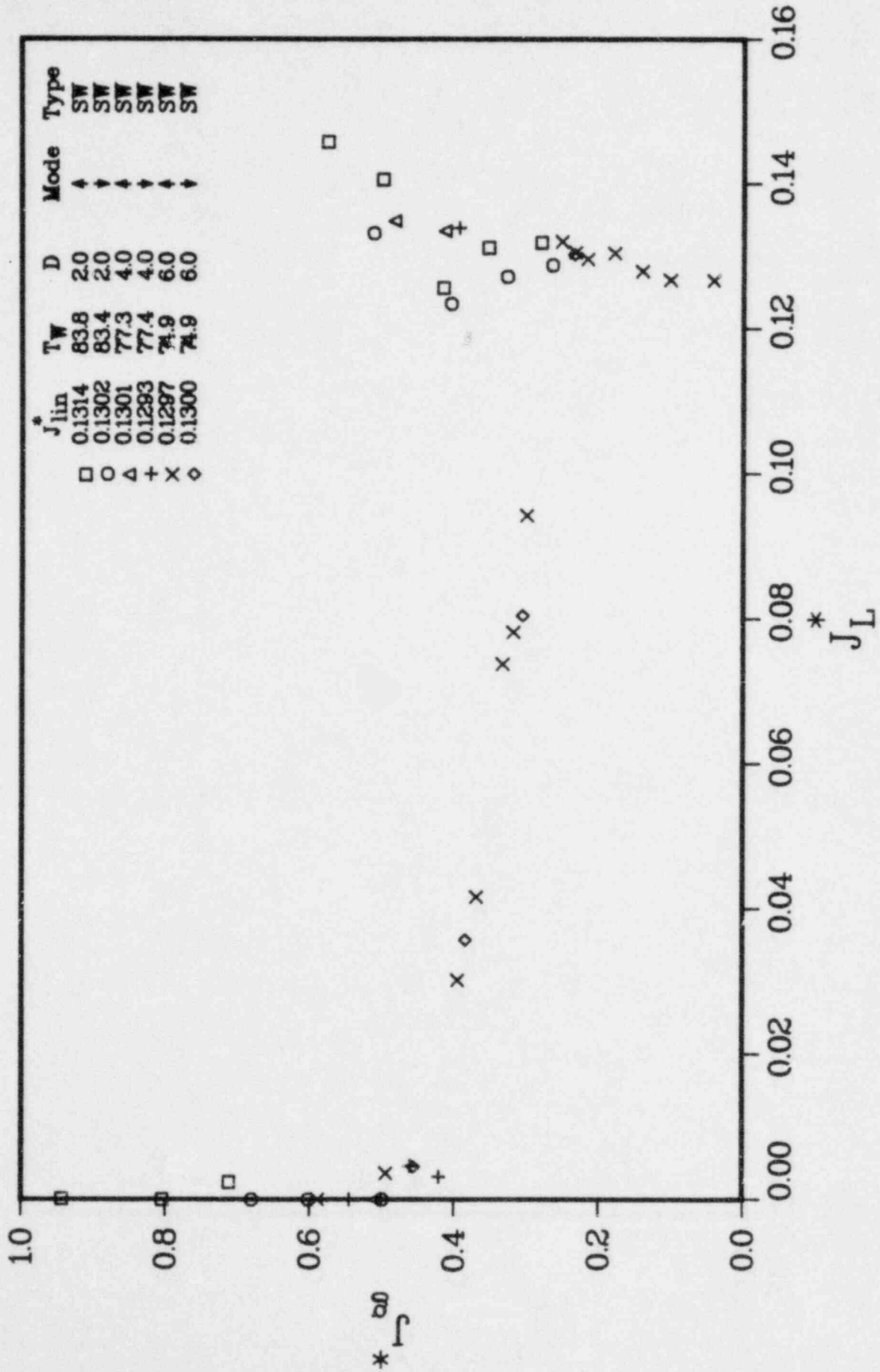


FIGURE 52. VARIATION OF FLOODING VELOCITIES AS A FUNCTION OF DIAMETER FOR STEAM-WATER FLOWS WITH $T_W = 75^\circ F$ AND $J_{LIN}^* = 0.13$

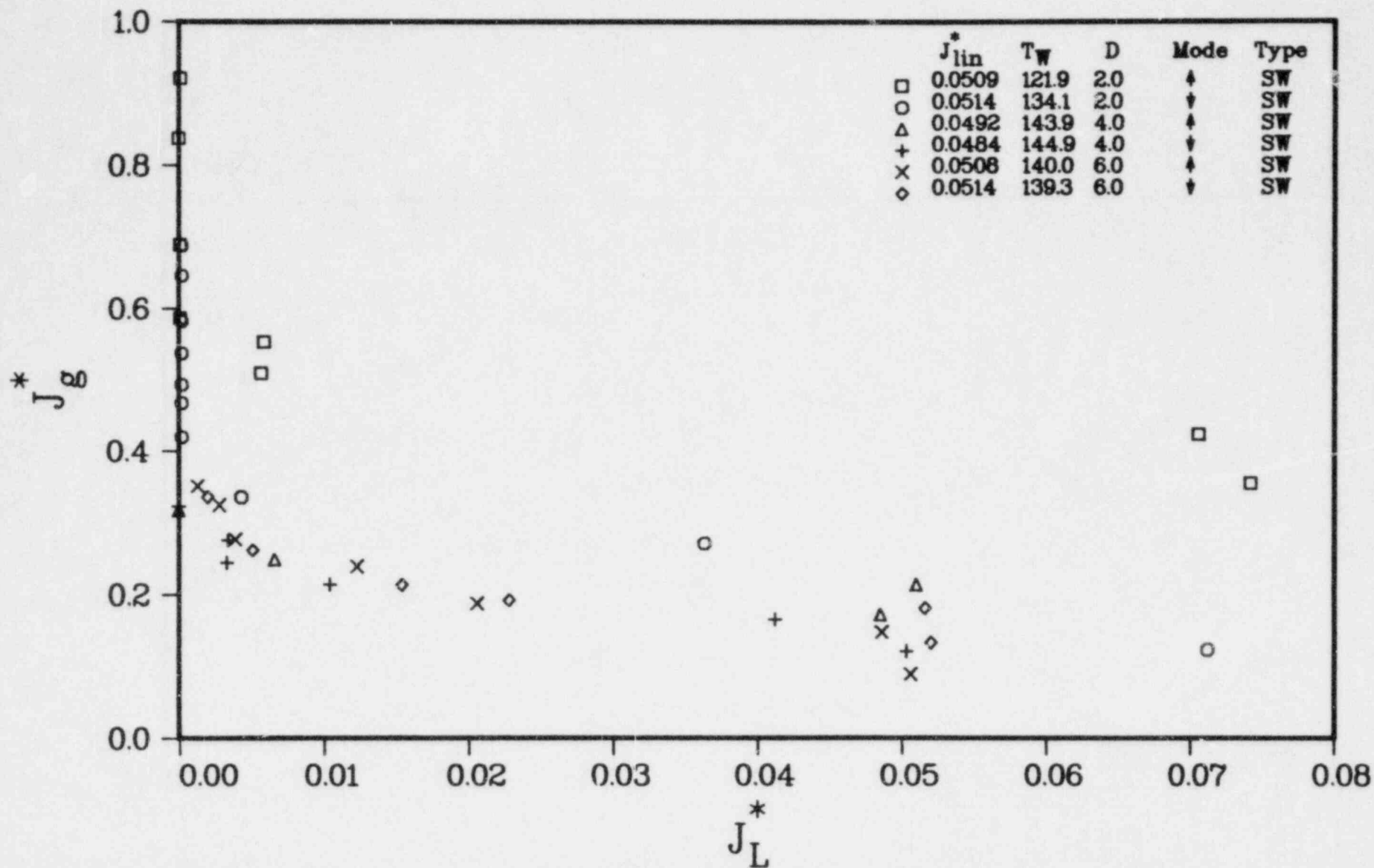


FIGURE 53. VARIATION OF FLOODING VELOCITIES AS A FUNCTION OF DIAMETER FOR STEAM-WATER FLOWS WITH $T_W = 140^\circ\text{F}$ AND $J_{LIN}^* = 0.05$

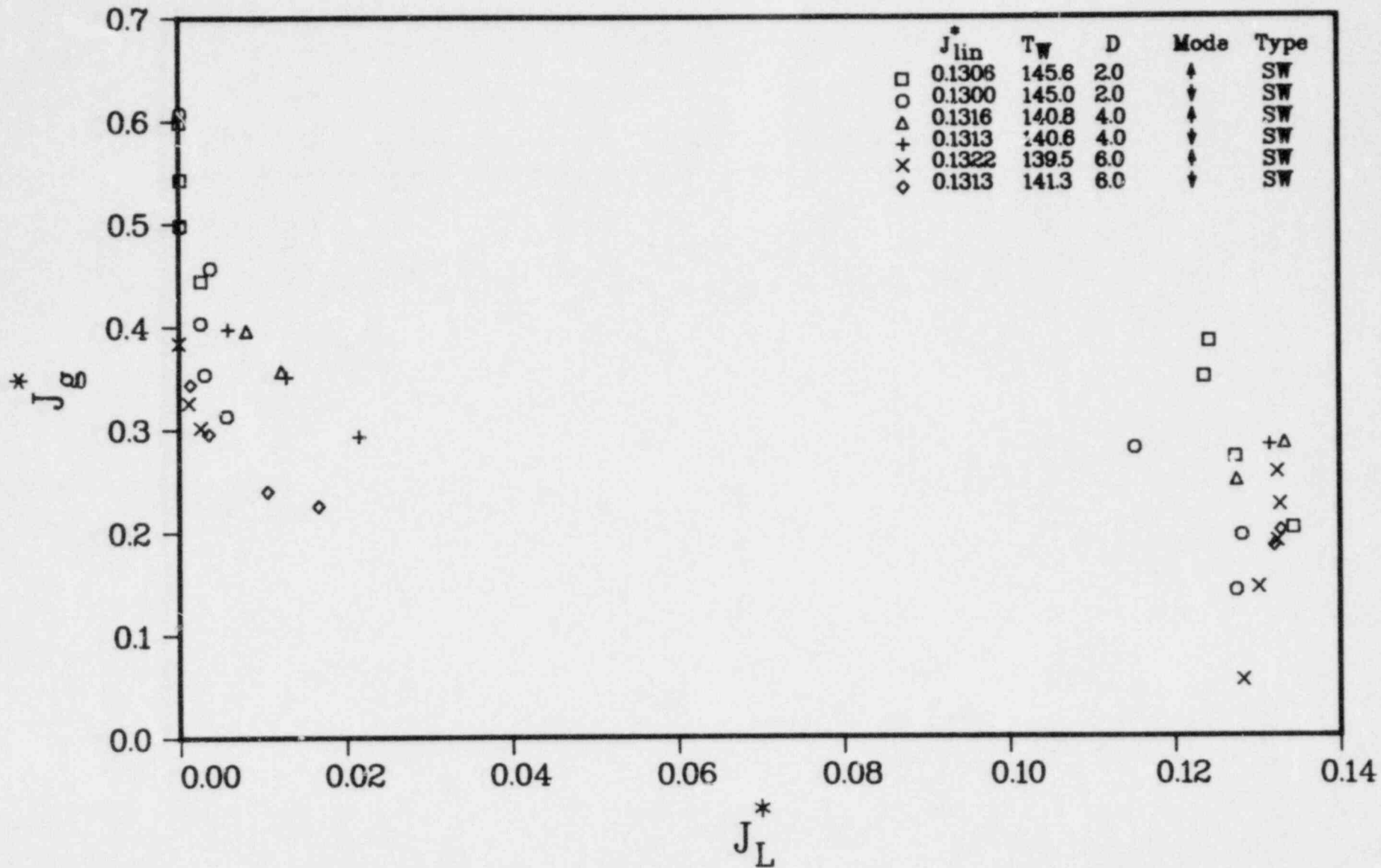


FIGURE 54. VARIATION OF FLOODING VELOCITIES AS A FUNCTION OF DIAMETER FOR STEAM-WATER FLOWS WITH $T_W = 140^\circ\text{F}$ AND $J_{LIN}^* = 0.13$

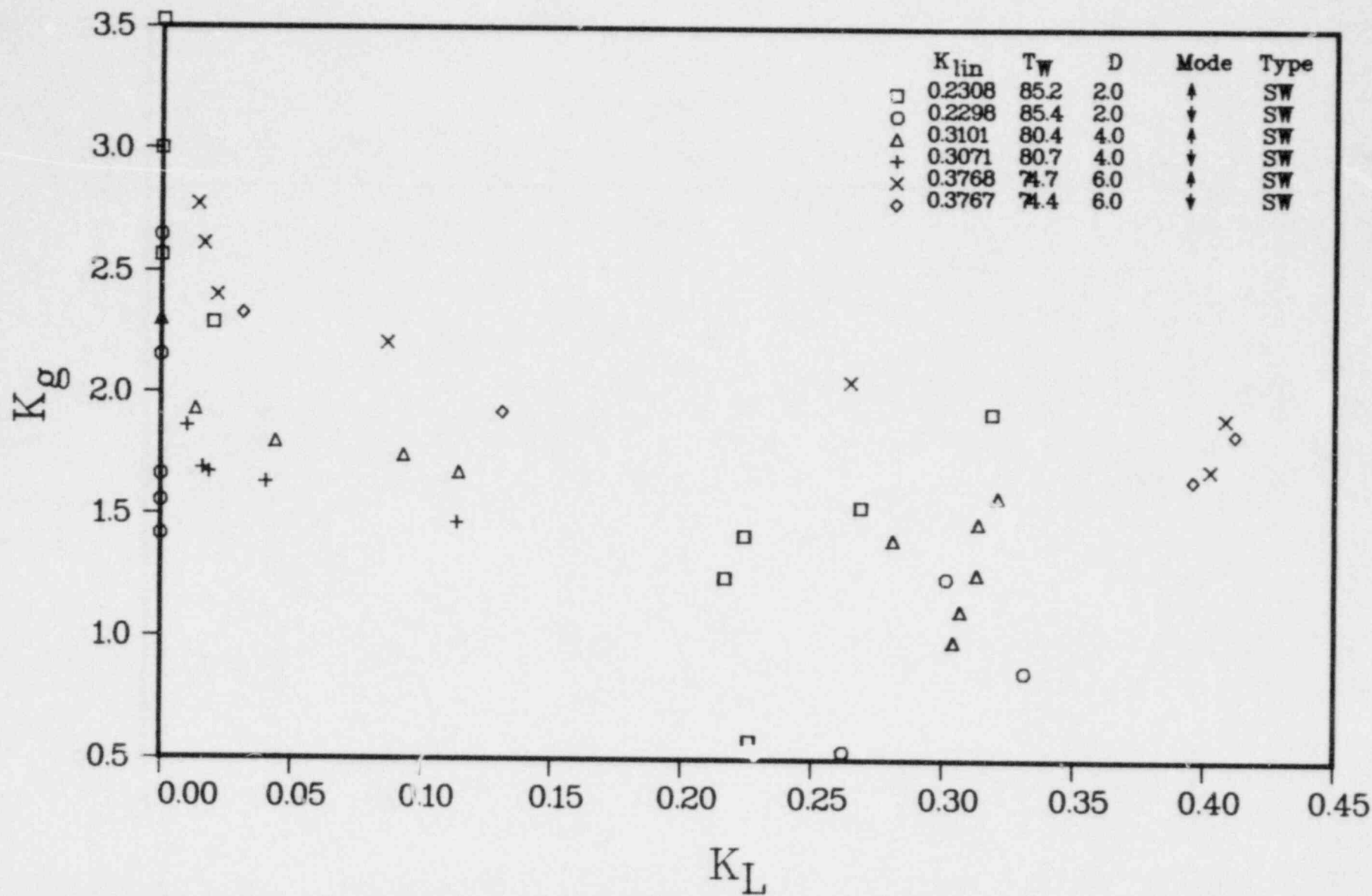


FIGURE 55. VARIATION OF FLOODING VELOCITIES AS A FUNCTION OF DIAMETER FOR STEAM-WATER FLOWS WITH $T_W = 80^\circ F$

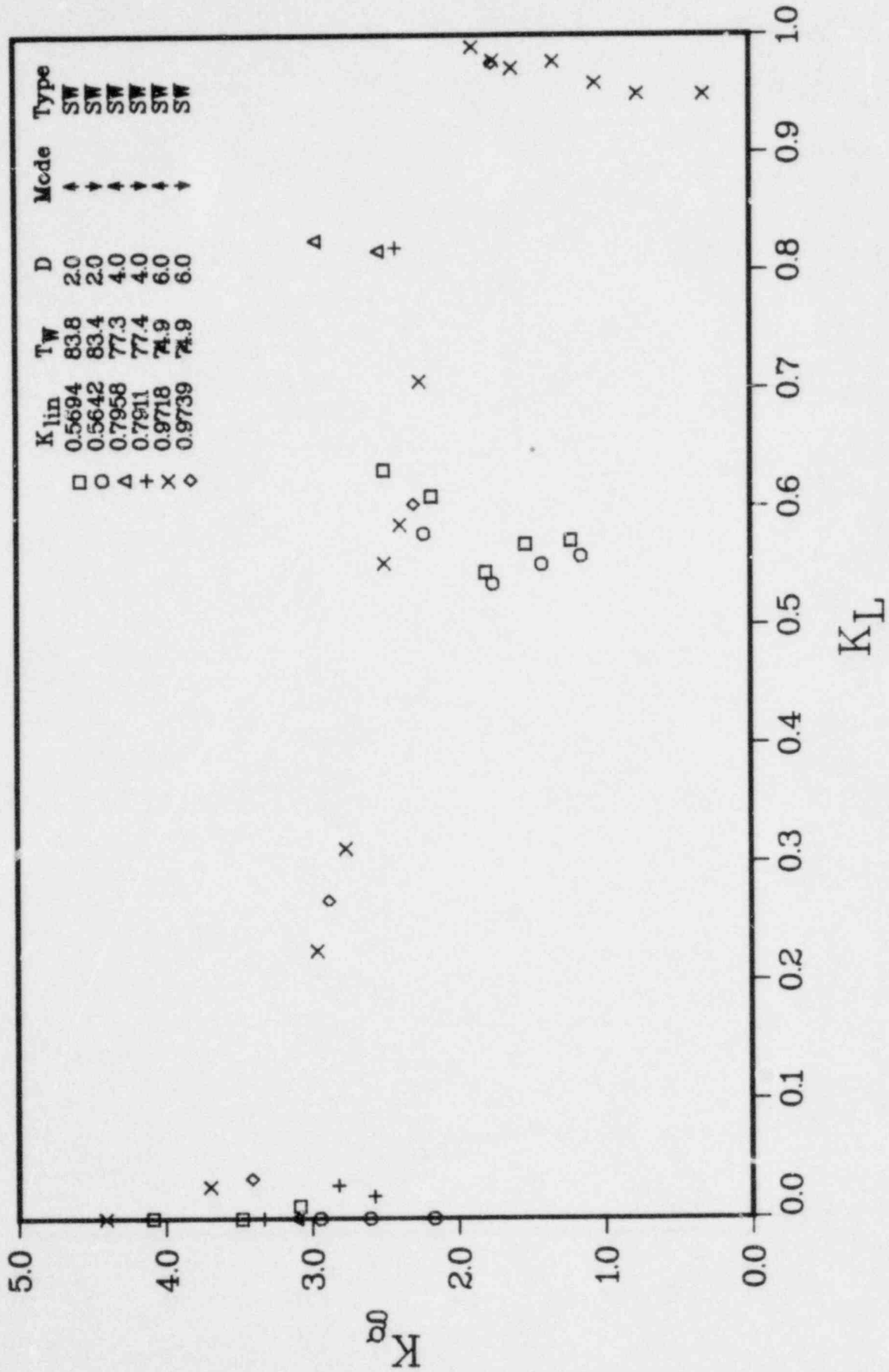


FIGURE 56. VARIATION OF FLOODING VELOCITIES AS A FUNCTION OF DIAMETER FOR STEAM-WATER FLOWS WITH $T_w = 80^\circ F$

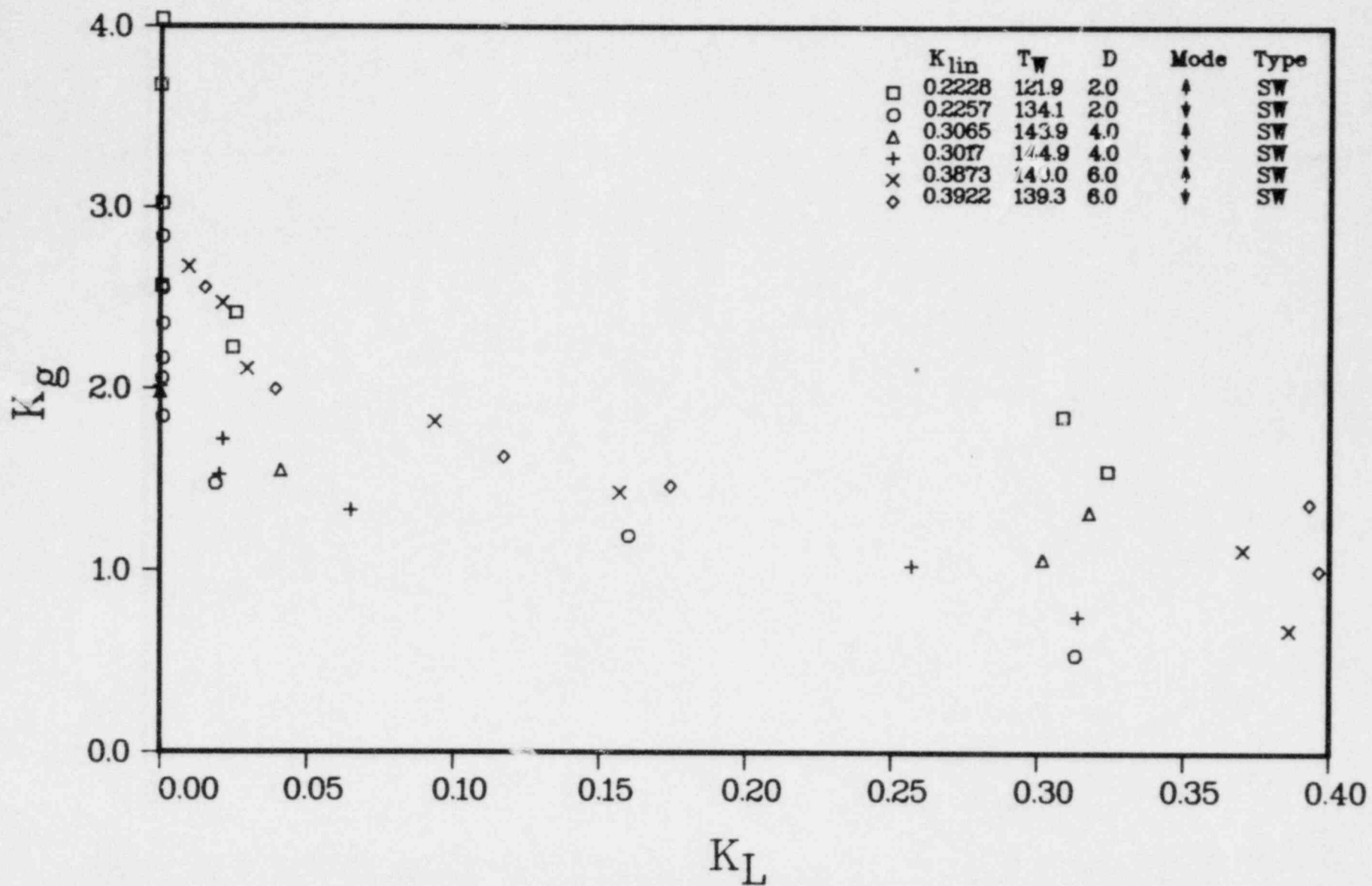


FIGURE 57. VARIATION OF FLOODING VELOCITIES AS A FUNCTION OF DIAMETER FOR STEAM-WATER FLOWS WITH $T_w = 140^\circ F$

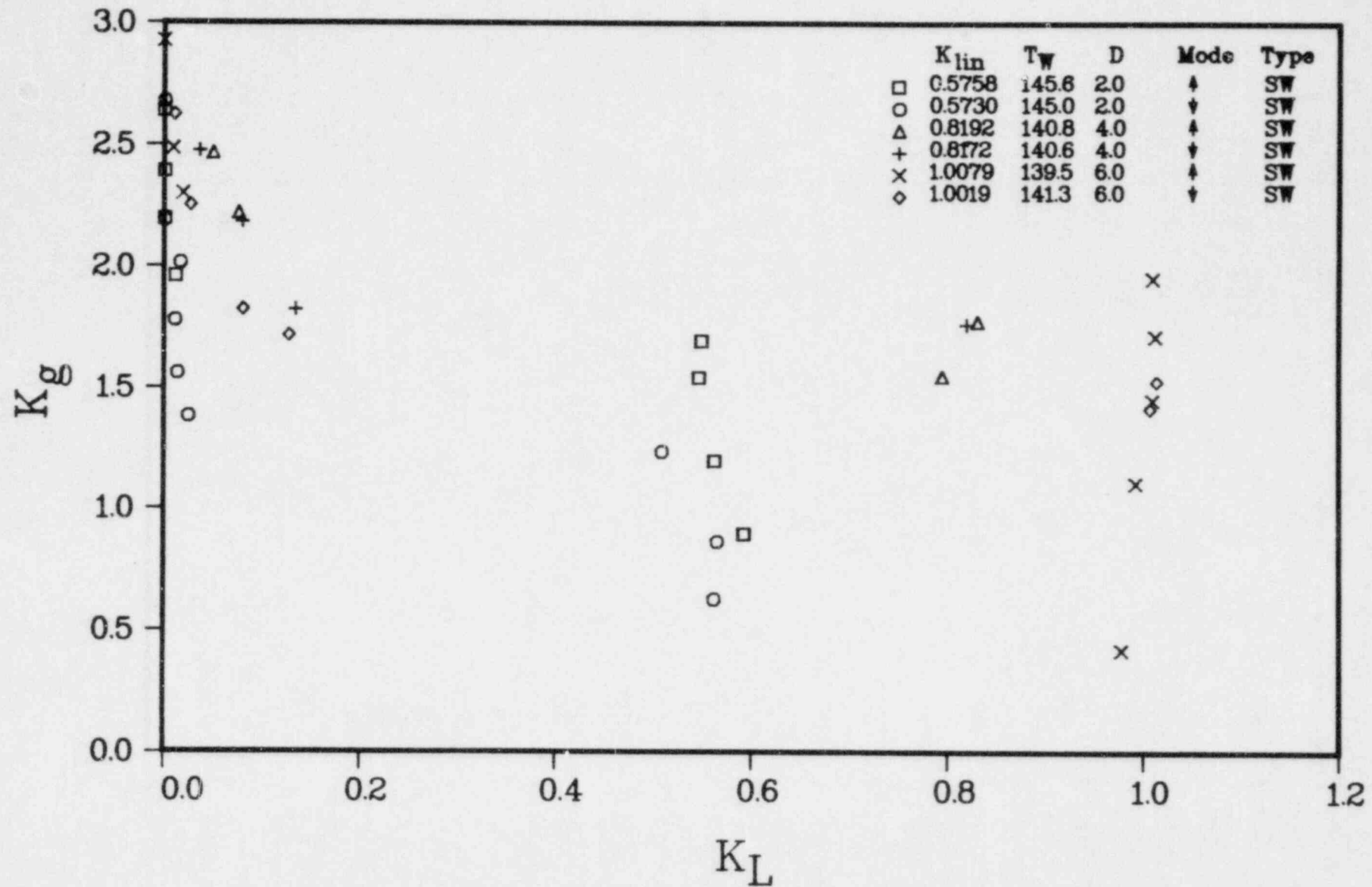


FIGURE 58. VARIATION OF FLOODING VELOCITIES AS A FUNCTION OF DIAMETER FOR STEAM-WATER FLOWS WITH $T_W = 140^\circ\text{F}$

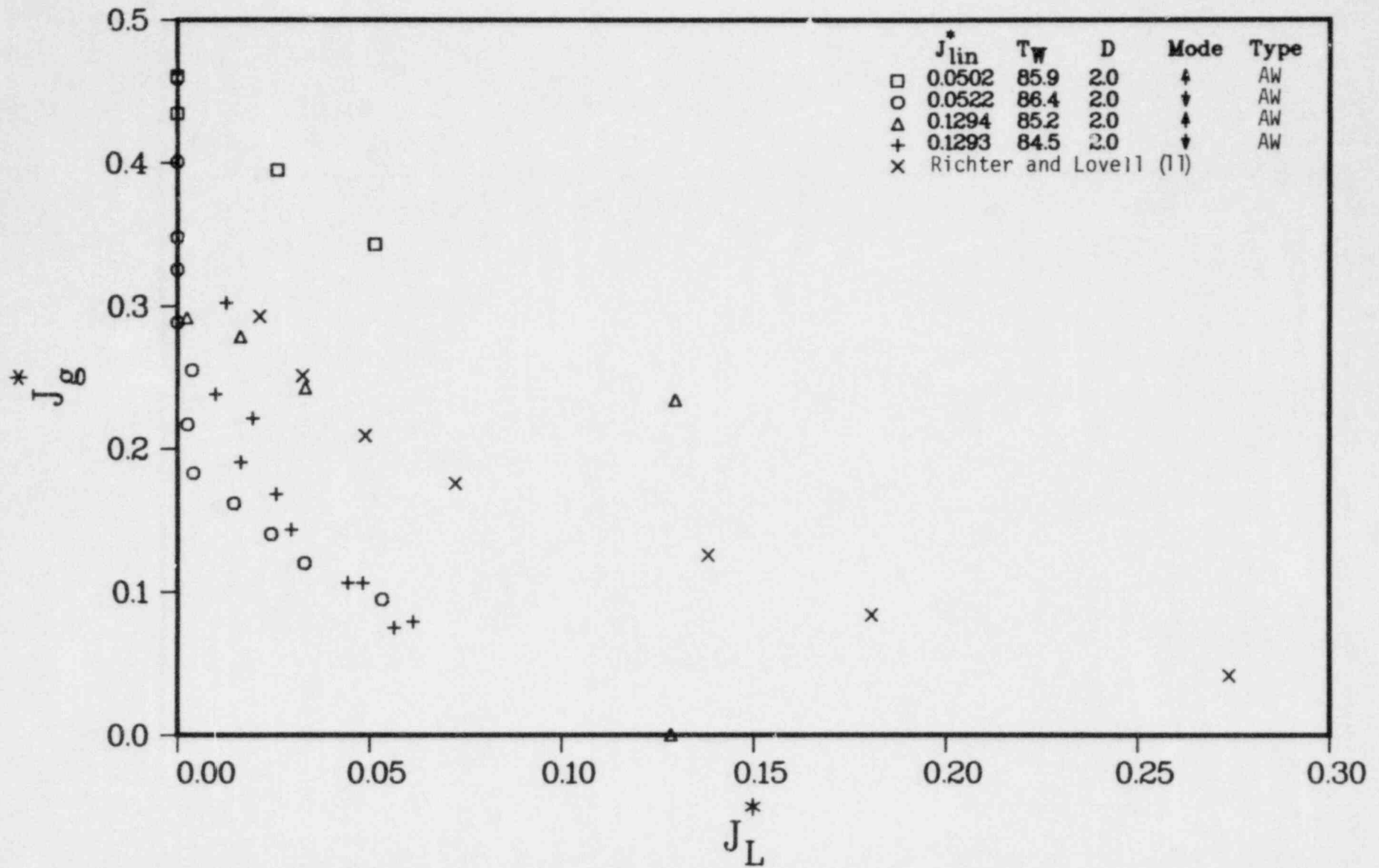


FIGURE 59. COMPARISON OF THE EXPERIMENTAL DATA FOR 2-INCH DIAMETER TUBE

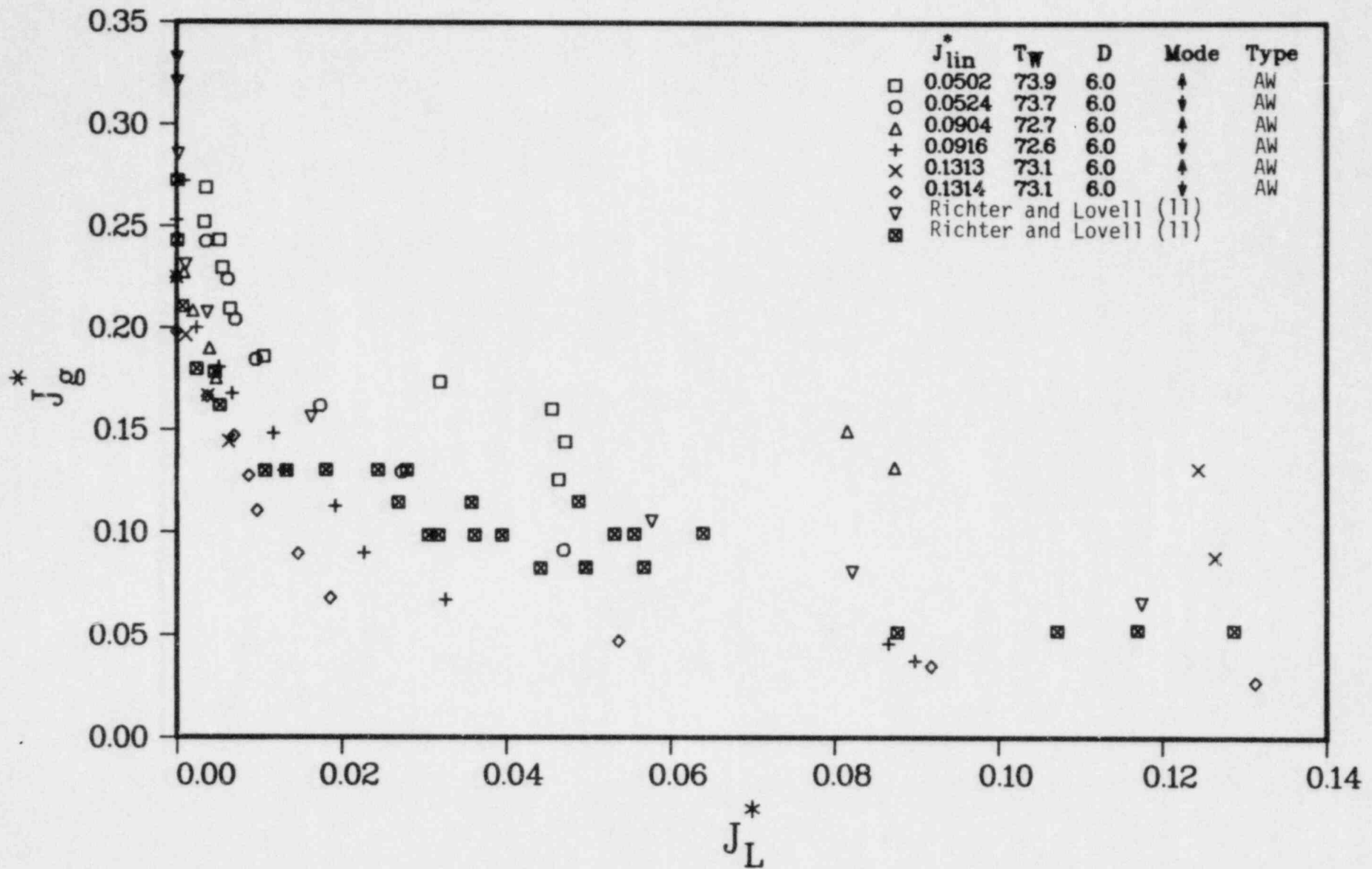


FIGURE 60. COMPARISON OF THE EXPERIMENTAL DATA FOR 6- AND 10-INCH DIAMETER TUBE

as shown in Figures 49 and 50. This partial penetration is the result of slug delivery, observed only for the 6-inch diameter tube.

The present results are somewhat different from previously published data. However, they show that neither the J^* nor the K parameter is entirely satisfactory for scaling the full range of countercurrent flooding data.

REFERENCES

- (1) Dworak, J. A., Segev, A., and Collier, R. P., "Scaling Air-Water Flooding in PWR Geometries", Trans. American Nuclear Society, 33, p. 973 (1979).
- (2) Beckner, W. D., Reyes, J. L., and Anderson, R., "Analysis of ECC Bypass Data", NUREG/CR-0570, USNRC (July, 1979).*
- (3) Collier, R. P., et al, "Steam-Water Mixing and Steam Hydrodynamics Program, Task 4", Quarterly Progress Report, April-June 1979, NUREG/CR-1557, BMI-2038 (June, 1980).*
- (4) Segev, A., and Collier, R. P., "Topical Report on Development of a Mechanistic Model for ECC Penetration in a PWR Downcomer", NUREG/CR-1426, BMI-2051 (June, 1980).*
- (5) Cudnik, R. A., et al, "Topical Report on Baseline Plenum Filling Behavior in a 2/15-Scale Model of a Four Loop Pressurized Water Reactor", NUREG/CR-0069, BMI-1997 (April, 1978).*
- (6) Crowley, C. J., and Block, J. A., "ECC Delivery Study-Experimental Results and Discussion", TN-217, Creare, Inc. (1975).
- (7) Wallis, G. B., One-Dimensional Two-Phase Flow, McGraw-Hill, New York (1969).
- (8) Cudnik, R. A., et al, "Steam-Water Mixing and Steam Hydrodynamics Program, Task 4", Quarterly Progress Report, January-March 1978, NUREG/CR-0147, BMI-2003 (June, 1978).*
- (9) Collier, R. P., et al, "Status Report on ECC Penetration Scaling Research", NUREG/CR-0651, BMI-2019 (February, 1979).*
- (10) Hewitt, G. F., "Influence of End Conditions, Tube Inclination, and Fluid Physical Properties on Flooding in Gas-Liquid Flows", HTFS-RS222, Harwell, England (1977).
- (11) Richter, H. J., and Lovell, T. W., "The Effect of Scale on Two-Phase Countercurrent Flow Flooding in Vertical Tubes", Final Report on Contract No. AT(49-24)-0329, Thayer School of Engineering, Dartmouth, College (1977).
- (12) Pushkina, O. L., and Sorokin, Y. L., "Breakdown of Liquid Film Motion in Vertical Tubes", Heat Transfer-Soviet Research, 1 (5), (1969).

- (13) Wallis, G. B., Richter, H. J., and Bharathan, D., "Air-Water Counter-current Annular Flow in Vertical Tubes", EPRI-NP-786 (1978).
- (14) Dukler, A. E., and Smith, L., "Two-Phase Interactions in Countercurrent Flow - Studies of the Flooding Mechanism", NUREG/CR-0617 (1979).*
- (15) Fan, C. K., and Schrock, V., "Flooding Phenomenon With Condensation", Trans. American Nuclear Society, 32, p 380 (1978).
- (16) de Sieyes, D. C., "Countercurrent Steam-Water Flow in Vertical Tubes", Bachelor of Engineering Report, Thayer School of Engineering, Dartmouth College (1978).
- (17) Tien, C. L., and Liu, C. P., "A Survey on Vertical Two-Phase Counter-current Flooding", EPRI-NP-984 (1979).
- (18) Bharathan, D., Wallis, G. B., and Richter, H. J., "Air-Water Countercurrent Flow", EPRI-NP-1165 (1979).
- (19) Tien, C. L., Chung, K. S., and Liu, C. P., "Topical Report on Flooding in Two-Phase Countercurrent Flows", EPRI-NP-1283 (1979).

* Available from National Technical Information Service (NTIS), Springfield, Virginia 22161. Also available for purchase from the NRC/GPO Sales Program, U. S. Nuclear Regulatory Commission, Washington, D.C. 20555.

APPENDIX A

2/15-Scale High Bypass Air-Water and Low
Subcooling Steam-Water Test Data

TABLE A-1. 2/15-SCALE AIR-WATER PLENUM FILL
PENETRATION DATA LISTING

Explanation of Column Titles

ID	- Identification number
WG	- Reverse core gas flow rate, lbm/sec
WL	- ECC water penetration flow rate, lbm/sec
WLIN	- ECC water injection flow rate, lbm/sec
JGS	- Dimensionless reverse core gas flow rate, $[\rho_g V_g^2 / g C_a (\rho_L - \rho_g)]^{1/2}$
JLS	- Dimensionless ECC water penetration flow rate, $[\rho_L V_L^2 / g C_a (\rho_L - \rho_g)]^{1/2}$
JSLIN	- Dimensionless ECC water injection flow rate, $[\rho_L V_{Lin}^2 / g C_a (\rho_L - \rho_g)]^{1/2}$
PV	- Lower plenum gas space pressure, psia
TLIN	- ECC water temperature, F
DTLIN	- ECC water subcooling, F
LAMBDA	- Condensation potential, $[C_p (T_{sat} - T_L) / h_{fg}] (\rho_L / \rho_g)^{1/2}$
DSTAR	- Dimensionless characteristic length, $C_a [g(\rho_L - \rho_g) / \sigma]^{1/2}$

Geometric data

Vessel scale	2/15
Vessel inner diameter, in	24.35
Annulus gap width, in	1.23
Annulus length, in	24.87
Annulus circumference, in	72.63
Cold leg diameter, in	4.02
Break leg diameter, in	7.63

ID	WG LBM/SEC	ML LBM/SEC	MLIN LBM/SEC	JGS	JLS	JLSIN	PV PSIA	TLIN F	DTLIN F	LAMBDA	OSTAR
25212	.478	26.530	35.00	.0212	.0493	.0650	21.82	75.83	0.00	0.000	678.81
25213	.918	7.459	35.23	.0427	.0138	.0654	19.62	75.43	0.00	0.000	678.91
25215	.298	32.206	35.02	.0155	.0598	.0650	16.15	75.96	0.00	0.000	679.20
25217	.431	23.428	34.87	.0209	.0435	.0647	18.49	75.92	0.00	0.000	679.13
25218	.588	19.792	34.78	.0270	.0367	.0646	20.42	75.94	0.00	0.000	679.08
25219	.692	16.019	34.71	.0306	.0297	.0644	22.13	75.98	0.00	0.000	679.04
25221	.892	9.768	34.74	.0397	.0181	.0645	21.49	75.98	0.00	0.000	679.06
25223	1.327	2.690	34.67	.0574	.0050	.0644	23.23	76.09	0.00	0.000	679.05
25224	1.648	1.862	34.79	.0744	.0035	.0646	21.49	76.18	0.00	0.000	679.14
25225	2.002	.915	34.69	.0860	.0017	.0644	23.84	76.26	0.00	0.000	679.10
25226	2.229	.616	34.58	.0929	.0011	.0642	25.50	76.33	0.00	0.000	679.08
25227	2.555	.504	34.51	.1021	.0009	.0641	27.94	76.45	0.00	0.000	679.02
25228	2.773	.187	34.44	.1073	.0003	.0640	29.88	76.57	0.00	0.000	678.99
25229	2.864	.249	34.40	.1089	.0005	.0639	31.01	76.72	0.00	0.000	679.01
25230	2.942	.044	34.38	.1106	.0001	.0639	31.85	76.88	0.00	0.000	679.05
25231	2.878	.087	34.40	.1083	.0002	.0639	31.87	76.87	0.00	0.000	679.05
25235	.217	46.013	52.72	.0090	.0855	.0979	24.63	77.16	0.00	0.000	679.39
25236	.405	28.882	52.16	.0154	.0537	.0969	29.74	77.25	0.00	0.000	679.20
25237	.542	23.207	52.30	.0210	.0431	.0972	28.44	77.38	0.00	0.000	679.30
25238	.668	18.283	51.84	.0243	.0340	.0963	32.34	77.48	0.00	0.000	679.21
25239	.774	9.642	53.09	.0344	.0179	.0986	21.80	77.61	0.00	0.000	679.63
25240	.972	5.409	53.02	.0425	.0100	.0985	22.56	77.71	0.00	0.000	679.65
25241	1.122	3.809	52.73	.0472	.0071	.0979	24.51	77.84	0.00	0.000	679.65
25242	1.281	2.583	52.57	.0521	.0048	.0977	26.26	77.92	0.00	0.000	679.61
25243	1.377	1.438	53.09	.0615	.0027	.0986	21.91	78.08	0.00	0.000	679.81
25244	1.691	.355	52.86	.0727	.0007	.0982	23.80	78.21	0.00	0.000	679.81
25245	1.952	.014	52.69	.0817	.0000	.0979	25.43	78.36	0.00	0.000	679.82
25246	2.105	.014	52.65	.0865	.0000	.0978	26.63	78.63	0.00	0.000	679.87
25247	.224	45.978	65.84	.0100	.0854	.1223	21.52	78.90	0.00	0.000	680.11
25249	.634	21.256	64.87	.0252	.0395	.1205	27.42	79.09	0.00	0.000	679.98
25250	.835	16.282	63.84	.0304	.0303	.1187	33.19	79.16	0.00	0.000	679.81
25251	.904	5.140	66.14	.0413	.0095	.1229	21.04	79.31	0.00	0.000	680.28
25252	1.061	3.790	65.98	.0474	.0070	.1226	22.18	79.45	0.00	0.000	680.31
25253	1.347	2.147	65.98	.0600	.0040	.1226	22.33	79.61	0.00	0.000	680.36
25254	1.635	1.158	65.61	.0703	.0022	.1219	24.13	79.71	0.00	0.000	680.35
25255	1.943	.473	65.12	.0796	.0009	.1210	26.78	79.83	0.00	0.000	680.30
25256	2.287	.014	64.73	.0899	.0000	.1203	29.13	79.97	0.00	0.000	680.25
25257	2.518	.014	64.23	.0951	.0000	.1194	31.67	80.13	0.00	0.000	680.22
25258	.336	28.107	65.80	.0154	.0530	.1240	20.54	141.70	0.00	0.000	703.93
25259	.473	25.109	64.77	.0192	.0473	.1221	26.80	141.40	0.00	0.000	703.65
25260	.664	22.003	62.73	.0226	.0415	.1182	38.40	140.90	0.00	0.000	703.14
25261	.592	15.295	65.67	.0266	.0288	.1237	21.78	140.50	0.00	0.000	703.42
25262	.779	10.257	65.42	.0339	.0193	.1232	23.29	140.10	0.00	0.000	703.22
25263	.888	7.033	65.32	.0377	.0132	.1230	24.37	139.90	0.00	0.000	703.11

ID	WG LBM/SEC	WL LBM/SEC	WLIN LBM/SEC	JGS	JLS	JLSIN	PV PSIA	TLIN F	DTLIN F	LAMBDA	DSTAR
25264	1.106	4.792	65.21	.0466	.0090	.1228	25.15	139.50	0.00	0.000	702.93
25265	1.242	3.537	64.96	.0507	.0067	.1223	26.83	139.30	0.00	0.000	702.81
25266	1.408	2.289	65.40	.0606	.0043	.1232	24.26	139.10	0.00	0.000	702.80
25267	1.577	2.185	65.28	.0666	.0041	.1229	25.31	138.90	0.00	0.000	702.69
25268	1.768	1.471	65.01	.0728	.0028	.1224	26.81	138.50	0.00	0.000	702.49
25269	2.044	.683	64.58	.0810	.0013	.1216	29.11	138.20	0.00	0.000	702.32
25270	2.281	.582	64.14	.0870	.0011	.1208	31.62	137.80	0.00	0.000	702.09
25271	2.578	.216	63.79	.0952	.0004	.1201	33.80	137.50	0.00	0.000	701.92
25272	2.553	.043	63.51	.0925	.0001	.1196	35.21	137.20	0.00	0.000	701.76
25273	2.684	.376	63.33	.0968	.0007	.1192	35.60	136.90	0.00	0.000	701.65
25274	2.723	.014	63.01	.0975	.0000	.1186	36.17	136.90	0.00	0.000	701.62
25275	.186	32.124	53.52	.0085	.0604	.1007	22.00	135.90	0.00	0.000	701.58
25276	.635	17.451	52.85	.0260	.0328	.0994	27.19	135.90	0.00	0.000	701.43
25277	.931	6.102	52.96	.0398	.0115	.0996	24.65	135.90	0.00	0.000	701.49
25278	1.129	2.363	53.30	.0517	.0044	.1003	21.79	135.60	0.00	0.000	701.45
25279	1.511	1.631	53.11	.0662	.0031	.0999	23.93	135.50	0.00	0.000	701.36
25280	1.716	.938	53.08	.0724	.0018	.0998	25.84	135.20	0.00	0.000	701.19
25281	2.094	.296	52.55	.0841	.0006	.0988	28.65	135.20	0.00	0.000	701.12
25282	2.371	.253	52.25	.0918	.0005	.0983	30.93	135.10	0.00	0.000	701.03
25283	2.500	.014	52.01	.0939	.0000	.0978	32.88	134.70	0.00	0.000	700.82
25284	2.671	.014	51.99	.0987	.0000	.0978	33.99	134.00	0.00	0.000	700.51
25302	.112	30.116	34.11	.0045	.0567	.0642	28.72	135.70	0.00	0.000	701.32
25304	.610	14.642	34.53	.0271	.0275	.0649	22.97	135.50	0.00	0.000	701.38
25305	.876	9.082	34.40	.0370	.0171	.0647	25.45	135.10	0.00	0.000	701.16
25306	1.015	5.054	34.42	.0430	.0095	.0647	25.27	134.50	0.00	0.000	700.92
25307	1.211	3.196	34.52	.0530	.0060	.0649	23.67	134.10	0.00	0.000	700.80
25308	1.352	2.785	34.44	.0575	.0052	.0648	24.81	133.90	0.00	0.000	700.68
25309	1.429	1.374	34.49	.0647	.0026	.0648	21.92	133.80	0.00	0.000	700.72
25310	1.755	.567	34.36	.0764	.0011	.0646	23.82	133.70	0.00	0.000	700.63
25311	1.943	.376	34.28	.0822	.0007	.0645	25.29	133.60	0.00	0.000	700.56
25312	2.173	.216	34.28	.0895	.0004	.0644	26.76	133.50	0.00	0.000	700.48
25313	2.316	.014	34.17	.0924	.0000	.0642	28.55	133.30	0.00	0.000	700.35
25314	2.589	.014	34.07	.1001	.0000	.0641	30.41	133.10	0.00	0.000	700.23
25315	.247	26.084	33.82	.0113	.0503	.0652	22.66	207.50	0.00	0.000	733.78
25316	.412	18.267	33.80	.0181	.0352	.0652	23.70	207.30	0.00	0.000	733.62
25317	.564	15.852	33.68	.0235	.0306	.0650	26.07	206.60	0.00	0.000	733.20
25318	.768	8.315	33.88	.0340	.0160	.0653	23.30	203.60	0.00	0.000	731.78
25319	.862	5.836	33.78	.0370	.0112	.0650	24.99	201.50	0.00	0.000	730.70
25320	1.113	3.320	33.84	.0495	.0064	.0651	23.22	201.90	0.00	0.000	730.94
25321	1.239	2.551	33.73	.0536	.0049	.0650	24.57	202.50	0.00	0.000	731.20
25322	1.212	1.957	33.66	.0514	.0038	.0648	25.64	202.40	0.00	0.000	731.13
25323	1.645	1.216	33.55	.0673	.0023	.0646	27.68	202.10	0.00	0.000	730.92
25324	1.878	.882	33.44	.0743	.0017	.0644	29.74	201.90	0.00	0.000	730.77
25325	2.045	.310	33.31	.0784	.0006	.0641	31.80	201.60	0.00	0.000	730.57
25326	2.236	.177	33.22	.0836	.0003	.0640	33.58	201.40	0.00	0.000	730.42
25327	2.416	.030	33.24	.0888	.0001	.0639	34.90	199.50	0.00	0.000	729.46

ID	WG LBM/SEC	WL LBM/SEC	WLIN LBM/SEC	JGS	JLS	JLSIN	PV PSIA	TLIN F	DTLIN F	LAMBDA	DSTAR
25328	2.719	.014	33.11	.0967	.0000	.0657	37.46	198.80	0.00	0.000	729.05
25329	.314	22.060	52.01	.0142	.0426	.1003	22.79	208.10	0.00	0.000	734.07
25330	.493	17.304	51.60	.0214	.0334	.0999	24.92	207.70	0.00	0.000	733.82
25331	.608	13.246	51.88	.0264	.0255	.1000	24.74	205.70	0.00	0.000	732.81
25332	.802	7.406	52.24	.0361	.0143	.1007	22.92	204.80	0.00	0.000	732.40
25333	.898	5.039	51.62	.0394	.0097	.0995	24.28	204.40	0.00	0.000	732.17
25334	1.084	4.037	51.19	.0464	.0078	.0986	25.60	204.40	0.00	0.000	732.13
25335	1.224	3.180	51.24	.0513	.0061	.0986	26.62	202.10	0.00	0.000	730.96
25336	1.336	2.485	51.21	.0545	.0048	.0985	27.94	200.90	0.00	0.000	730.33
25337	1.621	1.880	51.02	.0639	.0036	.0982	30.00	200.10	0.00	0.000	729.88
25338	1.880	1.214	50.78	.0711	.0023	.0977	32.62	199.80	0.00	0.000	729.66
25339	2.132	.729	50.63	.0784	.0014	.0974	34.57	198.90	0.00	0.000	729.16
25340	2.383	.492	50.47	.0852	.0009	.0970	36.75	197.70	0.00	0.000	728.52
25341	2.570	.377	50.32	.0900	.0007	.0967	38.56	196.30	0.00	0.000	727.79
25342	2.761	.122	50.78	.0952	.0002	.0975	40.06	194.40	0.00	0.000	726.84
25343	2.844	.134	51.36	.0966	.0003	.0986	41.32	194.60	0.00	0.000	726.90
25344	2.817	.006	51.14	.0948	.0000	.0982	41.96	194.40	0.00	0.000	726.79
25345	.241	26.393	63.97	.0107	.0510	.1235	23.71	209.10	0.00	0.000	734.56
25346	.444	19.962	63.60	.0192	.0385	.1228	25.26	208.90	0.00	0.000	734.42
25347	.582	16.322	63.35	.0247	.0315	.1223	26.00	208.60	0.00	0.000	734.24
25348	.732	9.537	63.52	.0326	.0134	.1226	23.80	208.20	0.00	0.000	734.10
25349	.884	6.793	63.43	.0384	.0131	.1222	24.90	204.70	0.00	0.000	732.38
25350	1.025	5.219	63.45	.0436	.0101	.1222	26.01	203.10	0.00	0.000	731.46
25351	1.034	3.977	63.34	.0426	.0077	.1219	27.78	201.70	0.00	0.000	730.73
25352	1.422	3.119	63.28	.0568	.0060	.1218	29.45	200.60	0.00	0.000	730.15
25353	1.651	2.387	63.02	.0636	.0046	.1212	31.67	199.90	0.00	0.000	729.74
25354	1.937	1.619	62.68	.0722	.0031	.1206	33.92	199.60	0.00	0.000	729.53
25355	2.067	1.153	62.37	.0748	.0022	.1199	36.04	198.60	0.00	0.000	728.98
25356	2.335	.784	61.93	.0817	.0015	.1190	38.55	197.30	0.00	0.000	728.28
25357	2.638	.821	61.59	.0896	.0016	.1183	40.77	195.90	0.00	0.000	727.53
25358	2.771	.651	61.32	.0924	.0013	.1177	42.28	194.20	0.00	0.000	726.67
25359	2.809	.512	61.90	.0950	.0010	.1188	42.88	191.90	0.00	0.000	725.55
25360	2.705	.518	63.49	.0888	.0010	.1217	43.57	190.80	0.00	0.000	725.01
25361	2.790	.281	63.56	.0917	.0005	.1218	43.62	189.20	0.00	0.000	724.25
25362	2.822	.073	63.59	.0930	.0001	.1218	43.41	188.30	0.00	0.000	723.83

IO	WG LBM/SEC	WL LBM/SEC	WLIN LBM/SEC	JGS	JLS	JLSIN	PV PSIA	TLIN F	DTLIN F	LAMBDA	DSTAR
25702	.070	37.070	35.53	.0033	.0689	.0660	19.78	81.16	0.00	0.000	680.96
25703	.116	36.306	35.55	.0054	.0675	.0660	19.94	81.30	0.00	0.000	681.01
25704	.379	29.295	35.02	.0163	.0544	.0651	22.87	81.47	0.00	0.000	680.98
25705	.300	30.545	35.16	.0135	.0568	.0653	20.84	81.52	0.00	0.000	681.04
25706	.528	20.957	35.17	.0232	.0389	.0654	21.64	81.63	0.00	0.000	681.06
25707	.591	19.416	35.15	.0256	.0361	.0653	22.27	81.74	0.00	0.000	681.08
25708	.712	16.909	34.96	.0299	.0314	.0650	23.79	81.87	0.00	0.000	681.09
25709	.728	18.153	35.04	.0311	.0337	.0651	23.26	81.99	0.00	0.000	681.15
25710	.859	15.094	34.87	.0350	.0281	.0648	25.63	82.02	0.00	0.000	681.09
25711	.813	14.201	34.82	.0329	.0264	.0647	26.17	82.13	0.00	0.000	681.11
25712	.976	10.424	34.74	.0372	.0194	.0646	29.62	82.25	0.00	0.000	681.01
25713	.990	11.321	34.81	.0379	.0210	.0647	29.26	82.27	0.00	0.000	681.03
25714	1.176	9.338	34.69	.0434	.0174	.0645	31.58	82.35	0.00	0.000	680.99
25715	1.185	8.315	34.72	.0435	.0155	.0646	31.95	82.43	0.00	0.000	681.01
25716	1.344	6.313	34.57	.0473	.0117	.0643	34.78	82.49	0.00	0.000	680.96
25717	1.374	7.204	34.56	.0486	.0134	.0643	34.53	82.56	0.00	0.000	680.99
25718	1.311	8.758	53.21	.0425	.0163	.0990	41.27	82.59	0.00	0.000	680.73
25719	1.375	8.244	53.19	.0445	.0153	.0990	41.38	82.71	0.00	0.000	680.78
25720	1.156	11.254	53.63	.0391	.0209	.0998	37.79	82.74	0.00	0.000	680.91
25721	1.171	12.295	53.72	.0399	.0229	.0999	37.20	82.84	0.00	0.000	680.98
25722	.916	15.242	54.17	.0327	.0283	.1008	33.89	82.84	0.00	0.000	681.11
25723	.998	14.583	54.12	.0353	.0271	.1007	34.48	82.94	0.00	0.000	681.13
25724	.895	16.722	54.52	.0328	.0311	.1014	32.17	82.96	0.00	0.000	681.20
25725	.844	17.706	54.60	.0313	.0329	.1015	31.32	82.98	0.00	0.000	681.23
25726	.662	22.368	55.16	.0264	.0416	.1026	27.22	83.09	0.00	0.000	681.42
25727	.679	20.945	55.01	.0267	.0309	.1023	28.12	83.10	0.00	0.000	681.39
25728	.382	28.274	55.61	.0163	.0526	.1034	23.39	83.15	0.00	0.000	681.56
25729	.433	30.895	55.66	.0188	.0574	.1035	22.39	83.21	0.00	0.000	681.60

ID	WG LBM/SEC	WL LBM/SEC	WLIN LBM/SEC	JGS	JLS	JLSIN	PV PSIA	TLIN F	DTLIN F	LAMBDA	DSTAR
25802	.250	33.023	35.04	.0105	.0615	.0652	23.73	92.86	0.00	0.000	685.04
25803	.488	21.721	34.86	.0198	.0405	.0650	25.35	102.00	0.00	0.000	688.35
25805	.863	11.039	34.74	.0334	.0206	.0649	28.20	106.10	0.00	0.000	689.81
25902	.194	47.400	53.16	.0081	.0883	.0990	24.34	92.03	0.00	0.000	684.74
25903	.377	35.162	53.21	.0158	.0655	.0991	24.15	91.81	0.00	0.000	684.66
25904	.630	23.594	53.01	.0253	.0439	.0987	25.98	91.67	0.00	0.000	684.55
25905	.503	30.292	53.19	.0204	.0564	.0990	25.28	91.59	0.00	0.000	684.54
25906	.786	21.195	52.93	.0306	.0395	.0985	27.40	91.52	0.00	0.000	684.46
25907	1.021	15.436	52.40	.0368	.0287	.0976	32.20	91.65	0.00	0.000	684.38
25908	1.335	10.545	51.78	.0444	.0196	.0965	37.70	91.71	0.00	0.000	684.18
25909	1.562	7.468	51.36	.0494	.0139	.0957	41.81	91.74	0.00	0.000	684.04
25910	1.700	6.903	52.89	.0521	.0129	.0986	44.73	91.77	0.00	0.000	684.01
25911	1.794	6.228	52.70	.0543	.0116	.0982	46.19	91.81	0.00	0.000	684.00
25912	1.780	5.808	52.76	.0541	.0108	.0983	45.91	91.89	0.00	0.000	684.04
26002	.257	32.712	34.80	.0106	.0608	.0646	24.39	76.45	0.00	0.000	679.11
26003	.439	30.500	34.98	.0187	.0566	.0650	22.57	76.53	0.00	0.000	679.20
26004	.579	24.354	34.82	.0234	.0452	.0647	25.25	76.65	0.00	0.000	679.15
26005	.780	16.975	34.86	.0315	.0315	.0648	25.26	76.64	0.00	0.000	679.15
26006	1.024	11.574	34.78	.0402	.0215	.0646	26.87	76.65	0.00	0.000	679.08
26007	1.283	7.462	34.60	.0467	.0139	.0643	31.21	76.67	0.00	0.000	678.92
26008	1.520	5.860	34.47	.0527	.0109	.0641	34.69	76.75	0.00	0.000	678.86
26009	1.684	5.346	34.38	.0567	.0099	.0639	36.99	76.75	0.00	0.000	678.77
26010	.915	13.669	35.05	.0372	.0254	.0651	25.18	76.60	0.00	0.000	679.15
26011	.699	18.352	35.29	.0313	.0341	.0655	21.04	76.59	0.00	0.000	679.28
26012	.665	21.667	35.11	.0271	.0402	.0652	24.99	76.55	0.00	0.000	679.13
26013	.524	29.569	35.01	.0205	.0549	.0650	27.26	76.55	0.00	0.000	679.04
26014	.516	29.295	35.27	.0218	.0544	.0655	23.23	76.47	0.00	0.000	679.16

TABLE A-2. 2/15-SCALE STEAM-WATER PLENUM FILL
PENETRATION DATA LISTINGExplanation of Column Titles

ID	-	Identification number
WG	-	Reverse core gas flow rate, lbm/sec
WL	-	ECC water penetration flow rate, lbm/sec
WLIN	-	ECC water injection flow rate, lbm/sec
JGS	-	Dimensionless reverse core gas flow rate, $[\rho_g V_g^2 / g C_a (\rho_L - \rho_g)]^{1/2}$
JLS	-	Dimensionless ECC water penetration flow rate, $[\rho_L V_L^2 / g C_a (\rho_L - \rho_g)]^{1/2}$
JSLIN	-	Dimensionless ECC water injection flow rate, $[\rho_L V_{Lin}^2 / g C_a (\rho_L - \rho_g)]^{1/2}$
PV	-	Lower plenum gas space pressure, psia
TLIN	-	ECC water temperature, F
DTLIN	-	ECC water subcooling, F
LAMBDA	-	Condensation potential, $[C_p (T_{sat} - T_L) / h_{fg}] (\rho_L / \rho_g)^{1/2}$
DSTAR	-	Dimensionless characteristic length, $C_a [g (\rho_L - \rho_g) / \sigma]^{1/2}$

Geometric data

Vessel scale	2/15
Vessel inner diameter, in	24.35
Annulus gap width, in	1.23
Annulus length, in	24.87
Annulus circumference, in	72.63
Cold leg diameter, in	4.02
Break leg diameter, in	4.02

ID	WG LBM/SEC	WL LBM/SEC	WLIN LBM/SEC	JCS	JLS	JLSIN	PV PSIA	TLIN F	DTLIN F	LAMBDA	DSTAR
25402	1.203	14.082	32.98	.0779	.0272	.0637	23.15	210.50	25.09	.872	735.64
25403	.989	17.060	33.06	.0661	.0329	.0638	21.69	210.10	21.95	.785	735.46
25404	.929	17.217	33.06	.0635	.0332	.0638	20.60	209.80	19.61	.715	735.32
25405	.930	16.692	33.04	.0634	.0322	.0638	20.77	209.50	20.32	.739	735.16
25406	.817	21.768	33.24	.0591	.0420	.0641	18.57	207.00	16.69	.641	733.92
25407	.691	23.254	33.34	.0515	.0448	.0643	17.60	208.30	12.49	.492	734.59
25408	1.273	15.032	33.00	.0797	.0290	.0637	24.65	208.90	30.32	1.022	734.80
25409	2.002	12.441	32.70	.1135	.0240	.0631	30.11	209.70	40.84	1.260	735.14
25410	2.197	9.088	32.45	.1179	.0175	.0626	33.78	209.80	47.31	1.392	735.15
25411	2.787	7.280	32.08	.1354	.0141	.0619	40.51	209.90	58.05	1.574	735.10
25412	3.411	5.632	31.60	.1513	.0109	.0610	49.01	210.40	69.26	1.736	735.25
25413	3.550	3.761	30.67	.1550	.00.2	.0591	50.64	205.40	76.37	1.888	732.69
25414	.588	32.363	32.99	.0271	.0626	.0638	44.97	212.60	61.49	1.600	736.42
25415	.623	34.584	32.95	.0287	.0669	.0637	44.95	212.90	61.17	1.591	736.58
25416	.949	34.640	32.93	.0438	.0670	.0637	44.91	212.30	61.71	1.606	736.27
25417	1.313	35.176	32.93	.0607	.0680	.0636	44.80	212.50	61.36	1.599	736.38
25418	1.379	32.828	32.56	.0647	.0635	.0629	44.82	212.70	61.19	1.602	736.50
25419	1.585	31.035	32.53	.0743	.0600	.0629	44.57	212.70	60.84	1.595	736.50
25421	2.075	18.796	32.17	.0963	.0363	.0621	45.88	211.00	64.35	1.669	735.62
25422	2.404	14.542	32.32	.1138	.0281	.0624	44.02	211.80	60.99	1.609	736.05
25424	3.115	3.959	32.91	.1391	.0077	.0636	48.00	212.20	66.07	1.670	736.18
25425	3.485	.120	32.76	.1535	.0002	.0633	49.53	212.00	68.37	1.703	736.06
25426	3.690	3.050	32.44	.1576	.0059	.0627	53.02	212.50	72.05	1.748	736.28
25427	.684	33.335	33.03	.0249	.0644	.0638	74.08	210.50	96.15	2.032	734.99
25428	1.043	34.747	32.92	.0377	.0671	.0636	74.82	210.20	97.12	2.044	734.83
25429	1.321	33.345	32.83	.0478	.0644	.0634	74.86	209.80	97.56	2.053	734.63
25430	1.728	33.584	32.90	.0627	.0648	.0635	74.61	208.10	99.03	2.088	733.77
25432	1.910	32.143	33.21	.0697	.0621	.0641	73.41	209.20	96.84	2.054	734.34
25433	1.968	33.463	33.25	.0719	.0646	.0642	73.21	209.50	96.35	2.046	734.49
25434	2.072	33.906	33.07	.0752	.0655	.0639	74.23	209.50	97.28	2.054	734.48
25435	2.312	31.912	33.12	.0840	.0616	.0640	74.13	209.50	97.19	2.054	734.48
25436	2.615	30.135	33.14	.0952	.0582	.0640	74.40	209.40	97.54	2.060	734.44
25437	2.982	26.070	33.06	.1079	.0503	.0639	74.73	209.30	97.94	2.063	734.37
25438	3.688	14.326	33.21	.1350	.0277	.0641	72.85	209.20	96.33	2.049	734.34
25439	4.296	6.110	32.91	.1550	.0118	.0635	75.17	208.80	98.84	2.077	734.11
25440	4.615	1.408	32.55	.1666	.0027	.0628	75.16	208.50	99.13	2.083	733.96
25441	4.620	3.758	32.68	.1678	.0073	.0631	74.15	207.60	99.11	2.094	733.51
25442	5.634	1.649	32.40	.2023	.0032	.0625	75.94	206.50	101.84	2.132	732.94
25443	1.656	43.221	50.52	.0773	.0835	.0976	45.43	212.40	62.33	1.623	736.34
25444	2.003	40.104	50.51	.0919	.0775	.0976	45.58	212.10	62.83	1.625	736.16
25445	2.206	36.190	50.27	.1011	.0699	.0972	46.97	211.90	64.95	1.666	736.06
25446	2.557	26.501	50.26	.1174	.0512	.0970	46.69	209.60	66.86	1.720	734.89
25447	2.714	23.389	50.47	.1254	.0451	.0974	45.74	208.20	67.23	1.741	734.18
25448	3.159	13.628	50.21	.1414	.0263	.0969	48.59	208.50	70.58	1.779	734.29
25449	3.441	17.498	50.07	.1504	.0338	.0966	50.06	208.50	72.59	1.799	734.26
25450	3.655	8.130	50.06	.1599	.0157	.0966	49.86	208.20	72.63	1.803	734.11

ID	WG LBM/SEC	WL LBM/SEC	WLIN LBM/SEC	JGS	JLS	JLSIN	PV PSIA	TLIN F	DTLIN F	LAMBDA	DSTAR
25451	3.722	8.460	49.73	.1607	.0163	.0960	51.66	208.10	74.86	1.835	734.04
25452	3.980	4.319	49.16	.1678	.0083	.0949	54.59	208.40	77.99	1.872	734.16
25453	4.332	3.521	48.29	.1757	.0068	.0932	59.02	209.30	82.26	1.908	734.57
25502	1.216	63.411	62.73	.0564	.1224	.1211	45.63	209.50	65.50	1.701	734.85
25503	2.027	50.220	62.50	.0930	.0969	.1206	46.69	208.00	68.46	1.761	734.07
25506	4.108	3.986	60.18	.1681	.0077	.1162	57.88	210.50	79.73	1.866	735.19
25507	4.812	9.181	58.42	.1866	.0177	.1129	65.00	210.70	87.12	1.944	735.21
25510	3.343	2.646	31.65	.1537	.0051	.0612	46.39	212.00	64.05	1.650	736.11
25511	.910	36.633	33.22	.0425	.0708	.0642	45.16	211.20	63.16	1.648	735.72
25514	2.275	28.251	33.18	.1063	.0546	.0641	45.33	210.10	64.49	1.681	735.17
25515	2.582	13.801	33.23	.1214	.0267	.0642	44.79	210.70	63.15	1.655	735.48
25516	2.868	5.803	33.27	.1333	.0112	.0643	45.33	211.20	63.39	1.650	735.72
25517	3.329	5.849	33.13	.1474	.0113	.0640	48.71	211.60	67.64	1.698	735.86
25518	3.621	6.684	32.88	.1536	.0129	.0635	53.55	211.50	73.67	1.780	735.75
25521	3.021	2.410	33.18	.1389	.0047	.0641	46.11	211.00	64.66	1.670	735.63
25522	2.945	12.417	33.25	.1394	.0240	.0642	43.50	211.10	60.97	1.613	735.69
25523	2.700	12.269	33.15	.1272	.0237	.0640	44.20	211.20	61.83	1.627	735.73
25524	2.473	13.154	32.87	.1174	.0254	.0635	43.82	211.30	61.21	1.618	735.79

APPENDIX B

Flooding Data for Countercurrent Air-Water and
Steam-Water Flows in Tubes

TABLE B-1. FLOODING DATA FOR COUNTERCURRENT
AIR-WATER FLOWS IN TUBES

ID - Identification number

WG - Air flow rate, lbm/sec

WL - Water penetration rate, lbm/sec

WLIN - Inlet water flow rate, lbm/sec

TLIN - Temperature of inlet water, °F

PLT - Lower tank pressure, psia

DIA - Tube diameter, inch

JLSIN - Dimensionless inlet water flow rate,

$$[\rho_L V_{Lin}^2 / gD(\rho_L - \rho_g)]^{1/2}$$

JGS - Dimensionless air flow rate,

$$[\rho_g V_g^2 / gD(\rho_L - \rho_g)]^{1/2}$$

JLS - Dimensionless water penetration rate,

$$[\rho_L V_L^2 / gD(\rho_L - \rho_g)]^{1/2}$$

KLSIN - Dimensionless inlet water flow rate,

$$\{\rho_L V_{Lin}^2 / [g\sigma(\rho_L - \rho_g)]^{1/2}\}^{1/2}$$

KGS - Dimensionless air flow rate,

$$\{\rho_g V_g^2 / [g\sigma(\rho_L - \rho_g)]^{1/2}\}^{1/2}$$

KLS - Dimensionless water penetration rate,

$$\{\rho_L V_L^2 / [g\sigma(\rho_L - \rho_g)]^{1/2}\}^{1/2}$$

ID	WG LBM/SEC	WL LBM/SEC	WLIN LBM/SEC	TLIN F	PL PSIA	DIA INCH	JLSIN -	JGS -	JLS -	KLSIN -	KGS -	KLS -
21834	.1014	.1077	2.1363	75.8	15.01	4.0	.1201	.1607	.0106	.7347	.9826	.0646
21835	.0796	.3196	2.1391	75.8	14.92	4.0	.1203	.1270	.0180	.7356	.7769	.1099
21836	.0592	.5732	2.1391	75.8	14.95	4.0	.1203	.0953	.0322	.7356	.5826	.1971
21837	.0409	.7345	2.1391	75.8	14.82	4.0	.1203	.0662	.0413	.7356	.4050	.2526
21838	.0390	1.0440	2.1377	75.8	14.81	4.0	.1202	.0645	.0587	.7352	.3945	.3590
21839	.0284	2.1460	2.1460	75.8	14.47	4.0	.1207	.0465	.1207	.7380	.2846	.7380
21840	.0771	2.8607	2.8607	75.0	14.61	4.0	.1609	.1254	.1610	.9835	.7669	.9800
21841	.1030	2.8704	2.8704	75.1	14.75	4.0	.1614	.1664	.1614	.9869	1.0172	.9900
21842	.1177	2.8635	2.8635	75.1	14.86	4.0	.1610	.1899	.1609	.9845	1.1612	.9800
21843	.1214	2.8578	2.8579	75.1	14.99	4.0	.1607	.1957	.1599	.9826	1.1964	.9800
21844	.1227	.2124	2.8524	75.0	15.17	4.0	.1604	.1939	.0117	.9807	1.1856	.0700
21845	.1386	.1707	2.8607	75.0	15.23	4.0	.1609	.2181	.0097	.9835	1.3334	.0600
21846	.1350	.1503	2.8440	75.1	15.28	4.0	.1599	.2136	.0084	.9778	1.3057	.0517
21847	.1192	.2313	2.8496	75.1	15.16	4.0	.1602	.1876	.0130	.9797	1.1469	.0795
21848	.1012	.2984	2.8551	75.1	15.04	4.0	.1605	.1601	.0160	.9816	.9790	.1026
21849	.0806	.4800	2.8579	75.1	14.94	4.0	.1607	.1203	.0225	.9826	.7845	.1375
21850	.0602	.4233	2.8593	75.1	14.88	4.0	.1608	.0965	.0238	.9831	.5903	.1455
21851	.0400	.6970	2.8593	75.1	14.35	4.0	.1608	.0646	.0392	.9830	.3947	.2396
21852	.0270	1.2761	2.8579	75.1	14.86	4.0	.1607	.0436	.0719	.9826	.2664	.4394
21853	.1549	.8632	.9074	79.2	15.22	4.0	.0510	.2461	.0486	.3125	1.5064	.2973
21854	.1639	.8718	.9028	79.3	15.48	4.0	.0508	.2556	.0040	.3109	1.5648	.0247
21855	.1565	.0631	.9032	79.4	15.35	4.0	.0508	.2447	.0036	.3111	1.4976	.0217
21856	.1355	.1071	.9047	79.4	15.20	4.0	.0509	.2175	.0060	.3116	1.3316	.0369
21857	.1190	.2288	.9051	79.4	15.06	4.0	.0509	.1879	.0129	.3117	1.1503	.0788
21858	.1013	.4719	.9066	79.4	14.93	4.0	.0510	.1610	.0266	.3123	.9858	.1625
21859	.0809	.7124	.9089	79.4	14.78	4.0	.0511	.1297	.0401	.3130	.7940	.2453
21860	.0609	.9100	.9100	79.5	14.57	4.0	.0512	.0989	.0512	.3134	.6054	.3134
21902	.1142	.8612	.8804	144.7	14.92	4.0	.0503	.1871	.0492	.3134	1.1659	.3066
21903	.1363	.8032	.9135	144.9	15.15	4.0	.0522	.2244	.0459	.3253	1.3989	.2860
21904	.1519	.8615	.8986	145.0	15.49	4.0	.0513	.2411	.0035	.3200	1.5029	.0219
21905	.1755	.1507	.8834	145.1	15.84	4.0	.0508	.2746	.0086	.3167	1.7118	.0537
21906	.2002	.1195	.8844	145.0	16.23	4.0	.0505	.3117	.0068	.3149	1.9428	.0426
21907	.1813	.1624	.8865	145.1	15.93	4.0	.0507	.2859	.0093	.3157	1.7821	.0578
21908	.1618	.1211	.8837	145.1	15.69	4.0	.0505	.2574	.0069	.3147	1.6044	.0431
21909	.1427	.0954	.8844	145.1	15.47	4.0	.0505	.2287	.0055	.3149	1.4256	.0340
21910	.1212	.1732	.8829	145.1	15.24	4.0	.0504	.1953	.0099	.3144	1.2172	.0617
21911	.0979	.2973	.9021	145.1	15.03	4.0	.0515	.1581	.0170	.3212	.9852	.1061
21912	.0802	.5041	.9004	145.0	14.90	4.0	.0514	.1311	.0288	.3206	.8172	.1795
21913	.0608	.7766	.8998	145.0	14.73	4.0	.0514	.1008	.0444	.3204	.6280	.2765
21914	.0430	.8985	.8985	144.9	14.52	4.0	.0513	.0719	.0513	.3199	.4463	.3199
21915	.1000	1.5310	1.5944	143.0	14.86	4.0	.0510	.1670	.0674	.5671	1.0403	.5445
21916	.1209	1.3140	1.5931	142.9	15.05	4.0	.0910	.2023	.0750	.5666	1.2602	.4673
21917	.1240	1.4630	1.5931	142.9	15.09	4.0	.0910	.2081	.0835	.5666	1.2964	.5203
21918	.1359	.0794	1.5904	142.8	15.44	4.0	.0908	.2184	.0045	.5656	1.3601	.0282
21919	.1547	.1084	1.5905	142.7	15.60	4.0	.0908	.2434	.0062	.5656	1.5160	.0386
21920	.1345	.1546	1.5905	142.7	15.51	4.0	.0908	.2239	.0088	.5656	1.3942	.0550
21921	.1295	.1287	1.5904	142.8	15.40	4.0	.0908	.2087	.0073	.5656	1.3000	.0458
21922	.1162	.1467	1.5905	142.8	15.27	4.0	.0908	.1860	.0084	.5655	1.1567	.0522
21923	.0968	.2915	1.5919	142.6	15.09	4.0	.0909	.1558	.0166	.5660	.9703	.1037
21924	.0787	.3056	1.5933	142.6	14.96	4.0	.0910	.1276	.0220	.5665	.7948	.1371

IG	WG LBM/SEC	WL LBM/SEC	WLIN LBM/SEC	FLIN F	PLT P_LIA	D.A INCH	JLSIN -	JGS -	JLS -	KLSIN -	KGS -	KLS -
21925	.0507	.4831	1.5933	142.6	14.86	4.0	.0910	.0969	.0247	.5665	.6037	.1540
21926	.0404	.7524	1.5933	142.6	14.80	4.0	.0910	.0682	.0447	.5665	.6248	.2792
21927	.0273	.9740	1.5933	142.5	14.75	4.0	.0910	.0468	.0556	.5665	.2915	.3463
21928	.0205	1.3927	1.5920	142.4	14.46	4.0	.0909	.0353	.0795	.5660	.2201	.4951
21929	.0583	2.3009	2.3009	140.9	14.59	4.0	.1313	.0985	.1313	.8173	.6131	.8200
21930	.0763	2.2901	2.2901	140.9	14.70	4.0	.1311	.1297	.1313	.8163	.8076	.6200
21931	.0901	.5776	2.2926	140.9	15.03	4.0	.1308	.1504	.0330	.8144	.9360	.2052
21932	.1019	.1454	2.2805	140.9	15.18	4.0	.1306	.1869	.0083	.8129	1.0389	.8517
21933	.1142	.1016	2.2872	140.9	15.29	4.0	.1305	.1854	.0058	.8125	1.1545	.8361
21934	.1168	.0963	2.2941	140.8	15.33	4.0	.1309	.1871	.0055	.8149	1.1648	.8342
21935	.1006	.1802	2.3023	140.8	15.17	4.0	.1314	.1614	.0103	.8178	1.0046	.8640
21936	.0904	.0971	2.3037	140.8	15.10	4.0	.1314	.1454	.0055	.8182	.9053	.8345
21937	.0783	.2033	2.3052	140.7	15.01	4.0	.1315	.1267	.0116	.8187	.7886	.8722
21938	.0575	.3430	2.3065	140.7	14.90	4.0	.1316	.0947	.0196	.8192	.5896	.8218
21939	.0390	.5132	2.3066	140.6	14.84	4.0	.1316	.0658	.0293	.8191	.4096	.8822
21940	.0220	.7751	2.3054	140.4	14.83	4.0	.1315	.0379	.0442	.8186	.2361	.2752
22002	.0566	2.0260	2.8260	140.8	14.69	4.0	.1612	.0964	.1612	1.0037	.6000	1.8000
22003	.0695	2.8205	2.8205	140.8	14.77	4.0	.1609	.1192	.1607	1.0018	.7421	1.8000
22005	.0765	2.5017	2.8166	140.6	14.81	4.0	.1607	.1307	.1427	1.0003	.8137	.8884
22008	.0918	2.4118	2.8802	139.7	14.95	4.0	.1643	.1564	.1376	1.0223	.9731	.8561
22009	.1009	.1441	2.8692	139.8	15.24	4.0	.1637	.1642	.0082	1.0185	1.0220	.8512
22010	.1505	.1515	2.8233	139.7	16.01	4.0	.1613	.2360	.0086	1.0039	1.4686	.8538
22011	.1067	.1239	2.8533	139.7	15.35	4.0	.1630	.1731	.0071	1.0146	1.0769	.8440
22012	.0307	.1692	2.8639	139.6	15.21	4.0	.1634	.1453	.0097	1.0165	.9042	.8601
22013	.0729	.1850	2.8694	139.6	15.10	4.0	.1637	.1176	.0106	1.0185	.7317	.8657
22014	.0542	.3329	2.8722	139.5	15.01	4.0	.1638	.0888	.0190	1.0194	.5528	.8182
22015	.0367	.4092	2.8735	139.5	14.96	4.0	.1639	.0615	.0233	1.0199	.3826	.8452
22016	.0246	.4824	2.8722	139.5	14.95	4.0	.1638	.0418	.0275	1.0194	.2598	.8712
22017	.0130	.3562	2.8708	139.5	14.94	4.0	.1637	.0306	.0203	1.0189	.1907	.8264
22018	.0113	.5516	2.8694	139.5	14.94	4.0	.1637	.0193	.0315	1.0184	.1203	.8958
22102	.2753	2.2735	2.4934	74.1	16.13	6.0	.0509	.1257	.0464	.3809	.9409	.3473
22103	.2627	2.3124	2.4643	73.9	16.71	6.0	.0503	.1443	.0472	.3764	1.0805	.3532
22104	.2968	2.2334	2.4338	73.9	17.30	6.0	.0497	.1604	.0456	.3717	1.2009	.3411
22105	.3274	1.5676	2.4695	73.9	17.93	6.0	.0504	.1738	.0320	.3770	1.3011	.2394
22106	.3582	.5210	2.4352	73.9	18.55	6.0	.0497	.1860	.0106	.3720	1.3923	.8796
22107	.4103	.3183	2.5060	73.9	19.80	6.0	.0511	.2095	.0065	.3828	1.5679	.8486
22108	.4726	.2760	2.4352	73.8	21.03	6.0	.0497	.2297	.0056	.3720	1.7196	.8422
22109	.5107	.2550	2.4365	73.9	21.38	6.0	.0507	.2432	.0052	.3798	1.8203	.8390
22110	.5363	.1653	2.4463	73.9	22.45	6.0	.0499	.2520	.0034	.3737	1.8864	.8252
22111	.5874	.1753	2.4203	73.9	23.71	6.0	.0496	.2687	.0036	.3709	2.0109	.8268
22112	.5093	.1760	2.5920	73.9	21.81	6.0	.0529	.2426	.0036	.3959	1.8161	.8269
22113	.4576	.3030	2.5962	73.8	20.60	6.0	.0530	.2240	.0062	.3965	1.6764	.8463
22114	.4057	.3492	2.5823	73.7	19.51	6.0	.0527	.2041	.0071	.3944	1.5279	.8533
22115	.3574	.4719	2.6332	73.7	18.55	6.0	.0539	.1845	.0096	.4031	1.3812	.8721
22116	.3046	.8552	2.5255	73.7	17.61	6.0	.0515	.1621	.0174	.3857	1.2137	1.306
22117	.2344	1.3381	2.5685	73.7	16.43	6.0	.0524	.1295	.0273	.3923	.9696	.2844
22118	.1592	2.3061	2.4616	73.7	15.41	6.0	.0502	.0912	.0470	.3759	.6828	.3522
22119	.2363	4.2867	4.4576	72.8	16.30	6.0	.0909	.1314	.0874	.6805	.9835	.6544
22120	.2731	3.9998	4.4077	72.7	16.38	6.0	.0899	.1493	.0816	.6729	1.1171	.6106
22121	.3364	.2355	4.4340	72.7	18.24	6.0	.0905	.1754	.0049	.6769	1.3129	.8359

ID	WG LBM/SEC	WL LBM/SEC	WLIN LPM/SEC	FLIN F	PLT PSIA	DIA INCH	JLSIN -	JGS -	JLS -	KLSIN -	KGS -	KLS -
22122	.3723	.1963	4.4239	72.6	10.98	6.0	.0904	.1099	.0040	.6763	1.4214	.0300
22123	.4160	.0995	4.4341	72.6	19.83	6.0	.0905	.2083	.0020	.6770	1.5584	.0152
22124	.4640	.0452	4.4230	72.6	20.91	6.0	.0902	.2273	.0009	.6753	1.7006	.0069
22125	.5351	.0419	4.3646	72.7	23.86	6.0	.0691	.2721	.0009	.6664	2.0357	.0064
22126	.5356	.0000	4.4434	72.6	22.39	6.0	.0908	.2529	0.0000	.6793	1.8925	0.0000
22127	.4586	0.0000	4.4702	72.6	20.68	6.0	.0912	.2244	0.0000	.6825	1.6794	0.0000
22128	.3942	.1188	4.4355	72.6	19.33	6.0	.0905	.2001	.0024	.6772	1.4972	.0181
22129	.3506	.2510	4.5063	72.6	19.49	6.0	.0919	.1808	.0051	.6880	1.3532	.0383
22130	.3210	.3260	4.5465	72.6	17.97	6.0	.0928	.1680	.0067	.6941	1.2570	.0498
22131	.2769	.5713	4.6007	72.6	17.19	6.0	.0939	.1484	.0117	.7023	1.1103	.0872
22132	.2379	.6357	4.4466	72.6	16.57	6.0	.0907	.1302	.0130	.6788	.9743	.0970
22133	.2019	.9408	4.4619	72.6	16.07	6.0	.0910	.1126	.0192	.6811	.8426	.1436
22134	.1583	1.1119	4.4966	72.6	15.55	6.0	.0917	.0898	.0227	.6864	.6720	.1697
22135	.1166	1.5972	4.5202	72.6	15.18	6.0	.0922	.0673	.0326	.6900	.5040	.2438
22136	.0700	4.2471	4.5424	72.6	14.30	6.0	.0927	.0457	.0866	.6934	.3421	.6483
22137	.0632	6.4010	4.5507	72.6	14.62	6.0	.0928	.0373	.0898	.6947	.2788	.6718
22138	.1532	6.1972	6.4695	73.2	15.25	6.0	.1370	.0878	.1264	.9878	.6572	.9463
22139	.2350	6.0984	6.4404	73.2	16.30	6.0	.1414	.1311	.1244	.9834	.9809	.9312
22140	.2661	.3072	6.4168	73.1	17.03	6.0	.1309	.1444	.0063	.9798	1.0811	.0469
22141	.3176	.1048	6.4571	73.1	17.94	6.0	.1317	.1669	.0038	.9860	1.2494	.0282
22142	.3378	.0550	6.4307	73.1	19.26	6.0	.1312	.1963	.0011	.9820	1.4692	.0085
22143	.4627	0.0000	6.4016	73.1	20.99	6.0	.1306	.2249	0.0000	.9775	1.6829	0.0000
22144	.4575	0.0000	6.4405	73.1	20.70	6.0	.1314	.2246	0.0000	.9835	1.6809	0.0000
22145	.3895	0.0000	6.4599	73.1	19.35	6.0	.1318	.1980	0.0000	.9864	1.4820	0.0000
22146	.3166	.1813	6.4863	73.1	17.91	6.0	.1323	.1664	.0037	.9904	1.2455	.0278
22147	.2743	.3377	6.4946	73.1	17.18	6.0	.1325	.1470	.0069	.9916	1.1000	.0516
22148	.2336	.4249	6.4113	73.1	16.56	6.0	.1308	.1275	.0097	.9789	.9544	.0649
22149	.1990	.4760	6.4169	73.1	16.09	6.0	.1309	.1103	.0627	.9798	.8253	.0727
22150	.1585	.7204	6.4266	73.1	15.61	6.0	.1311	.0894	.0147	.9812	.6691	.1100
22151	.1108	.9132	6.4377	73.1	15.26	6.0	.1313	.0691	.0186	.9820	.5100	.1394
22152	.0806	2.6349	6.4343	73.1	15.03	6.0	.1313	.0468	.0537	.9825	.3503	.4023
22153	.0593	4.4979	6.4322	73.1	14.93	6.0	.1312	.0346	.0918	.9821	.2589	.6867
22154	.0459	6.4363	6.4363	73.1	14.68	6.0	.1313	.0270	.1313	.9827	.2023	.9827
22202	.2489	2.4442	2.4768	141.4	17.08	6.0	.0513	.1396	.0506	.3912	1.0661	.3860
22203	.2953	2.1099	2.4496	141.3	17.89	6.0	.0507	.1634	.0454	.3868	1.2462	.3458
22204	.3099	2.0690	2.3740	135.9	17.96	6.0	.0491	.1721	.0428	.3737	1.3103	.3257
22205	.3350	.3595	2.3996	138.6	19.98	6.0	.0497	.1770	.0074	.3783	1.3489	.0567
22206	.3711	.3334	2.4222	141.3	19.90	6.0	.0502	.1904	.0069	.3825	1.4515	.0527
22207	.4086	.2662	2.4579	141.2	20.74	6.0	.0509	.2050	.0055	.3882	1.5630	.0420
22208	.4349	.2147	2.4319	141.2	21.33	6.0	.0504	.2149	.0044	.3841	1.6387	.0339
22209	.5077	.1466	2.4999	141.2	23.08	6.0	.0518	.2409	.0030	.3946	1.8368	.0232
22210	.4327	.2554	2.4743	141.1	21.15	6.0	.0513	.2142	.0053	.3907	1.6329	.0403
22211	.4093	.2295	2.5003	141.1	20.61	6.0	.0518	.2050	.0048	.3948	1.5628	.0362
22212	.3927	.3273	2.5291	141.0	20.00	6.0	.0524	.1947	.0068	.3994	1.4846	.0517
22213	.3464	.3389	2.4854	140.9	19.19	6.0	.0515	.1801	.0070	.3924	1.3732	.0535
22214	.3002	.5508	2.4787	140.8	18.27	6.0	.0513	.1605	.0114	.3913	1.2233	.0870
22215	.2690	.6344	2.4932	140.8	17.74	6.0	.0518	.1460	.0131	.3946	1.1128	.1002
22216	.2302	1.0327	2.4786	140.9	17.00	6.0	.0513	.1292	.0214	.3913	.9847	.1630
22217	.1933	1.5000	2.5074	140.8	16.24	6.0	.0519	.1122	.0312	.3958	.8552	.2381
22218	.1507	2.0500	2.4596	140.0	15.68	6.0	.0509	.0900	.0425	.3883	.6864	.3237

ID	WG LBM/SEC	WL LBM/SEC	WLIN LBM/SEC	TLIN F	PLT PSIA	DIA INCH	JLSIN -	JGS -	JLS -	KLSIN -	KGS -	KLS -
22219	.1123	2.3468	2.4705	140.0	15.28	6.0	.0512	.0683	.0486	.3900	.5204	.3705
22220	.1096	4.2325	4.3576	139.4	16.08	6.0	.0902	.1091	.0876	.6874	.8316	.6676
22221	.2183	4.1674	4.3751	139.4	16.45	6.0	.0906	.1258	.0663	.6906	.9588	.6573
22222	.2006	4.0761	4.4014	139.4	17.74	6.0	.0911	.1571	.0844	.6943	1.1976	.6430
22223	.3148	.2092	4.3435	139.3	18.73	6.0	.0900	.1672	.0056	.6861	1.2740	.8425
22224	.3374	.1492	4.4192	139.4	19.19	6.0	.0915	.1757	.0031	.6971	1.3391	.0235
22225	.3709	.1296	4.3468	139.3	19.39	6.0	.0900	.1888	.0027	.6857	1.4389	.0204
22226	.4124	.0951	4.3573	139.3	21.05	6.0	.0904	.2056	.0020	.6889	1.5666	.0150
22227	.4499	.0722	4.3565	139.2	21.95	6.0	.0902	.2138	.0015	.6872	1.6751	.0114
22228	.4468	.0493	4.3900	139.0	21.67	6.0	.0907	.2199	.0010	.6908	1.6753	.0078
22229	.3775	.1275	4.3760	138.9	20.03	6.0	.0906	.1930	.0026	.6901	1.4707	.0201
22230	.3464	.1346	4.4143	138.9	19.33	6.0	.0914	.1787	.0040	.6962	1.3613	.0307
22231	.3007	.3502	4.3433	138.8	18.38	6.0	.0899	.1593	.0072	.6849	1.2135	.0552
22232	.2671	.3374	4.3873	138.6	17.75	6.0	.0908	.1441	.0070	.6918	1.0979	.0532
22233	.2268	.6585	4.4024	138.6	17.12	6.0	.0911	.1261	.0136	.6941	.9606	.1038
22234	.1920	1.0300	4.3929	138.5	16.54	6.0	.0909	.1095	.0213	.6926	.8339	.1624
22235	.1514	1.2060	4.3340	138.6	15.97	6.0	.0897	.0982	.0250	.6833	.6723	.1901
22236	.1160	1.6721	4.3641	138.6	15.57	6.0	.0903	.0694	.0346	.6880	.5287	.2636
22237	.0758	3.0096	4.3819	138.6	15.23	6.0	.0907	.0464	.0623	.6908	.3532	.4745
22238	.0581	4.1800	4.3914	138.6	14.96	6.0	.0909	.0360	.0865	.6923	.2745	.6590
22239	.1867	6.0641	6.4011	138.6	16.10	6.0	.1325	.1091	.1255	1.0092	.8312	.9561
22240	.2217	5.9871	6.3342	138.6	16.63	6.0	.1323	.1276	.1239	1.0082	.9720	.9440
22241	.2502	.0669	6.3835	138.5	17.49	6.0	.1321	.1381	.0014	1.0064	1.0523	.8105
22242	.2646	.0777	6.3752	138.4	17.71	6.0	.1320	.1433	.0016	1.0055	1.0914	.0123
22243	.3022	.0600	6.3659	138.4	18.56	6.0	.1317	.1600	.0012	1.0036	1.2188	.0095
22244	.3724	0.0000	6.3442	138.3	20.11	6.0	.1313	.1903	0.0000	1.0002	1.4498	0.0000
22245	.3767	0.0000	6.3416	138.2	20.11	6.0	.1312	.1928	0.0000	.9997	1.4690	0.0000
22246	.3417	0.0000	6.3527	138.1	19.31	6.0	.1315	.1785	0.0000	1.0014	1.3599	0.0000
22247	.2637	.1074	6.3707	138.0	17.91	6.0	.1318	.1434	.0022	1.0041	1.0923	.0169
22248	.2323	.1227	6.3750	137.9	17.25	6.0	.1319	.1269	.0025	1.0048	.9665	.0193
22249	.1916	.2881	6.3832	137.9	16.59	6.0	.1321	.1072	.0060	1.0060	.8168	.0454
22250	.1544	.6795	6.3822	137.7	16.06	6.0	.1320	.0888	.0141	1.0057	.6763	.1071
22251	.1130	.3468	6.3933	137.6	15.60	6.0	.1323	.0671	.0175	1.0074	.5109	.1334
22252	.0749	2.2004	6.3948	137.5	15.30	6.0	.1323	.0455	.0455	1.0076	.3469	.3467
22254	.0607	3.4279	6.3938	137.3	15.22	6.0	.1323	.0372	.0709	1.0073	.2834	.5400
22255	.0447	5.5921	6.3942	137.2	15.12	6.0	.1322	.0276	.1157	1.0073	.2103	.8809

ID	MG LBM/SEC	WL LBM/SEC	WLIN LBM/SEC	TLAN F	PLT PSIA	DIA INCH	JLSIN -	JG -	JLS -	KLSIN -	KGS -	KLS -
22603	.0372	.1614	.1604	85.5	14.47	2.0	.0511	.3434	.0514	.2215	1.4888	.2229
22604	.0431	.0853	.1553	87.8	14.59	2.0	.0495	.3949	.0261	.2145	1.7120	.1100
22605	.0474	0.0000	.1503	86.0	14.63	2.0	.0481	.4345	0.0000	.2084	1.8839	0.0000
22606	.0503	0.0000	.1638	86.2	14.64	2.0	.0522	.4605	0.0000	.2264	1.9969	0.0000
22607	.0492	0.0000	.1637	86.3	14.64	2.0	.0537	.4503	0.0000	.2331	1.9895	0.0000
22608	.0429	0.0000	.1663	86.3	14.62	2.0	.0530	.4006	0.0000	.2298	1.7371	0.0000
22609	.0373	0.0000	.1637	86.3	14.61	2.0	.0522	.3482	0.0000	.2262	1.5098	0.0000
22610	.0349	0.0000	.1627	86.4	14.61	2.0	.0518	.3254	0.0000	.2248	1.4112	0.0000
22611	.0309	0.0000	.1606	86.4	14.61	2.0	.0512	.2894	0.0000	.2222	1.2507	0.0000
22612	.0273	.0043	.1593	86.3	14.61	2.0	.0507	.2548	.0038	.2201	1.1049	.0200
22613	.0235	.0075	.1575	86.3	14.61	2.0	.0502	.2167	.0026	.2176	.9399	.0100
22614	.0199	.0154	.1554	86.3	14.62	2.0	.0495	.1827	.0041	.2147	.7924	.0200
22615	.0176	.0490	.1690	86.4	14.62	2.0	.0538	.1615	.0147	.2335	.7002	.0600
22616	.0153	.0787	.1637	86.4	14.62	2.0	.0537	.1403	.0244	.2331	.6063	.1100
22617	.0131	.1078	.1678	86.4	14.55	2.0	.0535	.1202	.0331	.2319	.5210	.0140
22618	.0103	.1674	.1674	86.5	14.48	2.0	.0534	.0948	.0532	.2314	.4111	.2300
22619	0.0000	.4034	.4034	86.7	14.40	2.0	.1285	.0002	.1286	.5575	.0008	.5600
22620	.0253	.4068	.4068	85.3	14.44	2.0	.1296	.2337	.1296	.5618	1.0133	.5600
22621	.0265	.1063	.4063	85.0	14.64	2.0	.1294	.2426	.0334	.5610	1.0514	.1400
22622	.0303	.0470	.4070	84.7	14.65	2.0	.1296	.2782	.0165	.5619	1.2059	.0700
22623	.0317	.0072	.4072	84.5	14.66	2.0	.1297	.2916	.0025	.5621	1.2638	.0100
22624	.0326	.0396	.4096	84.5	14.66	2.0	.1305	.3024	.0128	.5656	1.3106	.0600
22625	.0258	.0290	.4090	84.4	14.66	2.0	.1303	.2380	.0100	.5646	1.0313	.0400
22626	.0241	.0543	.4083	84.4	14.66	2.0	.1300	.2211	.0197	.5636	.9581	.0900
22627	.0209	.0476	.4076	84.4	14.66	2.0	.1298	.1907	.0166	.5627	.8265	.0700
22628	.0184	.0762	.4062	84.5	14.67	2.0	.1294	.1681	.0250	.5608	.7287	.1100
22629	.0157	.0953	.4053	84.5	14.67	2.0	.1291	.1434	.0297	.5596	.6214	.1300
22630	.0116	.1347	.4047	84.5	14.68	2.0	.1289	.1066	.0444	.5587	.4619	.1900
22631	.0116	.1533	.4033	84.6	14.68	2.0	.1285	.1065	.0483	.5568	.4614	.2100
22632	.0086	.1923	.4023	84.5	14.68	2.0	.1281	.0791	.0613	.5554	.3426	.2700
22633	.0082	.1722	.4022	84.4	14.68	2.0	.1281	.0747	.0564	.5552	.3240	.2400
22702	.0297	.1567	.1557	142.9	14.39	2.0	.0506	.2793	.0505	.2229	1.2301	.2200
22703	.0320	.1492	.1492	143.1	14.40	2.0	.0482	.3012	.0481	.2123	1.3266	.2100
22704	.0360	.1541	.1541	143.4	14.42	2.0	.0498	.3396	.0497	.2193	1.4960	.2200
22705	.0372	.1537	.1537	143.5	14.42	2.0	.0496	.3510	.0496	.2187	1.5465	.2200
22706	.0412	.0229	.1529	143.7	14.56	2.0	.0494	.3832	.0062	.2175	1.6881	.0300
22707	.0431	0.0000	.1673	144.0	14.58	2.0	.0541	.4007	0.0000	.2382	1.7654	0.0000
22708	.0498	0.0000	.1573	144.3	14.60	2.0	.0508	.4628	0.0000	.2240	2.0398	0.0000
22709	.0429	0.0000	.1438	144.4	14.58	2.0	.0484	.3989	0.0000	.2133	1.7576	0.0000
22710	.0362	0.0000	.1528	144.5	14.56	2.0	.0494	.3563	0.0000	.2176	1.5789	0.0000
22711	.0325	0.0000	.1523	144.5	14.55	2.0	.0492	.3076	0.0000	.2166	1.3556	0.0000
22712	.0291	0.0000	.1568	144.6	14.55	2.0	.0507	.2754	0.0000	.2232	1.2335	0.0000
22713	.0256	0.0000	.1639	144.8	14.55	2.0	.0549	.2424	0.0000	.2419	1.0681	0.0000
22714	.0232	0.0000	.1662	145.1	14.55	2.0	.0537	.2193	0.0000	.2367	.9664	0.0000
22715	.0207	.0038	.1596	145.3	14.55	2.0	.0516	.1937	.0012	.2274	.8540	.0100
22716	.0148	.0529	.1529	145.2	14.56	2.0	.0494	.1385	.0167	.2178	.6104	.0700
22717	.0110	.0669	.1542	145.1	14.56	2.0	.0498	.1108	.0216	.2196	.4882	.0953
22718	.0082	.1542	.1542	145.0	14.43	2.0	.0498	.0766	.0458	.2196	.3377	.2200
22719	.0210	.4146	.4146	147.7	14.38	2.0	.1341	.1964	.1341	.5915	.8750	.5900
22720	.0242	.4036	.4036	147.4	14.39	2.0	.1305	.2245	.1305	.5757	1.0120	.5800

ID	WG LBM/SEC	WL LBM/SEC	WLIN LBM/SEC	TLIN F	PLT PSIA	DIA INCH	JLSIN -	JGS -	JLS -	KLSIN -	KGS -	KLS -
22721	.0277	.0071	.4071	147.0	14.58	2.0	.1316	.2577	.0283	.5805	1.1366	.1300
22722	.0323	.0261	.4061	146.7	14.60	2.0	.1313	.3002	.0084	.5791	1.3237	.0400
22723	.0377	0.0000	.4067	146.5	14.62	2.0	.1315	.3501	0.0000	.5798	1.5437	0.0000
22724	.0325	.0258	.4058	146.4	14.60	2.0	.1312	.3051	.0077	.5784	1.3450	.0300
22725	.0293	.0241	.4041	146.3	14.60	2.0	.1307	.2779	.0084	.5761	1.2252	.0400
22726	.0261	.0432	.4032	146.2	14.60	2.0	.1304	.2472	.0139	.5747	1.0898	.0600
22727	.0235	.0329	.4029	146.2	14.60	2.0	.1303	.2230	.0100	.5743	.9831	.0400
22728	.0206	.0307	.4007	146.2	14.60	2.0	.1296	.1944	.0110	.5712	.8569	.0500
22729	.0173	.0524	.4024	146.1	14.60	2.0	.1301	.1614	.0154	.5735	.7118	.0700
22730	.0147	.0823	.4023	146.1	14.60	2.0	.1300	.1373	.0278	.5733	.6055	.1200
22731	.0098	.1025	.4025	146.1	14.62	2.0	.1301	.0919	.0328	.5737	.4052	.1400
22732	.0075	.1106	.4006	146.1	14.62	2.0	.1295	.0708	.0358	.5710	.3122	.1600
21308	.1102	.7699	.9031	80.0	14.33	4.0	.0511	.1791	.0433	.3132	1.0967	.2652
21309	.1419	.6604	.9059	80.0	15.19	4.0	.0510	.2270	.0376	.3121	1.3945	.2303
21310	.1475	.0767	.9021	80.0	15.34	4.0	.0508	.2351	.0043	.3108	1.4396	.0264
21311	.1748	.0800	.8982	80.1	15.67	4.0	.0505	.2773	.0045	.3094	1.6976	.0276
21312	.1531	.0620	.8939	80.1	15.36	4.0	.0506	.2466	.0035	.3100	1.5095	.0213
21313	.1219	.1219	.9016	80.1	15.13	4.0	.0507	.1963	.0069	.3106	1.2018	.0420
21314	.1120	.2280	.9017	80.2	14.95	4.0	.0507	.1806	.0128	.3106	1.1055	.0786
21315	.0960	.4547	.9028	80.2	14.78	4.0	.0508	.1558	.0256	.3110	.9540	.1567
21316	.0829	.6262	.9029	80.2	14.67	4.0	.0508	.1351	.0352	.3111	.8273	.2157
21317	.0655	.7999	.9035	80.2	14.52	4.0	.0508	.1074	.0450	.3113	.6573	.2756
21804	.0002	1.5892	1.5979	76.4	14.41	4.0	.0899	.0003	.0894	.5497	.0020	.5467
21805	.0098	1.6322	1.5910	76.5	14.77	4.0	.0895	.1609	.0918	.5473	.9841	.5615
21806	.1163	1.4606	1.5868	76.5	14.90	4.0	.0892	.1869	.0826	.5459	1.1430	.5052
21807	.1326	1.5393	1.5854	76.5	15.03	4.0	.0892	.2126	.0866	.5454	1.3002	.5295
21808	.1454	1.4631	1.5826	76.5	15.14	4.0	.0890	.2323	.0823	.5444	1.4207	.5033
21809	.1582	.0498	1.5771	76.5	15.48	4.0	.0887	.2485	.0028	.5425	1.5198	.0171
21810	.1910	.1116	1.5701	76.6	15.84	4.0	.0883	.2959	.0063	.5402	1.8098	.0384
21811	.2091	.1166	1.5674	76.6	16.07	4.0	.0882	.3190	.0066	.5392	1.9513	.0401
21812	.2072	.0995	1.5646	76.6	16.10	4.0	.0880	.3155	.0056	.5383	1.9480	.0342
21813	.1695	.1495	1.5687	76.7	15.37	4.0	.0882	.2943	.0084	.5397	1.8002	.0514
21814	.1580	.1211	1.5743	76.8	15.51	4.0	.0885	.2431	.0068	.5416	1.5239	.0415
21815	.1440	.1126	1.5757	76.8	15.36	4.0	.0886	.2261	.0063	.5421	1.3833	.0387
21816	.1321	.1505	1.5770	76.8	15.26	4.0	.0887	.2072	.0085	.5426	1.2677	.0518
21817	.1152	.2154	1.5794	76.8	15.12	4.0	.0888	.1820	.0121	.5430	1.1131	.0741
21818	.0956	.3217	1.5704	76.8	15.03	4.0	.0888	.1359	.0181	.5430	.8315	.1107
21819	.0831	.3046	1.5704	76.8	15.04	4.0	.0888	.1319	.0171	.5430	.8068	.1048
21820	.0650	.5001	1.5730	76.8	14.90	4.0	.0889	.1038	.0281	.5435	.6349	.1720
21821	.0500	.6950	1.5794	76.8	14.31	4.0	.0888	.0805	.0391	.5430	.4922	.2391
21822	.0381	.9529	1.5794	76.8	14.76	4.0	.0888	.0617	.0536	.5430	.3774	.3278
21823	.0299	1.4606	1.5798	76.8	14.47	4.0	.0889	.0484	.0626	.5435	.2962	.5053
21826	.0764	2.1317	2.3375	75.6	14.66	4.0	.1314	.1231	.1199	.8038	.7531	.7330
21827	.0972	2.2011	2.3320	75.6	14.91	4.0	.1311	.1568	.1138	.8019	.9590	.7569
21828	.1160	2.0929	2.3236	75.6	15.00	4.0	.1307	.1876	.1177	.7990	1.1471	.7197
21829	.1194	.0581	2.3167	75.6	15.29	4.0	.1303	.1884	.0033	.7967	1.1523	.0200
21830	.1436	.0727	2.3054	75.6	15.43	4.0	.1298	.2249	.0041	.7938	1.3754	.0250
21831	.1774	.0715	2.3056	75.6	15.51	4.0	.1297	.2773	.0040	.7929	1.6960	.0246
21832	.1402	.1533	2.1308	75.6	15.27	4.0	.1198	.2230	.0086	.7328	1.3637	.0527
21833	.1209	.1676	2.1349	75.9	15.12	4.0	.1201	.1908	.0094	.7342	1.1670	.0576

TABLE B-2. FLOODING DATA FOR COUNTERCURRENT
STEAM-WATER FLOWS IN TUBES

- ID - Identification number
 WG - Steam flow rate, lbm/sec
 WL - Water penetration rate, lbm/sec
 WLIN - Inlet water flow rate, lbm/sec
 TLIN - Temperature of inlet water, °F
 PLT - Lower tank pressure, psia
 DIA - Tube diameter, inch
 THRM - Thermodynamic ratio,

$$[C_P(T_{SAT} - T_{Lin})/h_{fg}](\rho_L/\rho_g)^{1/2} J_{Lin}^*/J_g^*$$

- JLSIN - Dimensionless inlet water flow rate,

$$[\rho_L V_{Lin}^2/gD(\rho_L - \rho_g)]^{1/2}$$

- JGS - Dimensionless steam flow rate,

$$[\rho_g V_g^2/gD(\rho_L - \rho_g)]^{1/2}$$

- JLS - Dimensionless water penetration rate,

$$[\rho_L V_L^2/gD(\rho_L - \rho_g)]^{1/2}$$

- KLSIN - Dimensionless inlet water flow rate,

$$\{\rho_L V_{Lin}^2/[g\sigma(\rho_L - \rho_g)]^{1/2}\}^{1/2}$$

- KGS - Dimensionless air flow rate,

$$\{\rho_g V_g^2/[g\sigma(\rho_L - \rho_g)]^{1/2}\}^{1/2}$$

- KLS - Dimensionless water penetration rate,

$$\{\rho_L V_L^2/[g\sigma(\rho_L - \rho_g)]^{1/2}\}^{1/2}$$

ID	MG LBM/SEC	ML LBM/SEC	WLIN LBM/SEC	T LIN F	PLT P:IA	THRMF -	DIA INCH	JLSIN -	JGS -	JLS -	KLSIN -	KGS -	KLS -
22413	.2317	1.1036	2.4894	139.3	15.09	.0225	6.0	.0515	.1922	.0228	.3926	1.4646	.1741
22414	.2141	2.4928	2.4909	139.1	14.73	.0758	6.0	.0515	.1802	.0516	.3928	1.3733	.3931
22415	.1563	2.5144	2.4909	139.0	14.66	1.1970	6.0	.0515	.1319	.0520	.3928	1.0052	.3965
22416	.0986	4.2604	4.3627	137.5	14.66	3.7901	6.0	.0902	.0832	.0883	.6873	.6337	.6724
22417	.1823	4.2518	4.3616	137.2	14.66	1.8334	6.0	.0902	.1539	.0879	.6878	1.1721	.6697
22418	.2262	4.3011	4.3577	137.2	14.69	1.4657	6.0	.0901	.1906	.0889	.6864	1.4521	.6775
22419	.3021	4.2681	4.3438	136.9	14.70	1.1153	6.0	.0899	.2545	.0882	.6858	1.9383	.8718
22420	.3369	.5591	4.3457	136.9	15.12	1.0210	6.0	.0899	.2791	.0116	.6844	2.1260	.0881
22421	.7711	.0998	4.3457	136.9	15.09	.9755	6.0	.0899	.3132	.0021	.6844	2.3055	.0157
22422	.4409	.0369	4.3268	136.7	15.36	.7701	6.0	.0895	.3754	.0008	.6813	2.8589	.0058
22423	.4549	0.0800	4.3700	136.3	15.39	.7489	6.0	.0895	.3691	0.0000	.6817	2.7629	0.0000
22424	.3971	.0973	4.3931	136.2	15.10	.8660	6.0	.0908	.3392	.0020	.6916	2.5828	.0153
22425	.3277	.3161	4.4002	136.0	15.08	1.0731	6.0	.0910	.2718	.0065	.6926	2.0693	.0498
22426	.3140	.6115	4.3947	136.0	15.17	1.1228	6.0	.0908	.2598	.0126	.6917	1.9782	.0963
22427	.2657	.8630	4.3893	135.9	15.40	1.2454	6.0	.0907	.2351	.0178	.6909	1.7904	.1358
22428	.2483	1.2161	4.3826	135.8	15.56	1.4419	6.0	.0906	.2036	.0251	.6898	1.5499	.1914
22429	.2097	4.2106	4.3953	135.5	14.65	1.6562	6.0	.0908	.1762	.0870	.6916	1.3414	.6626
22430	.1333	4.2612	4.3941	135.4	14.65	2.5967	6.0	.0908	.1125	.0881	.6914	.8564	.6785
22431	.0649	6.1988	6.3914	140.2	14.60	7.2511	6.0	.1323	.0549	.1283	1.0084	.4188	.9780
22432	.1712	6.2912	6.3906	139.9	14.62	2.7623	6.0	.1322	.1448	.1302	1.0081	1.1039	.9925
22433	.2247	6.4011	6.3923	139.7	14.62	2.1112	6.0	.1323	.1900	.1325	1.0083	1.4486	1.0097
22434	.2660	6.4200	6.3911	139.6	14.62	1.7858	6.0	.1322	.2249	.1328	1.0080	1.7144	1.0126
22435	.3030	6.4040	6.3887	139.4	14.53	1.5722	6.0	.1322	.2561	.1325	1.0076	1.9520	1.0100
22436	.3653	.1239	6.3877	139.2	15.26	1.3498	6.0	.1322	.3018	.0076	1.0073	2.3002	.0195
22437	.3823	.0580	6.3808	139.0	15.09	1.2621	6.0	.1322	.3260	.0012	1.0077	2.4849	.0091
22438	.4454	0.0000	6.3912	138.8	15.00	1.0758	6.0	.1322	.3840	0.0000	1.0076	2.9261	0.0000
22439	.4010	.0684	6.3495	141.3	15.08	1.1534	6.0	.1314	.3440	.0014	1.0025	2.6237	.0108
22440	.3545	.1724	6.3440	141.3	15.20	1.3324	6.0	.1313	.2955	.0036	1.0017	2.2536	.0272
22441	.2906	.5118	6.3454	141.3	15.40	1.6477	6.0	.1314	.2393	.0106	1.0019	1.8250	.0888
22442	.2743	.0082	6.3469	141.2	15.53	1.7577	6.0	.1314	.2252	.0167	1.0021	1.7176	.1276
22443	.2365	6.4206	6.3428	141.2	14.60	1.9447	6.0	.1313	.2003	.1329	1.0014	1.5273	1.8137
22444	.2189	6.3788	6.3442	141.2	14.60	2.1023	6.0	.1313	.1853	.1321	1.0016	1.4131	1.0071

NRC FORM 335 (7-77)		U.S. NUCLEAR REGULATORY COMMISSION BIBLIOGRAPHIC DATA SHEET		1. REPORT NUMBER (Assigned by DDC) NUREG/CR-1625	
4. TITLE AND SUBTITLE (Add Volume No., if appropriate) Steam-Water Mixing and System Hydrodynamics Program - Task 4 - Quarterly Progress Report July 1, 1979 - September 30, 1979				2. (Leave blank)	
7. AUTHOR(S) Robert P. Collier and others				5. DATE REPORT COMPLETED MONTH: July YEAR: 1980	
9. PERFORMING ORGANIZATION NAME AND MAILING ADDRESS (Include Zip Code) Battelle, Columbus Laboratories 505 King Avenue Columbus, Ohio 43201				DATE REPORT ISSUED MONTH: August YEAR: 1980	
12. SPONSORING ORGANIZATION NAME AND MAILING ADDRESS (Include Zip Code) Division of Reactor Safe ⁺ , Research U. S. Nuclear Regulatory Commission Washington, D. C. 20555				6. (Leave blank)	
				8. (Leave blank)	
				10. PROJECT TASK/WORK UNIT NO.	
				11. CONTRACT NO. FIN No. A4048	
13. TYPE OF REPORT Quarterly Progress Report			PERIOD COVERED (Inclusive dates) July 1, 1979 - September 30, 1979		
15. SUPPLEMENTARY NOTE				14. (Leave blank)	
16. ABSTRACT (200 words or less) During this quarter we analyzed results from high bypass air-water tests and from low subcooling steam-water tests in the 2/15-scale model, continued development of a mechanistic model for ECC penetration, and analyzed results from steam-water tests in the simple tube facility. The experimental efforts during this quarter were directed to completion of the installation of the annulus void measurement system and the instrumented spool piece for the break leg, and subsequent check out and acquisition of initial data.					
17. KEY WORDS AND DOCUMENT ANALYSIS ECC Bypass Scaling Condensation Analysis Experiments			17a. DESCRIPTORS		
17b. IDENTIFIERS OPEN-ENDED TERMS					
18. AVAILABILITY STATEMENT Unlimited			19. SECURITY CLASS (This report) Unclassified		21. NO. OF PAGES
			20. SECURITY CLASS (This page) Unclassified		22. PRICE \$